Chelated N^N and N^O Donor Nickel(II) Complexes as Ethylene Oligomerization Catalysts

By

Makhosonke Ngcobo

Thesis

Submitted in accomplishment for

Master's Degree

in

Chemistry

in the

Faculty of Agriculture, Engineering and Sciences

based in the

University of KwaZulu Natal Pietermaritzburg

Supervisor: Prof S. O. Ojwach

November 2016

DECLARATION

I declare that this thesis, Chelated N^N and N^O donor nickel(II) complexes as potential catalysts for ethylene oligomerization reactions is genuinely my own work and all the information, sources and quotes that I have used have been acknowledged by means of a complete physical reference.

Student Name: Makhosonke Ngcobo

Signature: ……. Date: ……

Supervisor: Prof Stephen O Ojwach

Signature: ……. Date: ……

DEDICATIONS

Dedicated to my whole family and friends

ABSTRACT

A series of nickel(II) complexes chelated by N^N benzimidazolylmethylamine and N^O 2-[(ethylimino)ethyl]phenol ligands have been synthesized, characterized and applied as catalysts for ethylene oligomerization reactions. A total of twelve ligands and thirteen nickel(II) complexes was synthesized. The formation of ligands and complexes was confirmed using ^{1}H NMR and $^{13}C\{^{1}H\}$ NMR, IR spectroscopy, mass spectrometry, magnetic moment measurements, elemental analyses and single crystal X-ray crystallography. The N^N benzimidazolylmethylamine ligand **L3** gave a mononuclear complex **3a** whilst the N^O 2-[(ethylimino)ethyl]phenol ligand **L7** gave a binuclear nickel(II) complex **9a** and both ligand systems resulted in formation of complexes possessing a distorted octahedral geometries. The nickel(II) complexes were then tested for the oligomerization reactions of ethylene and the oligomeric products were characterized using GC and a combination of GC-MS.

Upon activation with $EtAlCl_2$ and MAO all the nickel (II) complexes showed high catalytic activities in the range of 337 kg mol^{-1} h^{-1} to 3 330 kg mol^{-1} h^{-1} to produce C_4 and C_6 and toluene alkylated products depending on the solvent system and co-catalyst utilized. The catalytic activities of the complexes and the products formed were largely governed by the nature of the nickel(II) complex structure. The most catalytically active catalyst **10** gave activity of 3 330 kg mol^{-1} h^{-1} and selectivity of 25% and 75% for butene and hexene respectively. The use of toluene resulted in formation of Friedel-Craft alkylated products whilst chlorobenzene predominantly gave C_4 and C_6 oligomers. Activation with MAO co-catalyst also gave C_4 and C_6 oligomers as major products irrespective of the solvent system used. In addition, the reaction parameters such as pressure, time and Al/Ni ratio had a significant effect on catalytic activity and selectivity of the nickel(II) complexes and therefore were also optimized.

TABLE OF CONTENTS

DECLARATION ii

DEDICATIONS iii

ABSTRACT iv

LIST OF FIGURES x

LIST OF SCHEMES xiii

LIST OF TABLES xiv

ABBREVIATIONS xv

ACKNOWLEDGEMENTS xvi

CHAPTER ONE

Introduction and literature review of ethylene oligomerization reactions by late transition metal catalysts

1.1. Background information 1

1.2. Mechanism for ethylene oligomerization and polymerization reactions 3

1.3. The role of the co-catalyst 5

1.4. Properties and applications of linear α-olefins (LAOs) 6

1.5. Literature review of nickel(II) complexes as ethylene oligomerization catalysts 7

1.5.1. Nickel(II) complexes chelated by N^O bidentate ligands 8

1.5.2. N^N bidentate nickel(II) complexes 11

1.5.3. N^N^N tridentate nickel(II) complexes 15

1.5.4. Mixed oxygen^nitrogen tridentate nickel(II) complexes 19

1.5.5. Friedel-Craft alkylation in the oligomerization reactions of ethylene 22

1.6. Statement of the problem 26

1.7. Justification of the research project 26

1.8. Aim of the research project 27

1.9. Objectives of the study 27

1.10. References 28

CHAPTER TWO

Nickel(II) complexes chelated by N^N benzimidazolyl-methylamine ligands: Synthesis, structural characterization and catalytic behavior in ethylene oligomerization reactions.

2.1. Introduction 33

2.2. Experimental section 34

2.2.1. Materials and instrumentation 34

2.2.2. Synthesis of ligands and nickel(II) complexes 35

*2.2.2.1. N-(1H-benzimidazol-2-ylmethyl)-2-analine (**L1**)* 35

*2.2.2.2. N-(1H-benzimidazol-2-ylmethyl)-2-bromoanaline (**L2**)* 36

*2.2.2.3. N-(1H-benzimidazol-2-ylmethyl)-2-methoxyanaline (**L3**)* 37

*2.2.2.4. N-(1H-benzimidazol-2-ylmethyl)-2-phenolanaline (**L4**)* 38

*2.2.2.5. [{N-(1H-benzoimidazol-2-ylmethyl)-2-analine} $NiBr_2$] (**1**)* 39

*2.2.2.6. [{N-(1H-benzoimidazol-2-ylmethyl)-2-bromoanaline} $NiBr_2$] (**2**)* 39

*2.2.2.7. [{N-(1H-benzoimidazol-2-ylmethyl)-2-methoxyanaline} $NiBr_2$] (**3**)* 40

*2.2.2.8. [{N-(1H-benzoimidazol-2-ylmethyl)-2-methoxyanaline} $NiCl_2$] (**4**)* 41

*2.2.2.9. [{N-(1H-benzoimidazol-2-ylmethyl)-2-phenolanaline} $NiBr_2$] (**5**)* 41

*2.2.2.10. [{N-(1H-benzimidazol-2-ylmethyl)-2-phenolanaline} $NiCl_2$] (**6**)* 42

2.2.3. X-ray Crystallography 42

2.2.4. General procedure for ethylene oligomerization reactions 43

2.3. Results and discussion 45

2.3.1. Syntheses and characterization of nickel(II) complexes 45

2.3.2. Ethylene oligomerization reactions catalyzed by nickel(II) complexes **1**–**6** 54

2.3.2.1. Effect of catalyst structure on ethylene oligomerization reactions 57

2.3.2.2. Effect of reaction condition on ethylene oligomerization reactions using nickel(II) complex **3** 59

*2.3.2.2.1. Effect of Al/Ni ratio on the catalytic behaviour of complex **3*** 59

*2.3.2.2.2. Effect of time on the catalytic behaviour of the nickel(II) complex **3*** 60

*2.3.2.2.3. Effect of ethylene pressure on the catalytic behaviour of the nickel(II) Complex **3*** 61

*2.3.2.2.4. Effect of the nature of the co-catalyst on the catalytic behaviour of the nickel(II) complex **3*** 62

2.3.2.3. The effect of the solvent on the catalytic activities and selectivities of nickel(II) complexes **1**, **3** and **4** 63

2.4. Conclusions 65

2.5. References 66

CHAPTER THREE

Chelated N^O donor nickel(II) complexes of 2-[(ethylimino)ethyl]phenol ligands: Coordination chemistry and catalytic behavior on ethylene oligomerization reactions.

3.1. Introduction 69

3.2. Experimental section 71

3.2.1. Materials and methods 71

3.2.2. Preparation of ligands and their respective nickel(II) complexes 72

3.2.2.1. Phenol, 2-[1-[(2-methxyethyl) imino] ethyl] (**L5**) 72

3.2.2.2. Phenol, 2-[1-[(2-hydroxyethyl) imino] ethyl] (**L6**) 73

3.2.2.3. Phenol, 2-[(E)-[(2-hydroxyethyl) imino] methyl] (**L7**) 74

3.2.2.4. Phenol, 2-[(E)-{[2-(diethylamino) ethyl] imino} methyl] (**L8**) 74

3.2.2.5. Phenol, 2-[1-[(2-methxyethyl) amino] ethyl] (**L9**) 75

3.2.2.6. Phenol, 2-[1-[(2-hydroxyethyl) amino] ethyl] (**L10**) 76

3.2.2.7. Phenol, 2-{[(2-hydroxyethyl) amino] methyl} (**L11**) 77

3.2.2.8. Phenol, 2-({[2-(diethylamino)ethyl]amino}methyl) (**L12**) 77

3.2.2.9. Phenol, 2-[1-[(2-hydroxyethyl) imino] ethyl] $NiBr_2$ (**7**) 78

3.2.2.10. Phenol, 2-[1-[(2-hydroxyethyl) imino] ethyl] $NiCl_2$ (**8**) 79

3.2.2.11. Phenol, 2-[1-[(hydroxyethyl) imino] methyl $NiCl_2$ (**9**) 79

3.2.2.12. Phenol, 2-[1-[(2-methxyethyl) amino] ethyl] $NiBr_2$ (**10**) 80

3.2.2.13. Phenol, 2-[1-[(2-hydroxyethyl) amino] ethyl] $NiBr_2$ (**11**) 80

3.2.2.14. Phenol, 2-[1-(2-Hydroxyethyl)amino] methyl] $NiCl_2$ (**12**) 81

3.2.2.15. Phenol, 2-(1-{[2-(diethylamino)ethyl] amino} methyl) $NiCl_2$ (**13**) 81

3.2.3. X-ray Crystallography 82

3.2.4. Ethylene oligomerization reactions general procedure 82

3.3. Results and Discussion 84

3.3.1. Syntheses of ligands and their respective nickel(II) complexes 84

3.3.2. Molecular structure of nickel(II) complex **9a** 96

3.3.3. Ethylene oligomerization reactions catalyzed by nickel(II) complexes **7**–**13** 99

3.3.3.1. The effect of the catalyst structure on the catalytic activities and product distribution 99

3.3.3.2. The effect of the reaction parameters on the catalytic behavior of the nickel(II) complex **9** 102

*3.3.3.2.1 The effect of Al/Ni ratio on ethylene oligomerization reaction of complex **9*** 103

*3.3.3.2.2 The effect of time on the catalytic behavior of the nickel(II) complex **9*** 103

*3.3.3.2.3 The effect of ethylene pressure on the catalytic ability of complex **9*** 104

*3.3.3.2.4 The effect of solvent on the catalytic activity and selectivity of the complex **9*** 104

3.4. Conclusions 105

3.5. References 105

CHAPTER FOUR

General concluding remarks and future prospects

4.1. General conclusions 108

4.2. Future prospects 110

LIST OF FIGURES

Figure **Page**

1.1 Market volume of the products from LAOs in 2004 7

1.2 The coordination chemistry of the hemilabile catalytic system 9

1.3 The previously studied neutral nickel catalysts with N^O-type ligands 10

1.4 The *bis*-(4,6-dibenzhydryl-2-[(arylimino)methyl]phenoxylate) nickel(II) complex 11

1.5 The α-di-imine nickel(II) catalyst precursors, developed by Brookhart and co-workers 12

1.6 Nickel(II) complexes of 8-(1-aryliminoethylidene)quinaldinyl ligands (**1-VII**) and N-(2-substituted-5,6,7-trihydroquinolin-8-ylidene)arylamino (**1-VIII**) 13

1.7 Nickel(II) complex of 2-iminopyridyl ligands 14

1.8 The nickel(II) complexes supported by (amino)pyridine ligands 15

1.9 Nickel(II) catalysts bearing N-(2-(1H-benzo[d]imidazol-2-yl)quinolin-8-yl) benzamine derivatives 16

1.10 Nickel(II) dibromide complexes bearing *bis*-(benzimidazolyl)amine (**1-XII**) and *bis*-(benzimidazolyl)pyridine (**1-XIII**) ligands 18

1.11 Nickel(II) complex bearing 2-(benzimidazole-2-yl)-1,10-phenathrolines ligands 19

1.12 Nickel(II) dihalides bearing 2-benzimidazol-8-ethoxyquinolines 20

1.13 Nickel(II) complexes bearing tridentate ligands used in ethylene oligomerization 21

1.14 Nickel(II) complexes chelated by 2,6-pyridinedicarboxamide 22

Figure **Page**

1.15 The nickel(II) complexes anchored by [2-(3,5-dimethyl-pyrazol-1-yl)-ethanol] (**3**) and [1-(2-chloro-ethyl)-3,5-dimethyl-1H-pyrazole] ligands (**7**) 25

2.1 ^{1}H NMR spectrum of N-(1H-benzoimidazol-2-ylmethyl)-2-aniline (**L1**) in $CDCl_3$ 46

2.2 $^{13}C\{^{1}H\}$ NMR spectrum of N-(1H-benzoimidazol-2-ylmethyl)-2-aniline (**L1**) in $CDCl_3$ 47

2.3 FT-IR spectrum of compound **L3** displaying N-H (broad) and C=N (sharp) peaks at 3149.45 cm^{-1} and 1600.93 cm^{-1} 48

2.4 Mass spectrum of ligand **L3** showing a molecular ion peak at m/z of 276.1121 amu 48

2.5 The mass spectrum of **1** showing the complex peak at 441.8250 amu and fragmentation of a bromide ion at m/z of 359.9186 amu 50

2.6 The IR spectra of ligand **L2** and its corresponding complex **2** showing N-H peaks at 3060.84 cm^{-1} and 3151.64 cm^{-1} 51

2.7 Molecular structure of complex **3a** showing the presence of two ligands units in the nickel(II) coordination sphere 53

2.8 A typical gas chromatogram obtained for ethylene oligomerization by complex **3** using $EtAlCl_2$ as co-catalyst in toluene solvent 55

2.9 The GC-MS of the product obtained when using complex **3**, showing the butyl-alkylated toluene product 56

Figure **Page**

2.10 Gas chromatogram showing C_4 and C_6 oligomers obtained when complex **3** is activated with $EtAlCl_2$ in chlorobenzene solvent 65

3.1 ^1H NMR spectrum of ligand **L5** in $CDCl_3$ 85

3.2 ^{13}C NMR of spectrum of ligand **L5** in $CDCl_3$ 86

3.3 The mass spectrum of **L5** showing $[M + Na]^+$ fragment at m/z =216.0995 amu 86

3.4 ^1H NMR spectrum of ligand **L9** in $CDCl_3$ 88

3.5 $^{13}C\{^1H\}$ NMR spectrum of compound **L9** in $CDCl_3$ 88

3.6 Mass Spectrum of **L9** showing a peak at 195.1189 amu corresponding to a molecular ion peak 89

3.7 The IR spectra of the imine ligand **L8** characterized by a sharp C=N peak and the amine ligand **L12** 90

3.8 The mass spectrum of **9** showing a peak at m/z of 222.0113 amu when two chlorines are fragmented and a peak at 443.0172 corresponding to $[(L7)_2Ni]^+$ molecular ions 92

3.9 The mass spectrum of **10** showing a molecular ion peak at 326.9061 amu (60 %) 93

3.10 The infrared spectra of ligand **L12** and its nickel (II) complex **13** showing strong and broad N-H signal in complex **13** 94

3.11 Molecular structure diagram of nickel(II) complex **9a** 98

LIST OF SCHEMES

Scheme	Page
1.1 The β-hydride elimination step that leads to chain termination of oligomer or polymer product	2
1.2 The mechanism of ethylene oligomerization and polymerization reactions	4
1.3 The activation of the nickel(II) complex with the aluminium based co-catalyst	5
1.4 Ethylene oligomerization by (Pyrazo-1-ylmethyl)pyridine nickel(II) complexes and unusual Friedel Crafts alkylation	24
2.1 The synthetic protocol of the benzimidazolylmethylamine N^N donor ligands	45
2.2 The syntheses of benzimidazolylmethylamine N^N chelated nickel(II) complexes	49
2.3 Ethylene oligomerization reactions and unusual Friedel alkylation catalysts	54
3.1 Syntheses of 2-[(ethylimino)ethyl]phenol, N^O donor ligands	84
3.2 Reduction of imine ligands to form 2-[(ethylimino)ethyl]phenol, N^O donor ligands	87
3.3 Syntheses of imine and amine N^O chelated nickel(II) complexes	91
4.1 The proposed synthesis for the heterogenized nickel(II) complexes of N^N benzimidazolylmethylamine ligands	111

LIST OF TABLES

Table	**Page**
2.1 The spectroscopic and physical data obtained for nickel(II) complexes **1-6**	52
2.2 The Effect of the catalyst structure on ethylene oligomerization reactions using complexes **1-6** and $EtAlCl_2$ as a co-catalyst in toluene solvent	57
2.3 The effect of reaction conditions on ethylene oligomerization reactions using nickel(II) complex **3**	60
2.4 The effect of the solvents on the catalytic activities and selectivities of nickel(II) complexes **1**, **3** and **4**	63
3.1 The IR, mass spectral and magnetic moments data of the ligands **L5**–**L12** and their nickel(II) complexes **7**–**13**	95
3.2 The selected bond lengths [Å] and angles [°] for nickel(II) complex **9a**	96
3.3 Crystal data and structure refinement for nickel(II) complex **9a**	97
3.4 Ethylene oligomerization data obtained for nickel(II) complexes **7**-**13** using $EtAlCl_2$ as a co-catalyst in chlorobenzene	100
3.5 Ethylene oligomerization reactions of the **9**/$EtAlCl_2$ system	102

ABBREVIATIONS

LAO	Linear alpha olefins
GC	Gas chromatography
GC-MS	Gas chromatography-mass spectrometry
ESI	Electron spray ionisation
IR	Infrared spectroscopy
L	Ligand
MS	Mass spectrometry
NMR	Nuclear magnetic resonance
MAO	Methylaluminoxane
MMAO	Modified methyaluminoxane
$EtAlCl_2$	Ethylaluminum dichloride
Et_2AlCl	Diethylaluminum chloride
Et_3Al	Triethylaluminium
LDPE	Low density polyethylene
HDPE	High density polyethylene
SHOP	Shell higher olefin process

ACKNOWLEDGEMENTS

- Firstly I would like to pass my sincere gratitude to my pillar of strength, the Almighty God for His spiritual guidance throughout the course of this research project.
- I am also very thankful to Prof Stephen Ojwach who has not only been a supervisor to me but also a role model and a father, I feel honoured to be part of his research group and also one of his product. I am grateful for all his guidance and informative pieces of advice.
- Catalysis research group for their assistant and my fellow Masters candidates for social support and all the events we had.
- Technical and laboratory assistance from Sizwe Zamisa (single crystal X-ray Crystallography), Mr Craig Grimmer (NMR Spectroscopy), Mrs Caryl Jense Van Rensburg (GC-MS, MS and CHN analyses), Mrs Prudence Lubanyana and Marvin Makhathini (GC), Bheki Dlamini (IR Spectroscopy) and Shawn Ball (Solvents) is also acknowledged.
- University of KwaZulu Natal and the school of Chemistry and Physics for the opportunity to further my laboratory skills and to broaden my knowledge and also providing such a clean and user friendly environment.
- I would also like to acknowledge the National Research Foundation for their funding, I am grateful.
- My whole family especially my parents for their unfailing support and for believing in me all the time and also for being there for me during the time of need.
- Lastly but not least, I am thankful to my ever-loving, caring, patient and supportive sweetheart, Thabsile Mthembu. Honey, your loving kindness kept me going.

Chapter One

Introduction and literature review of ethylene oligomerization reactions by late transition metal catalysts.

1.1. Background information

Catalysis remains the backbone of the chemical transformation in industrial processes with over 85% of both domestic and industrial products being produced using catalysts.[1] The importance of catalysis is witnessed in energy processing, bulk chemicals, fine chemicals and food processing.[1] One of the major areas where catalysis has played a significant role is in the conversion of olefins to useful products. There exist two different types of catalysis, that is, heterogeneous catalysis and homogeneous catalysis. The latter catalysis is a subset of catalysis and utilizes soluble organometallic compounds as catalysts for various organic transformations.[2] For example, the well-known Shell-Higher Olefin Process using nickel-based catalyst, Albermarle and Chevron Processes with aluminium catalyst, and the Idemitsu Process, which also employs aluminium/zirconium catalysts are counted amongst the most important processes for ethylene oligomerization reactions.[3]

Designing a suitable homogeneous catalysts for a given reaction is a crucial step since catalyst stability, selectivity and activity need to be taken into account and consequently be well balanced.[4] In the field of linear olefin transformation, the synthesis of C_4-C_{20} linear α-olefins in a selective

manner has become an area of immense interest in both the industrial and academic sector owing to their rapidly growing demand in the market.[5] As a result, Brookhart and his co-workers[6] initiation resulted in an increased interest in the development of new late transition metal based complexes for the transformation of α-olefins both in academia and industries.[7] The tolerance of polar monomers displayed by late transition metal catalysts is one of the most vital characteristic which have made them more attractive over early transition metal catalysts and therefore their relevance is also noticed in copolymerization reactions of polar monomers.[8] In addition, they are less oxophillic hence more stable and easier to handle. In contrast, early transition metal catalysts limitations include their sensitivity to impurities in the monomer feed and their oxophillic nature.[8]

The late transition metal catalysts are also suitable candidates for the oligomerization of ethylene reaction. This is because the β-elimination step (Scheme 1.1) is facile for the late transition metals such as Co, Ni, Rh and Pd, as a result these metals preferentially lead to the formation of oligomerization products such as butenes and hexenes.[7] In contrast, chain propagation is favoured for early transition metals (Ti or Cr) and therefore are suitable for the production of polymers.[9]

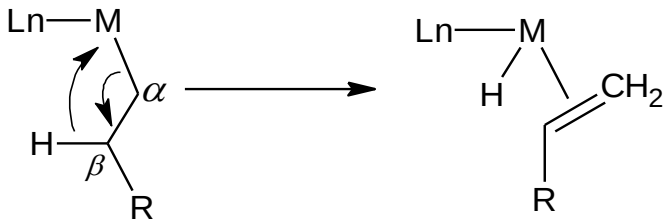

Scheme 1.1 The β-hydride elimination step that leads to chain termination of oligomer or polymer product.

1.2. Mechanism for ethylene oligomerization and polymerization reactions.[7]

The mechanism for ethylene oligomerization and polymerization reactions proceeds *via* three consecutive steps i.e. initiation, propagation and termination steps. During the initiation step, the co-catalyst knock out the halide directly bonded to the metal pre-catalyst (Scheme 1.2, (**A**)) and introduces an alkyl group which results in the formation of a metal to carbon bond which is required for the propagation step. The substrate binding site is then created through the dissociation of the second halide which subsequently forms an active metal complex (**B**). The nucleophilic olefin which is the substrate is then attached to the metal vacant site leading to olefin/alkyl complex (**C**). The subsequent step is propagation and proceeds *via* migratory insertion. The olefin is inserted to the metal-alkyl bond thereby forming an unsaturated metal/alkyl complex with another vacant site where another olefin is introduced and propagated (**D**) until termination step takes place (**E**). This step occurs through a reversible process whereby a β-hydrogen is abstracted as the hydride leading to a formation of an olefin/hydride complex and olefinic product (**F**). Depending on the reaction conditions, the olefinic product can be a polymer or an oligomer. Polymers are formed if the olefin/hydride complex undergoes hydride re-insertion under the condition that the rate of chain re-insertion is greater than the rate of chain termination. On the other hand, the oligomers are produced when the olefin-terminated chain is removed by another olefin and the catalytic cycle repeated again (**G**).

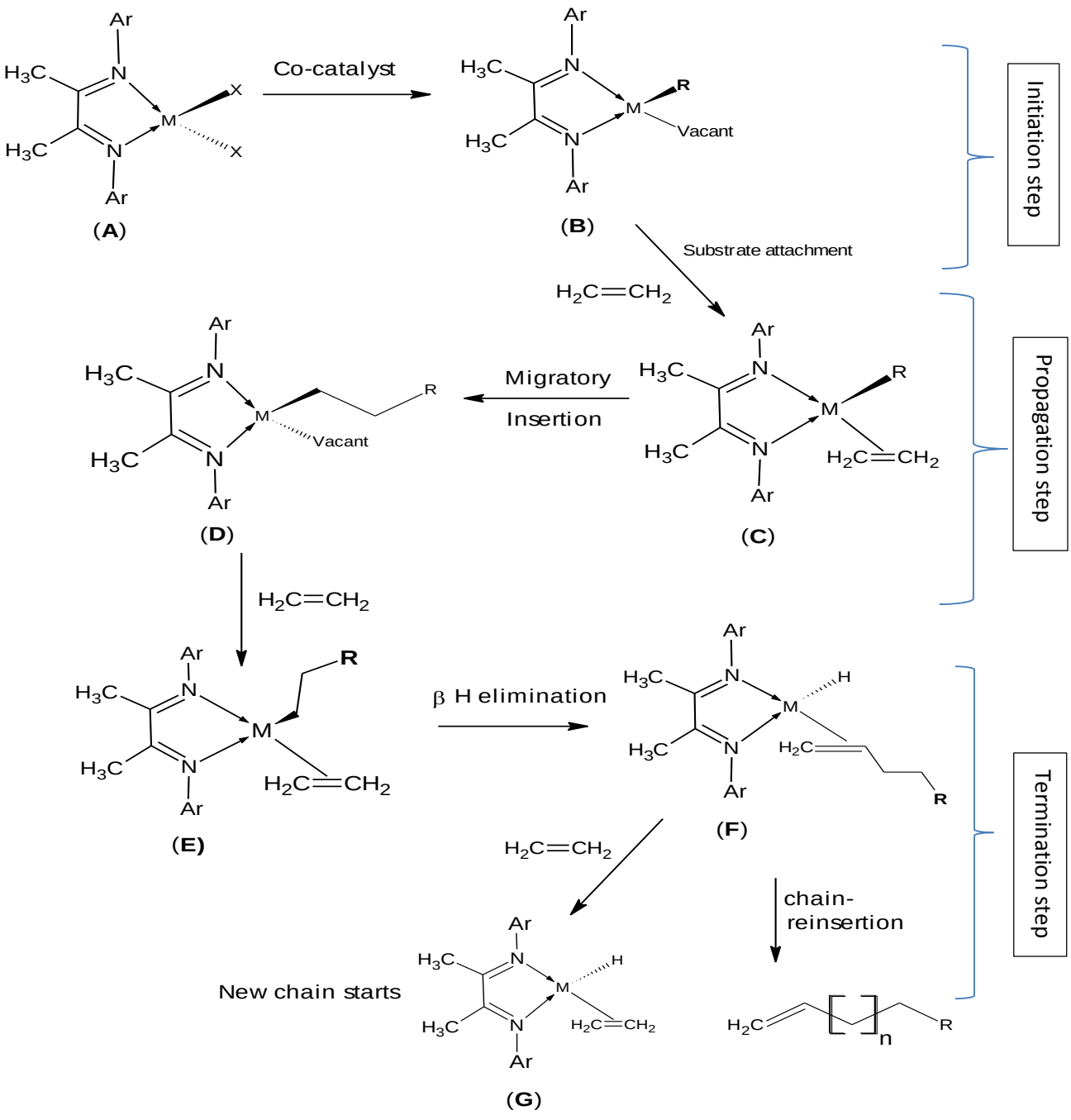

Scheme 1.2 The activation, propagation and termination steps for ethylene oligomerization reaction using late transition based metal catalysts.

1.3. The role of the co-catalyst

The mechanism in Scheme 1.3 shows that organometallic complexes require a co-catalyst which is usually a strong Lewis acid to form a cationic metal centre which is active in ethylene oligomerization reactions (Scheme 1.3).[2]

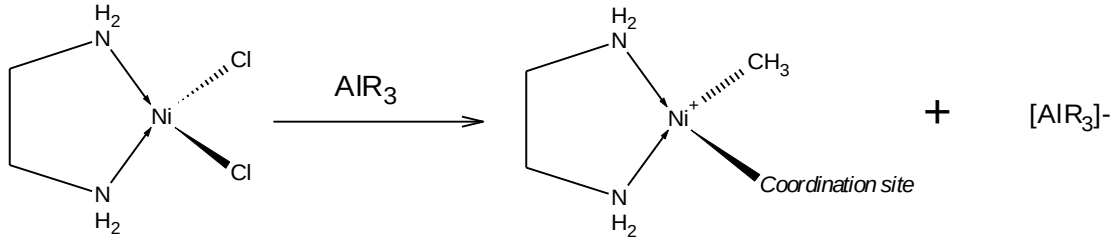

Scheme 1.3 The activation of the nickel(II) complex with the aluminium based co-catalyst.

The activation with aluminium based co-catalyst is a two steps process whereby the complex is first alkylated by the co-catalyst which is then followed by the activation of the neutral metal complex via the formation of a coordination site leading to a cationic metallic centre (Scheme 1.3). The commonly employed Lewis acids in olefin oligomerization activation includes Et_3Al, MAO, MMAO, Et_2AlCl and $EtAlCl_2$.[10-11] It is also noteworthy to mention that for effective activation, favourable co-catalyst to catalyst precursor interactions are vital and also kinetic and thermodynamic need to be taken into considerations. The co-catalyst also forms weakly coordinated anion after activation and forms a vital part of a catalytically active cation-anion pair which may greatly influence the catalytic activity of the metal catalyst and the nature of the products produced.[11] The acidity of the co-catalyst also plays a crucial role in the activation of the pre-catalysts and the effect of the co-catalyst is also witnessed in the resultant catalytic activity and selectivity of the catalysts.[12] For example, the O^N^O system reported by Zhang *et al.*[13] show

moderate catalytic activity when activated with MAO while activation with $EtAlCl_2$ or Et_2AlCl resulted in enhanced catalytic activity of the nickel(II) complexes.

1.4. Properties and applications of linear α-olefins (LAOs)

The ethylene oligomerization process was discovered in 1933.[2] The ethylene oligomers are characterized by their flexibility, durability, chemically resistance and recyclability. The transition metal catalyzed olefin transformation reactions are currently adding value and plays a vital role in the petrochemical fine chemical and pharmaceutical manufacturing.[2] For example, the oligomerization of lighter α-olefins (C_2-C_8) to higher α-olefins (C_{10}-C_{20}) provides feedstocks for the manufacture of fine and bulk chemicals, plastics, adhesives, detergents, plasticisers and pharmaceutical products.[12, 14-18] Figure 1.1, shows the uses of LAOs in bulk chemical production with respect to their market volume.[19]

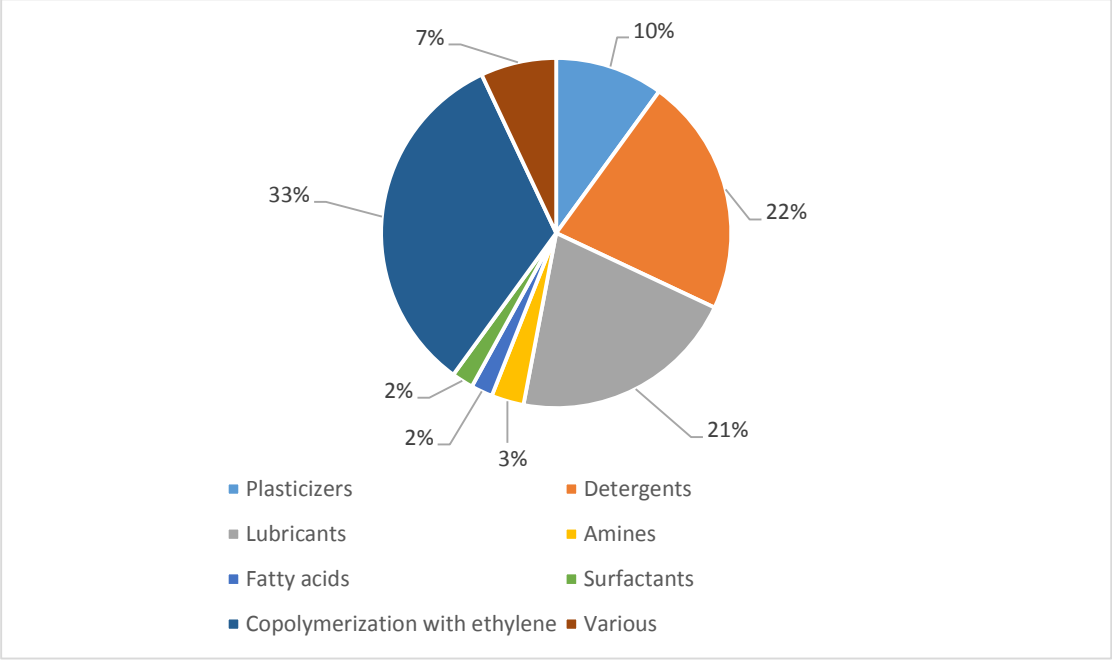

Figure 1.1. Market volume of the products from LAOs in 2004.[19]

LAO's also serve as co-monomers in the production of linear low density polyethylene (LLDPE). It was also estimated in 2004 that a total of 35 million tons of LLDPE/LDPE and 25 million tons of HDPE were consumed world-wide and this consumption was predicted to increase annually by 5% until 2010,[20] signifying the need for large supplies of LAO's. Due to the great demand of LAO's such as 1-hexene and 1-octene, the industrial demand of LAO's have become particularly more attractive and worth time investment and researching.[1]

1.5. Literature reviews of nickel(II) complexes as ethylene oligomerization catalyst.

Nickel(II) based metal catalysts have displayed vital properties in ethylene oligomerization reactions which includes high catalytic activity and thermal stability. Consequently, nickel has receive huge interest in the design and synthesis of new catalysts for the oligomerization reactions of ethylene. This is because nickel favours β-hydride elimination step over chain propagation step which mainly results in oligomerization products.[7] In addition, the phenomenon called "nickel effect" also highlights the oligomerizing character of the nickel catalysts which favours the chain transfer over chain growth.[21] The role of nickel complexes as catalysts has been emphasized by the high industrial demand for linear α-olefin (LAO), particularly in the range C_4-C_{20+}.

The electron-donating abilities of oxygen, nitrogen, and phosphorus in hetero-organic compounds make these compounds good ligands for transition metals. Nevertheless, bidentate and tridentate ligands of the type N^N, N^O, N^P, O^P, P^P, N^N^N, N^N^O, P^N^N or P^O^P have been widely studied.[22] The results obtained from these complexes show that the ligand architecture plays a crucial role in regulating the catalytic activity and selectivity of the respective complexes.

In the following sections we discuss different ligand systems that have been chelated to nickel late transition metal. This subsequent discussion is particularly based on the bidentate (N^O and N^N) and tridentate (N^N^N, N^N^O and O^N^O) donor ligands chelated to nickel(II) late transition metal and then further explores Friedel-Craft alkylation in ethylene oligomerization reactions in broader details.

1.5.1. Nickel(II) complexes chelated by N^O bidentate ligands

The N, O donor ligands are considered as unsymmetrical bidentate ligands and are often called mixed or hybrid ligands.[23] These hetero-functional ligands usually display distinct dynamic features including hemilability,[24] which provides efficient molecular activation procedure under mild conditions. The term "hemilabile" ligand was first introduced by Jeffrey and Rauchfuss[25] and refers to the multi-dentate ligand which contains at least one substitutionally labile donor group. Hemilabile group also plays a crucial role in stabilizing the active cationic species and subsequently the catalyst. Figure 1.2 shows the interesting behaviour in the coordination chemistry of the hemilabile ligand which is initiated by the co-catalyst or the solvent molecule.[26]

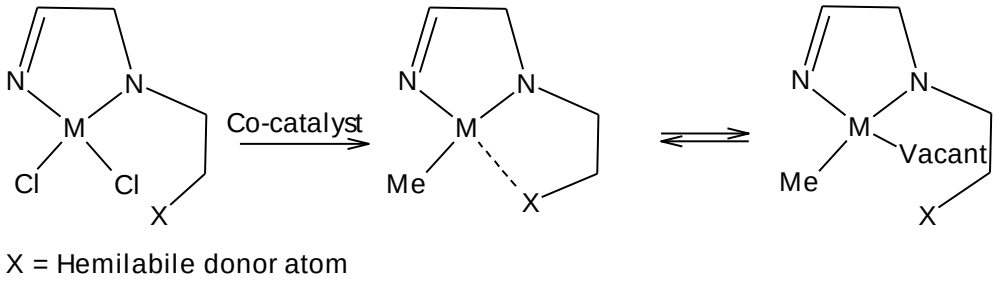

Figure 1.2. The coordination chemistry of the hemilabile catalytic system.[26]

Even though the nickel(II) P^O chelates have been successfully applied in the SHOP, there are reported major drawbacks including low catalytic activity and poor selectivity.[27] The discovery of the N^O chelated complexes was aimed to circumvent major drawbacks associated with P^O chelated systems. In a recent review by Gao *et al*,[28] it was reported that N^O ligated nickel(II) pre-catalysts, such as the salicylaldimito nickel(II) complex have high activity in catalyzing ethylene oligomerization reactions.

The neutral nickel(II) catalysts with N^O-type ligands have been proven to be highly active for the polymerization of ethylene.[21] These includes the nickel(II) complexes explored by the research groups of Grubbs (**1-I**), Mecking (**1-II**) and others with salicylaldimine ligands and Brookhart and co-workers with anilinotropone ligands (**1-III**) and also anilinoperinaphthenone ligands (**1-IV**) shown in Figure 1.3.

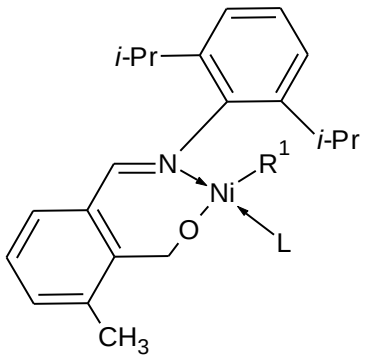

R=I, H, *t*Bu, Ph
R^1 = Me, Ph
X=I, H, OMe, NO_2
L=PPh_3, MeCN

1-I

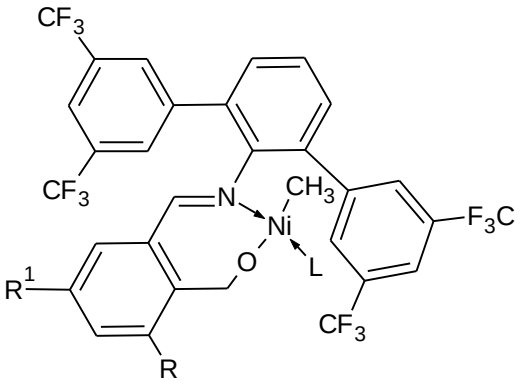

R=I, 9 - anthyl
R^1=I, H
L=Py, TPPTS, TPPDS, H_2N - PEG

1-II

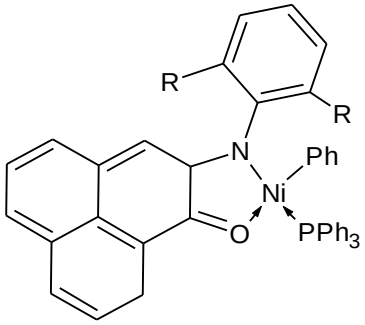

R=Me, *i*Pr

1-III

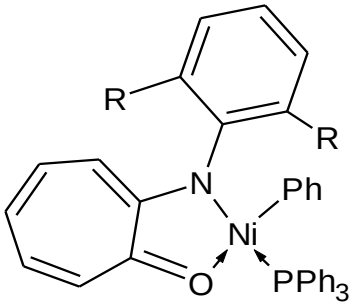

R=Me, iPr, *t*Bu, Ph, F, Br, CF_3

1-IV

Figure 1.3. The previously studied neutral nickel catalysts with N^O-type ligands by Kermagoret *et al.*[21]

Another series of N^O-type ligands was reported by Zhou and his co-workers in 2012.[4] Their ligand systems were based on 4,6-dibenzhydryl-2-[(arylimino)methyl]phenol derivatives (Figure 1.4, **1-V**). Activated with ethylaluminium sesquichloride (EASC), the nickel(II) complexes display good catalytic activities of up to 2.89 x 10^6 g mol^{-1} (Ni) h^{-1} for the dimerization of ethylene. Ligand

back-bone has a profound effect on the resultant catalytic activities of the nickel(II) complexes. As an illustration, the catalytic activities of the nickel(II) complexes were observed to increase on increasing the bulkiness of the *ortho* substituents at the arylimino group which alluded to increased solubility of the nickel(II) complexes.[4] The reaction conditions also have significant effect on the chemo- and regioselectivity toward target olefin products as witnessed by Carlini *et al*.[29] on their *bis*-(salicylaldiminate) nickel(II) complexes.

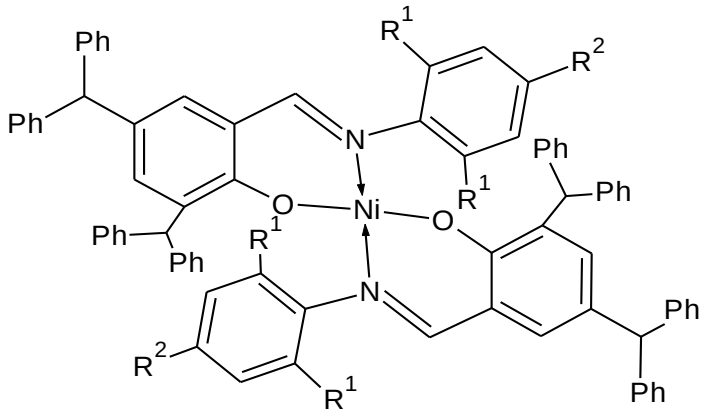

1-V

Figure 1.4. The *bis*-(4,6-dibenzhydryl-2-[(arylimino)methyl]phenoxylate) nickel(II) complex.[4]

1.5.2. N^N bidentate nickel(II) complexes

This class of bidentate nickel(II) complexes have also been extensively studied and have displayed vital properties for ethylene oligomerization reactions such as better catalytic activity, selectivity and thermal stability. The nickel(II) based catalyst developed by Brookhart produces highly branched short-chain polyethylene in the absence of comonomers.[2] These highly active catalysts are supported on N^N α-diimine ligands (Figure 1.5, **1-VI**). Grubbs and co-workers introduced another highly active nickel(II) catalyst anchored by salicylaldehyde ligands.[30] This neutral nickel

catalyst is the modification of the one used in the Shell Higher Olefin Process and polymerizes ethylene to polyethylene. The SHOP utilizes P^O chelates of neutral nickel catalysts.[31] Evidently, these chelating P^O ligands for neutral nickel(II) complexes have been successfully used in the SHOP to produce linear α-olefins but with major drawbacks.[32]

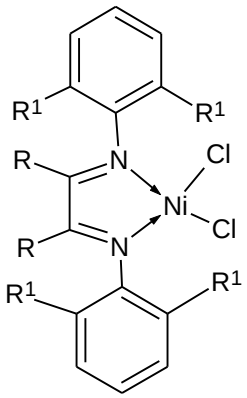

R = Me, H

R^1 = Me, *i*Pr

Y^- = BAr_4^-, SbF_6^-

1-VI

Figure 1.5. The α-di-imine nickel(II) catalyst precursors, developed by Brookhart and co-workers.[2]

In a recent work by Song and his co-workers,[33] they discovered that nickel(II) complexes supported by 8-(1-aryliminoethylidene)quinaldinyl ligands (Figure 1.6. **1-VII**) form active species for ethylene oligomerization upon activation with Et_2AlCl. These nickel(II) complexes display good catalytic activities in the range of 1.24 x 10^6 g mol^{-1} (Ni) h^{-1} - 1.83 x 10^6 g mol^{-1} (Ni) h^{-1} in ethylene oligomerization reactions with high selectivity for C_4 oligomer. The better thermal stability and solubility was an attribute to the more electron-donating group present in the ligand architecture. These properties are advantageous for industrial purposes.

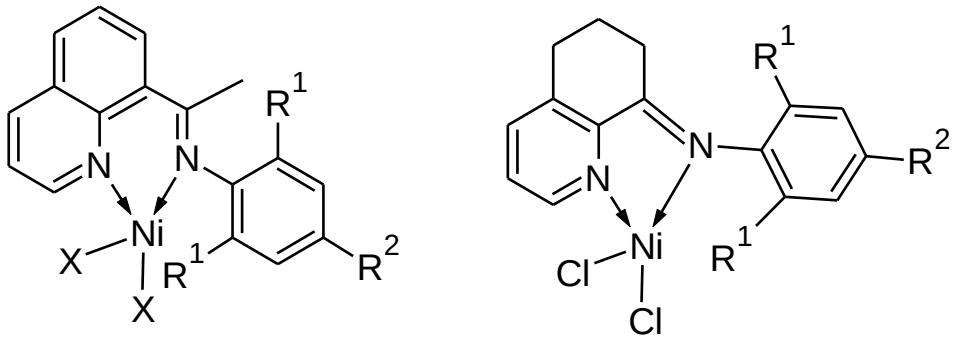

R^1 = Me, Et, *i*Pr; R^2 = Me, H

1-VII **1-VIII**

Figure 1.6. Nickel(II) complexes of 8-(1-aryliminoethylidene)quinaldinyl ligands (**1-VII**) and N-(2-substituted-5,6,7-trihydroquinolin-8-ylidene)arylamino nickel dichlorides (**1-VIII**).

In a subsequent study by Yu *et al.*[34] using N-(2-substituted-5,6,7-trihydroquinolin-8-ylidene)arylamino nickel dichlorides (Figure 1.6. **1-VIII**), they were able to show that N^N bidentate nickel(II) complexes form active catalysts for ethylene dimerization and trimerization reactions. Activities as high as 9.5 x 10^6 g mol^{-1} h^{-1} were achieved upon the activation of the complexes with ethylaluminium sesquichloride ($Et_3Al_2Cl_3$).

Generally, N^N bidentate type nickel(II) complexes have been studied extensively,[35-41] and display advantageous properties including ease in preparation, improved catalytic performances and better thermal stability when used in the synthesis of branched polyethylene of narrow polydispersity.[28] Nevertheless, the majority of ligands reported in literature are α-diimino derivatives and the examples of benzimidazolyl and imino pyridyl nickel(II) complexes are still rare.[42]

The catalytic properties of the resulting complexes are greatly dependent on the back bone and substituents of the ligand, which provides various coordination environments for the metal. To give a supporting example, 2-iminopyridyl nickel(II) complexes (Figure 1.7, **1-IX**) activated with $EtAlCl_2$ forms catalytic active catalysts for the oligomerization and polymerization of ethylene.[43] Higher catalytic activities of 10^7 g mol^{-1} (Ni) h^{-1} magnitude were observed with increased steric hindrance of the substituent, such as having a dibenzhydryl group on the *ortho* position of the phenyl or a dibenzhydryl naphthyl group on the imino nitrogen atom.

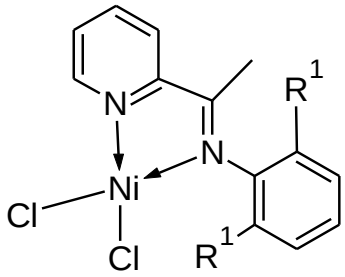

R^1 = Me, Et, *i*Pr

1-IX

Figure 1.7. Nickel(II) complex of 2-iminopyridyl ligands.

Most recently, Nyamato *et al.*[44] reported potential hemilabile N^N-bidentate nickel(II) complexes chelated by (amino) pyridine ligands as nickel(II) catalysts in ethylene oligomerization reactions with intriguing results (Figure 1.8, **1-X**). Activation of the complexes with $EtAlCl_2$ co-catalyst results in more active species than when MAO was used as an activator. This fundamental effect of MAO to form highly active species than $EtAlCl_2$ takes into account the acidity of the co-catalyst and the type of active species formed upon activation.[2] The catalytic activities of the complexes are also affected by the nature of the pendant donor group. For example, replacement of the OCH_3

pendant group (**2**) with NH_2 pendant group (**4**) results in increased catalytic activity from 2 380 kg oligomer mol^{-1}(Ni) h^{-1} to 2 740 kg oligomer mol^{-1}(Ni) h^{-1}. The explanation behind these high and low activities of the complexes relied on the Hard-Soft Acid Base theory. Lower activity was due to the to the incoming ethylene oligomer competing for the vacant site with the oxygen since there is a strong interaction between O and Ni atoms, and this is the rate determining step.

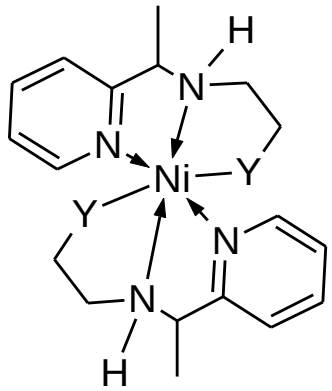

Y = OMe, NEt_2, OH

1-X

Figure 1.8. The nickel(II) complexes supported by (amino)pyridine ligands.[44]

1.5.3. N^N^N tridentate nickel(II) complexes

There exists nickel(II) complexes of tridentate ligands for the oligomerization of ethylene. Incorporation of nickel late transition metal to tridentate ligands have brought about another intriguing results and have developed a great interest in ethylene oligomerization reactions. Brookhart and Gibson independently reported nickel(II) complexes coordinated to 2,6-(bis(arylimino)pyridyl, N^N^N tridentate ligands.[45] These complexes are based on Fe(II) and

Co(II) metal centres. They form active species for the oligomerization and polymerization of ethylene and higher α-olefins upon activation with MAO. In addition, they are highly active than metallocene catalysts and more stable. For example the nickel(II) complexes bearing N-(2-(1H-benzo[d]imidazole-2-yl)quinolone-8-yl)benzamine ligands reported by Wang *et al.*[46] (Figure 1.9, **1-XI**).

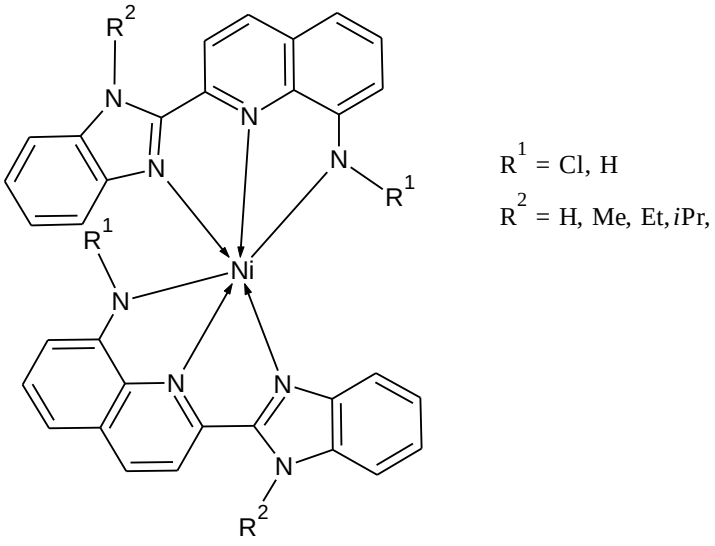

1-XI

Figure 1.9. Nickel(II) catalysts bearing N-(2-(1H-benzo[d]imidazol-2-yl)quinolin-8-yl)benzamine derivatives.[46]

These complexes displayed high activities in the oligomerization of ethylene to give C_4 oligomers as major products. In this work, changing the alkyl substituent of the ligand influences the catalytic activity of the catalyst. For example replacing methyl group with a propyl group increases the catalytic activity of the catalyst from 2.0 x 10^6 g mol^{-1} (Ni) h^{-1} to 5.5 x 10^6 g mol^{-1}(Ni) h^{-1}. In

addition, the complexes bearing R^1 and R^2 as bromide or chloride were observed to have much lower activity.

The ligand framework plays an important role in the resultant catalytic activity, stability and selectivity of the catalyst as also observed by Lee *et al.*[47] in their research work on nickel(II) dibromides complexes supported by tridentate ligands of *bis*-(benzimidazolyl)amine and bis-(benzimidazolyl)pyridine ligands.[47] Their findings show that *bis*-(benzimidazolyl)pyridine nickel(II) complexes (Figure 1.10 **1-XII**) have higher catalytic activities and selectivity towards ethylene dimerization than *bis*-(benzimidazolyl)amine nickel(II) complexes (Figure 1.10 **1-XIII**). In addition, the catalytic activity of the complexes derived from pyridine ranged from 1.662 to 2.803 X 10^6 (oligomer) $(mol\text{-}Ni)^{-1}\ h^{-1}\ bar^{-1}$ whilst the catalytic activity of the complexes derived from methylamine were found within the range of 1.086 to 1.622 X 10^6 (oligomer) $(mol\text{-}Ni)^{-1}\ h^{-1}\ bar^{-1}$. The catalytic activity differences are assigned to the variation of the electronic effect as a result of the differences in the structures of these two sets of complexes. For instance, *bis*-(benzimidazolyl)pyridine ligands results in a more electropositive metal centre as they are electron deficient and favour rapid substrate attachment leading to higher catalytic activities whilst *bis*-(benzimidazolyl)amine ligands are more electron rich and results in a less electropositive metal centre which subsequently reduces the catalytic activity of the nickel(II) catalyst.

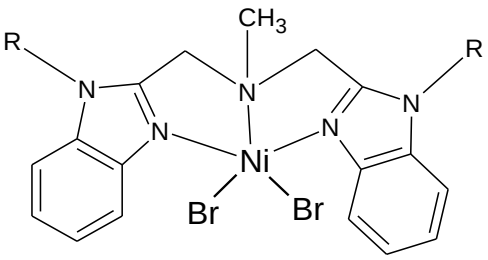

R = H, Me, Bn

1-XII

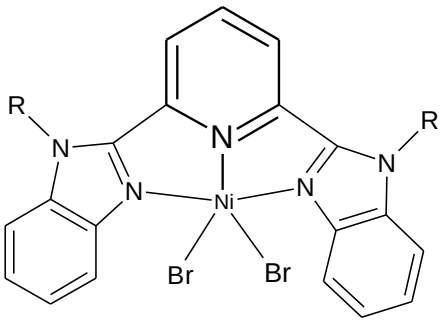

R = H, Me, Bn

1-XIII

Figure 1.10. Nickel(II) dibromide complexes bearing *bis*-(benzimidazolyl)amine (**1-XII**) and *bis*-(benzimidazolyl)pyridine (**1-XIII**) ligands.

The catalytic performance of the complex is also influenced by the nature of the co-catalyst employed. Shi *et al.*[48] used Et_2AlCl, MAO and MMAO to activate nickel complexes bearing 2-(1H-benzimidazol-2-yl)phenoxy ligands. In their studies they found that activation of the complexes by Et_2AlCl with Al/Ni ratio of 100 exhibit substantially high catalytic activities (2.19 x 10^5 g mol^{-1} h^{-1}) for ethylene oligomerization producing C_4-C_6 oligomers as the major products. On the other hand, MAO and MMAO show low catalytic activities toward ethylene oligomerization of 0.20 x 10^5 and 1.19 x 10^5 g mol^{-1} h^{-1} respectively also giving C_4-C_6 olefins as the major products. Further studies by Zhang *et al.*[49] show that higher catalytic activity can be attained by using an auxiliary ligand such as PPh_3. For example, the catalytic activity of 2-(benzimidazole-2-yl)-1,10-phenathrolines nickel(II) complex (Figure 1.11, **1-XIV**) increase from 2.77 x 10^6 g mol^{-1}(Ni) h^{-1} to 3.95 x 10^7 g mol^{-1}(Ni) h^{-1} upon addition of 20 equivalents of PPh_3.

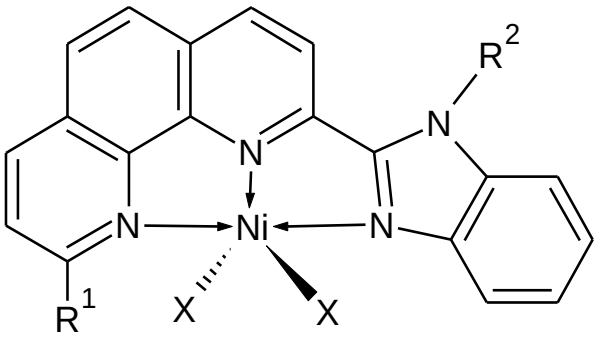

R^1 = H, Me R^2 = H, Me, Et, *i*Pr, Bn

X= Cl, Br

1-XIV

Figure 1.11. Nickel(II) complex bearing 2-(benzimidazole-2-yl)-1,10-phenathroline ligands.

1.5.4. Mixed oxygen^nitrogen tridentate nickel(II) complexes

This class of ligands is composed of oxygen and nitrogen as donor atoms and can either be N^N^O, N^O^O, N^O^N and O^N^O forms. Apart from their differences in the donor atoms arrangements, these ligands share common characteristics since they all form tridentate metal complexes which are characteristically catalytic active and stable. Tridentate nickel(II) complexes bearing mixed oxygen and nitrogen donor atoms have been intensively studied and are of particular interest, but herein we focus on the N^N^O and O^N^O tridentate systems. These nickel(II) complexes usually exhibit distorted octahedral geometry with the nickel(II) metal coordination sphere having two ligand motifs.[50] The nickel(II) metal high electropositivity and coordination number plays a crucial part in the resultant catalytic activities and also geometries of these complexes as not all late transition metals allow octahedral geometry.[50]

Liu *et al.*[15] has reported the oligomerization of ethylene using nickel dihalides bearing 2-benzimidazol-8-ethoxyquinolines ligands (Figure 1.12, **1-XV**). All the nickel(II) complexes show high catalytic activities for the oligomerization of ethylene reactions after they have been activated with Et_2AlCl. The catalytic activities of the nickel(II) bromide pre-catalysts increased with more electron donating capabilities of the alkyl substituent on the N-atom of the imidazole. In contrasts, this property decreased the catalytic activities of the nickel(II) chloride pre-catalysts. In addition, the effect of halides in the catalyst structure is also noted in the product distribution. Nickel(II) chloride catalysts predominantly produce oligomers in the rage C_1-C_6 whilst nickel(II) bromide catalysts solely form oligomers in the rage of C_7-C_{12}. In 2006, Yang and his co-workers also reported another ligand system of the N^N^O tridentate form which successfully oligomerize ethylene to predominantly C_4 and C_6 with also high catalytic activities.[51]

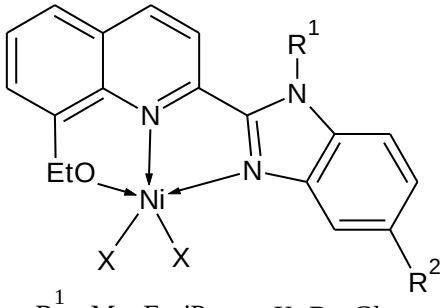

R^1 = Me, Et, *i*Pr X=Br, Cl
R^2 = H, Cl

1-XVI

Figure 1.12. Nickel(II) dihalides bearing 2-benzimidazol-8-ethoxyquinolines.

The mixed oxygen and nitrogen tridentate nickel(II) complexes have been well-researched and Figure 1.13, gives a summary of other previously synthesized nickel(II) complexes that have been applied in the oligomerization reactions of ethylene.

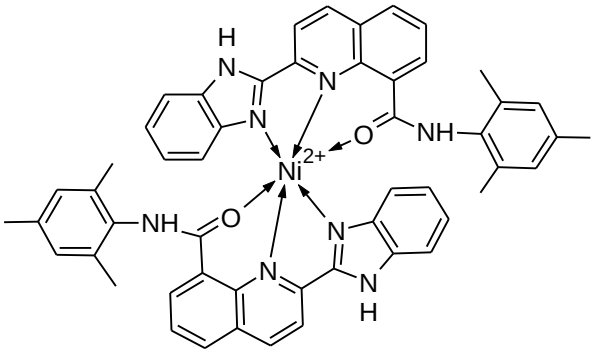

He *et al.*[50]

1-XVII

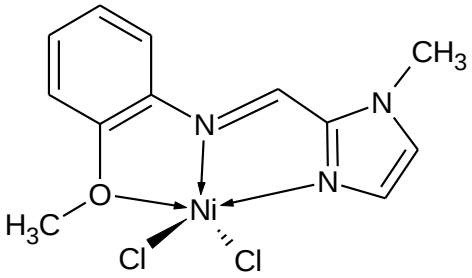

Olivier-Bourbigou *et al.* [52]

1-XVIII

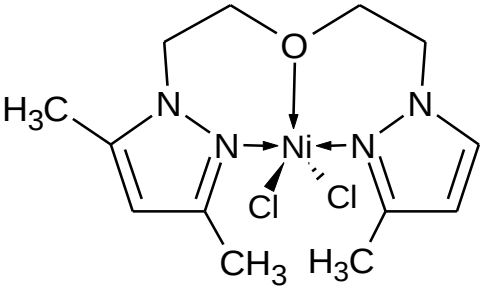

Carpentier *et al.* [53]

1-XIX

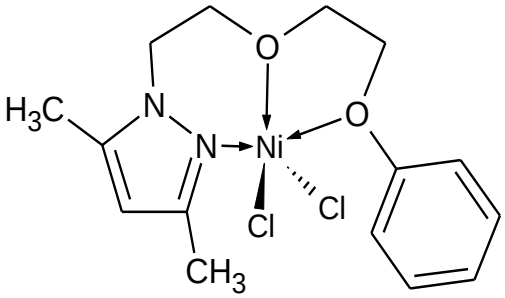

Casagrande *et al.*[54]

1-XX

Figure 1.13. Nickel(II) complexes bearing tridentate ligands used in ethylene oligomerization reactions.

Inspired by pioneering research and remarkable catalytic activities displayed by the tridentate systems of the mixed donor ligands, Zhang *et al*.[13] recently reported nickel(II) complexes chelated by tridentate 2,6-pyridinedicarboxamine ligands (Figure 1.14, **1-XXI**). These nickel(II) complexes show high catalytic activities of up to 7.55 x 10^5 g mol^{-1} (Ni) h^{-1} atm^{-1} upon activation with Et_2AlCl with high selectivity towards the formation of C_4. The substituents in the ligand motif play a crucial role on the resultant catalytic activity and selectivity of the nickel(II) complexes. For instance the complexes bearing chloride and fluoride as alkyl groups show very low catalytic activities with high selectivity for α-C_4 (76 % – 84 %) while complexes bearing H, Me, Et, ^{i}Pr alkyl substituent show high catalytic activities but with somewhat lower selectivity for α-C_4 (67 % – 77 %).

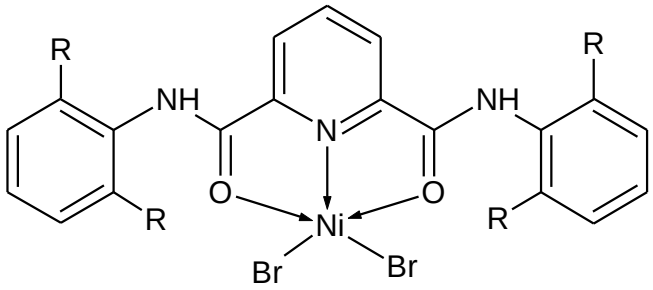

R = H, CH_3, Et, *i*Pr, Cl, F

1-XXI

Figure 1.14. Nickel(II) complexes chelated by 2,6-pyridinedicarboxamide.

1.5.5. Friedel-Craft alkylation in the oligomerization reactions of ethylene

This phenomenon whereby an aromatic solvent is alkylated with the oligomer product or monomer has become common in oligomerization reactions of ethylene.[55] Likewise, Friedel-Craft alkylation depends on the ligand structure, aromatic solvent and co-catalyst employed. For example Dyer *et*

al.[56] using nickel(II) complexes anchored on *N*-phosphinoguanidine ligands showed that activation with $EtAlCl_2$ promotes *in situ* Friedel-Crafts alkylation of toluene solvent by the previously formed oligomers.

In a subsequent work by Ojwach *et al.*[57] they demonstrated that nickel(II) complexes supported on (pyrazo-1-ylmethyl) pyridine ligands (Scheme 1.4) when activated with $EtAlCl_2$ oligomerize ethylene to C_4, C_6 and C_8 which subsequently undergo Friedel-Craft alkylation of the toluene solvent by the pre-formed oligomers. The active species predominantly produce toluene alkylated butenes, hexenes and octenes as major products and no alkylation of ethylene detected. Likewise, the solvent used has a major influence on the oligomeric products and as result when hexane solvent is used, the catalysts produce butenes, hexenes and octenes as major products and only traces of alkylated hexane products are observed but with extremely low catalytic activity. Dyer *et al.*[56] also postulated that Friedel-Crafts alkylation of the aromatic solvent by the olefinic products is a two-steps process whereby the first step involves ethylene oligomerization catalyzed by $Ni/EtAlCl_2$ to give higher olefins. The second step is the alkylation of the aromatic solvent toluene by the olefins obtained in the first step.

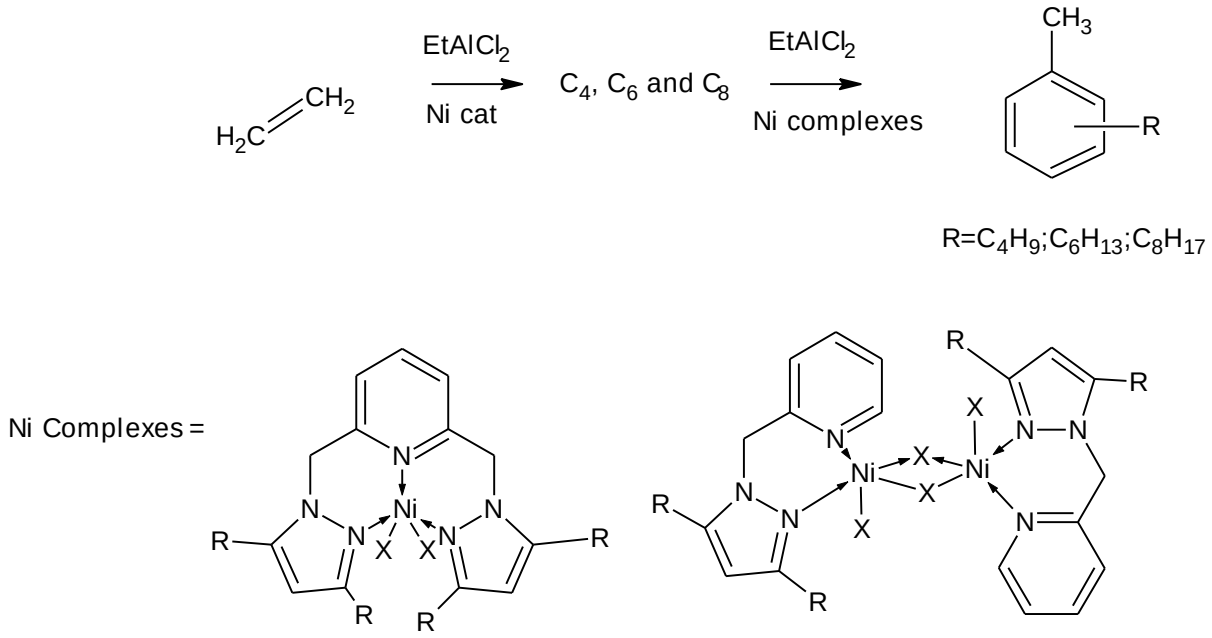

Scheme 1.4. Ethylene oligomerization by (Pyrazo-1-ylmethyl)pyridine nickel(II) complexes and unusual Friedel Crafts alkylation.

Following Ojwach work, Ainooson *et al.*[58] reported late transition metal catalysts anchored on [2-(3,5-dimethyl-pyrazol-1-yl)-ethanol] and [1-(2-chloro-ethyl)-3,5-dimethyl-1H-pyrazole] (Figure 1.15, **1-XXII** and **1-XXIII** respectively). Catalytic activity as high as 4 329 kg mol^{-1}(Ni) h^{-1} were observed upon activation with $EtAlCl_2$. It is noteworthy to mention that nickel(II) catalysts **3** and **7** produced mainly butenes (57 % and 90 % respectively) and hexenes (43 % and 10 % respectively) of which 20 % of the olefinic products produced by catalyst **3** combined undergo Friedel-Crafts alkylation while the oligomers produced by catalyst **7**, all were converted to Friedel-Crafts alkylated-toluene products. The hydroxyl pendant group present in catalyst **3** played a major

role in the observed difference in product distribution. It is believed that catalyst **3** resembles the catalytic performance of N^O type chelates due to the presence of N^OH chelate[59] and the role of the OH pendant functional group in catalyst **3** is to bind to the $EtAlCl_2$ co-catalyst and reduce Friedel-Crafts alkylation of the toluene solvent by the oligomers. In contrast, no such binding of Cl to $EtAlCl_2$ in catalyst **7** can be attained and consequently, higher alkylation of toluene observed.

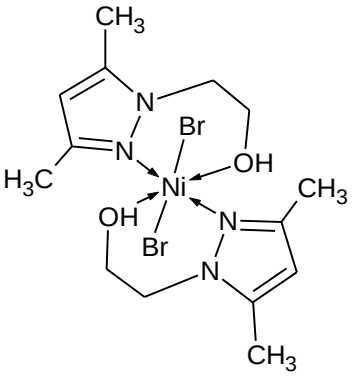

Catalyst = **3**

1-XXII

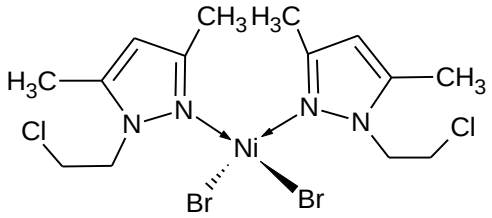

Catalyst = **7**

1-XXIII

Figure 1.15. The nickel(II) complexes anchored by [2-(3,5-dimethyl-pyrazol-1-yl)-ethanol] (**3**) and [1-(2-chloro-ethyl)-3,5-dimethyl-1H-pyrazole] ligands (**7**).

It is apparent that pyrazole based nickel(II) complexes activated with $EtAlCl_2$ co-catalyst in toluene solvent results in the formation of oligomers which then undergo subsequent Friedel-Crafts alkylation of the solvent toluene by the preformed oligomers as also reported by Nyamato *et al.*[60] in their (pyrazolylmethyl)pyridine nickel(II) complexes. In this work, the activation of the complexes with $EtAlCl_2$, in toluene solvent produces Friedel-Crafts toluene-alkylated products while the use of hexane and chlorobenzene solvents produces predominantly C_4 and C_6 oligomers.

Furthermore, activation with MAO in toluene also lead to the production of predominantly C_4, C_6 and C_8 oligomers and no Friedel-Craft alkylation is observed.

1.6. Statement of the problem

Nickel(II) complexes have been widely applied in the transformation of lower olefins to higher olefins. However, most industrial processes still lack selective catalyst systems that can selectively produce the exact desired oligomer or polymer products in ethylene oligomerization reactions. This lack of selectivity in ethylene oligomerization reactions is one of the major problems since separating mixtures of olefins involves high costs and also comes with the inevitable limitations in the atom economy and purity. Consequently, due to the major challenges encountered during catalyst design which includes identification and modification of the factors that influence the catalytic activity and selectivity of the transition metal complexes more research is required to acquire complexes with balanced catalytic activity and selectivity. In addition, striking a balance between the catalyst activity and stability still remains a mystery in ligand design and catalyst development for any given catalytic transformation.

1.7. Justification of the research project

Single-sited catalysts applied in homogeneous catalysis provides routes by which a desired product can be selectively produced and considerably high rates through the modification of the ligand and pre-catalyst structure. Therefore, based on the knowledge that the structure of the catalyst controls the product distribution and properties, these projects seek to investigate the catalytic behaviour of N^N and N^O nickel(II) chelated complexes based on benzimidazolylmethylamine and 2-

(aminomethyl)phenol ligands respectively with respect to their catalytic activity, selectivity and stability. These projects are also aimed to discover a balance between catalysts stability, activity and selectivity through the modification of the electronic and steric properties of the ligands framework and therefore the resultant catalysts.

1.8. Aim of the research project

The overall aim of these projects was to attempt and discover catalytically active and selective catalysts for the oligomerization reactions of ethylene using nickel(II) based complexes anchored by N^N bidentate ligands of benzimidazolylmethylamine and N^O bidentate ligands of 2-(aminomethyl)phenol moieties.

1.9. Objectives of the study

Thus the specific objectives can be formulated as follows:

1. To synthesize and structurally characterize the N^N benzimidazolylmethylamine and N^O 2-[(ethylimino)ethyl]phenol chelating ligands.
2. To synthesize and structurally characterize the nickel(II) complexes of the respective ligands.
3. To examine the behaviour of the nickel(II) complexes in the oligomerization reactions of ethylene.

4. To study the influence of the reaction parameters which includes pressure, temperature, time, co-catalyst/complex ratio, nature of the co-catalyst and solvent on the catalytic performance of the nickel(II) complexes.

1.10. References

1. Kissin, Y. V., *Kirk Othmer Encyclopedia of Chemical Technology.* Wiley & Sons: New York, **2005**; pp 253-260.
2. Piel, C., Kaminsky, W., Kulickle, Ing. W. -M., *Dissertation: Hamburg, Chem.* **2005**.
3. Skupinska, J., *Chem. Rev.* **1991**, *91*, 613-616.
4. Zhou, Z., Hao, X., Redshaw, C., Chen, L., Sun, W-H., *Catal. Sci. Technol.* **2012**, *2*, 1340-1345.
5. Keim, W., *Angew. Chem. Int. Ed.* **2013**, *52*, 12492-12496.
6. Johnson, L. K., Killian, C. M., Brookhart, M., *J. Am. Chem. Soc.* **1997**, *117*, 6414-6415.
7. Speicer, F., Braunstein, P., Saussine, L., *Acc. Chem. Res.* **2005**, *38*, 783-793.
8. Britovsek, G. J. P., Gibson, V. C., Kimberly, B. S., Maddox, P. J., McTavish, S. J., Solan, G. A., White, A. J. P., Williams, D. J., *Chem. Commun.* **1998**, *28*, 849-850.
9. Bianchini, C., Giambastiani, G., Rios, I. G., Mantovani, G., Meli, A., Segarra, M. A., *Coord. Chem. Rev.* **2006**, *250*, 1391-1418.
10. Alt, H. G., Koppl, A., *Chem. Rev.* **2000**, *100*, 1205-1222.
11. Chen, E. Y.-X., Marks, T. J., *Chem. Rev.* **2000**, *100*, 1391-1434.
12. Elowe, P. R., Mc Cann, C., Pringle, P. G., Spitzmesser, S. K., Bercaw, J. E., *Organometallics.* **2006**, *25*, 5255-5260.
13. Zhang, J., Liu, S., Li, A., Ye, H., Li, Z., *New. J. Chem.* **2016**, *40*, 7027-7032.

14. Cotton, F. A., Wilkinson, G., Murillo, C. A., Bochmann, M., Advanced Inorganic Chemistry 6th Ed. John Wiley and Sons: New York, **1999**; p 835.

15. Liu, H., Zhang, L., Chen, L., Redshaw, C., Li, Y., Sun, W. -H., *Dalton Trans.* **2011**, *40*, 2614-2621.

16. Nelana, S. M., Darkwa, J., Guzei, A. L., Mapolie, S. F., *J. Organomet. Chem.* **2004**, *689*, 1835-1842.

17. Wang, S., Sun, W. -H., Redshaw, C., *J. Organomet. Chem.* **2014**, *751*, 714-717.

18. Zhang, M., Zhang, S., Hao, P., Jie, S., Sun, W. -H., Li, P., Lu, X., *Eur. J. Inorg. Chem.* **2007**, 3816-3826.

19. Morgan, D., *PERP report 02/04, Nexant Chem Systems.* **2004**.

20. PlasticEurope Deutschland, W. S. a. M. R., **2004**.

21. Kermagoret, A., Braunstein, P., *Dalton Trans.* **2008**, *4*, 1564-1573.

22. Sun, W.-H., Zhang, D., Zhang, S., Jie, S., Hou, J., *Kinetics and Catalysis.* **2006**, *47*, 278-283.

23. Braunstein, P., Naud, F., *Engew. Chem. Int. Ed.* **2001**, *40*, 680-699.

24. Tribo, R., Munoz, S., Pons, J., Yanez, R., Alvarez-Larena, A., Piniella, J. F., Ros, J., *J. Organomet. Chem.* **2005**, *690*, 4072-4079.

25. Jeffrey, C. J., Rauchfuss, T. B. , *Inorg. Chem.* **1979**, *18*, 2658-2666.

26. Britovsek, G. J. P., Keim, W., Mecking, S., Sainz, D., Wagner, T., *J. Am. Chem. Soc.* **1993**, *23*, 1632-1634.

27. Keim, W., Kowldt, F. H., Goddard, R., Kruger, C., *Angew. Chem. Int. Ed.* **1978**, *17*, 466-469.

28. Gao, R., Sun, W-H., Redshaw, C., *Catal. Sci. Technol.* **2013**, *3*, 1172-1179.

29. Carlini, C., Isola, M., Liuzzo, V., Galletti, A. M. R., Sbrana, G., *Appl. Catal. A: Gen* **2002**, *231*, 307-320.

30. Sinn, H., Kaminsky, W., *Adv. Organomet. Chem.* **1980**, 99-149.

31. Masuda, D. J., Wei, P., Stephan, D. W., *Dalton Trans.* **2003**, *00*, 3500-3505.

32. Sun, W.-H., Li, Z., Hu, H., Wu, B., Yang, H., Zhu, N., Leng, X., Wang, H., *New. J. Chem.* **2002**, *26*, 1474-1478.

33. Song, S., Xiao, T., Liang, T., Wang, F., Redshaw, C., Sun, W-H., *Catal. Sci. Technol.* **2011**, *1*, 69-75.

34. Yu, J., Hu, X., Zeng, Y., Zhang, L., Ni, C., Hao, X., Sun, W-H., *New. J. Chem.* **2011**, *35*, 178-183.

35. Johnson, L. K., Killian, C. M., Brookhart, M., *J. Am. Chem. Soc.* **1995**, *117*, 6414-6425.

36. Killian, C. M., Johnson, L. K., Brookhart, M., *Organometallics.* **1997**, *16*, 2005-2007.

37. Kinnunen, T.-J. J., Haukka, M., Pakkanen, T. A., Pakkanen, T. T., *J. Organomet. Chem.* **2000**, *613*, 257-262.

38. Li, Z., Sun, W.-H., Ma, Z., Hu, Y., Shao, C. , *Chin. Chem. Lett.* **2001**, *12*, 691-692.

39. Shao, C., Sun, W. -H., Li, Z., Hu, Y., Han, L., *Catal. Commun.* **2002**, *3*, 405-411.

40. Spencer, L. P., Altwer, R., Wei, P., Gelmini, L., Gauld, J., Stephan, D. W., *Organometallics.* **2003**, *22*, 3841-3854.

41. Trofymchuk, O. S., Gutsulyak, D. V., Quintero, C., Parvez, M., Daniliuc, C. G., Piers, W. E., Rojas, R. S., *Organometallics.* **2013**, *32*, 7323-7333.

42. Wang, S., Du, S., Zhang, W., Asuha, S., Sun, W.-H., *Chemistry Open.* **2015**, *00*, 1-8.

43. Laine, T. V., Lappalainen, K., Liimatta, J., Aitola, E., Lofgren, B., Leskela, M., *Macromol. Rapid. Commun.* **1999**, *20*, 487-491.

44. Nyamato, G. S., Ojwach, S. O., Akerman, M. P., *Dalton. Trans.* **2016**, *45*, 3507-3416.

45. Small, B. L., Brookhart, M., Bennet, A. M. A., *J. Am. Chem. Soc.* **1998**, *120*, 4049-4079.

46. Wang, K., Shen, M., Sun, W-H., *Dalton Trans.* **2009**, *568*, 4085-4095.

47. Lee, G. M., Appukuttan, V. K., suh, H., Ha, C.-S., Kim, I., *Catal. Lett.* **2011**, *141*, 1608-1615.

48. Shi, Q., Zhang,S., Chang, F., Hao, P., Sun, W. -H., *C. R. Chimie.* **2007**, *10*, 1200-1208.

49. Zhang, C., Sun, W.-H., Wang, Z,-X., *Eur. J. Inorg. Chem.* **2006**, *23*, 4895-4903.

50. He, F., Hao, X., Cao, X., Redshaw, C., Sun, W., *J. Organomet. Chem.* **2012**, *712*, 46-51.

51. Yang, Q. Z., Kermagoret, A., Agostinho, M., Siri, O., Braunstein, P., *Organometallics.* **2006**, *25*, 5518-5526.

52. Boudier, A., Breuil, P. R., Magna, L., Olivier-Bourbigou, H., Braunstein, P., *J. Organomet. Chem.* **2012**, *718*, 31-37.

53. Ajellal, N., Kuhn, M. C. A., Boff, A. D. G., Hoener, M., Thomas, C. M., Carpentier, J.-F., Casagrande Jr., O. L., *Organometallics* **2006**, *25*, 1213-1219.

54. Ulbrich, A. H. P. S., Bergamo, A. L., Casagrande Jr, O. L., *Catal. Commun.* **2011**, *16*, 245-251.

55. Song, K., Gao, H., Liu, F., Pan, J., Guo, L., Zai, S., Wu, Q., *Eur. J. Inorg. Chem.* **2009**, *394*, 3016-3024.

56. Dyer, P. W., Fawcett, J., Hanton, M. J., *Organometallics.* **2008**, *27*, 5082-5087.

57. Ojwach, S. O., Guzei, I. A., Benade, L. L., Mapolie, S. F., Darkwa, J., *Organometallics.* **2009**, *28*, 2127-2133.

58. Ainooson, M. K., Ojwach, S. O., Guzei, I. A., Spencer, L. C., Darkwa, J., *J. Organomet. Chem.* **2011**, *696*, 1528-1535.

59. Keim, W., Lodewick, R., Peiukett, M., Schimtt, G., *J. Mol. Catal.* **1979**, *6*, 79-85.

60. Nyamato, G. S., Ojwach, S. O., Akerman, M. P., *J. Mol. Catal. A: Chem.* **2014**, *394*, 274-282.

Chapter Two

Nickel(II) complexes chelated by N^N benzimidazolylmethylamine ligands: Synthesis, structural characterization and catalytic behavior in ethylene oligomerization reactions.

2.1. Introduction

Nickel(II) based complexes have become a subject of diverse study in the design and development of late transition based homogeneous catalysts for various organic transformations.[1] These catalysts play a very important role in converting olefins to useful industrial and domestic products such as lubricants, surfactants, detergents and polymers. Like other late transition metals, nickel(II) metal displays various vital properties such as less oxophilicity, tolerance of heteroatoms and high co-ordination number. Nickel(II) complexes are applied and used in the Shell Higher Olefin Process (SHOP processes).[2] For example, a highly active nickel(II) catalyst supported by salicylaldimine ligands discovered by R. H. Grubbs was capable of polymerizing ethylene to polyethylene without any use of a co-catalyst. Nickel(II) complexes have been reported to possess good catalytic activity and better thermal stability.[3]

Regardless of the metal used, ligand architecture still plays a very crucial role in controlling the stability, activity and selectivity of the resulting catalysts.[4] On that note, nickel have been incorporated with different N^N, P^O, N^O, P^N and N^N^N ligand designs to attain balanced

nickel(II) complexes in terms of activity, selectivity and stability for ethylene oligomerization reactions. The diversified number of studies have focussed on the N^N bidentate ligands due to their distinctive advantages which includes ease in synthesis and handling, good catalytic activity for ethylene oligomerization reactions and also high thermal stability.[5-7] The N^N ligands based on the benzimidazole moiety have been studied extensively over the past years and have showed a good abilities in converting substrates like ethylene to oligomers and polymers. Nevertheless creating a balance between activity, selectivity and stability of these ligands is still considered a major problem to date. This chapter details the synthesis and characterization of nickel(II) complexes anchored by N^N benzimidazolylmethylamine ligands. Their catalytic performance towards ethylene oligomerization reactions has been also investigated.

2.2. Experimental section

2.2.1. Materials and instrumentation

All the synthetic manipulations were performed using standard Schlenk-line techniques under a nitrogen atmosphere. The solvents obtained from Merck were dried by distillation using appropriate drying agent prior to use. The reagents; 2-chloromethylbenzimidazole (96%), aniline (99.5%) 2-bromoaniline (98%), 2-methoxyaniline (99%), 2-aminophenol (99%), nickel(II) bromide (98%), nickel(II) bromide-1,2-dimethoxyethane complex [$NiBr_2$(DME)] (97%), nickel(II) chloride (98%) and nickel(II) chloride hexahydrates (98%) were obtained from Sigma Aldrich and used as received. The Infrared spectra were recorded from the Perkin Elmer, Spectrum 100 FT-IR spectrometer at the University of KwaZulu-Natal. ^{1}H NMR and $^{13}C\{^{1}H\}$ NMR (100 MHz) spectra were obtained from a 400 MHz proton NMR on a Bruker Ultra shield in $CDCl_3$ and DMSO-d_6 solvent at room temperature using tetramethylsilane (TMS) as a reference compound.

LC Premier micro-mass Spectrometer was used for the mass spectral analyses. The magnetic susceptibilities and magnetic moments of the nickel(II) complexes were determined using Evans balance (Sherwood MK-1). GC analyses were performed on a Varian CP-3800 gas chromatograph fitted with a flame ionisation detector and a 30 m (0.2 mm i.d., 0.25 µm film thickness) CP-Sil 5 CB capillary column while Shimadzu GC-MS QP2010 equipped with a quadrupole mass detector was used for GC-MS analyses.

2.2.2. Synthesis of ligands and nickel(II) complexes

*2.2.2.1. N-(1H-benzimidazol-2-ylmethyl)-2-analine (**L1**)*

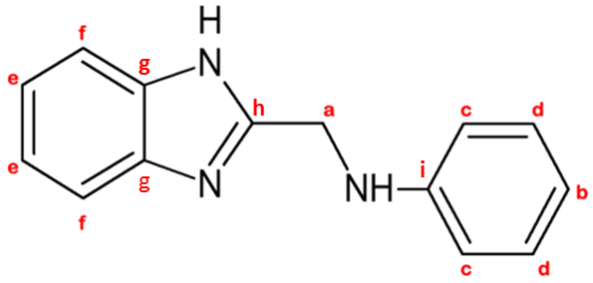

2-(chloromethyl) benzimidazole (1.67 g, 10.00 mmol) was dissolved in absolute ethanol (20 ml) followed by the addition of aniline (0.94 ml, 10.00 mmol) and KI (1.67 g, 10.00 mmol). The reaction mixture was allowed reflux for 6 h with temperature maintained at 80 °C. KOH (0.56 g, 10.00 mmol) was dissolved in water and ethanol mixture (10.00 ml) in a 1:1 ratio and poured to the reaction mixture and the reaction was further refluxed for 2 h. The hot brown solution was then cooled to room temperature, poured into ice/water (30 ml) to form a dark brown precipitate. The precipitate was filtered and re-dissolved in methanol (20 ml) insoluble impurities filtered off and the solvent removed under vacuum. The product was finally allowed to dry at the bench top to afford ligand **L1** as a brown solid. Yield: 0.93g (42%). ^{1}H NMR (400 MHz, $CDCl_3$): δ_H/ppm: 4.65

(s, 2H, H_a); 6.74 (t, 1H, $^3J_{HH}$ = 8.0 Hz, H_b); 6.62 (d, 2H, $^3J_{HH}$ = 8.0 Hz, H_c); 7.15 (t, 2H, $^3J_{HH}$ = 8.0 Hz, H_d); 7.27 (dd, 2H, $^3J_{HH}$ = 8.0 Hz, H_e); 7.55 (dd, 2H, $^3J_{HH}$ = 8.0 Hz, H_f). $^{13}C\{^1H\}$ NMR ($CDCl_3$): δ/ppm: 42.51 (C_a), 113.16 (C_b), 115.18 ($2C_f$), 118.94 (C_c), 123.37 ($2C_e$), 129.46 (C_d), 136.69 ($2C_g$), 146.90 (N=C, C_h), 153.35 (NH-C, C_i). FT-IR (cm^{-1}): $\nu_{(N-H)}$: 3054; $\nu_{(C=N)}$:1675; $\nu_{(Ph)}$: 1602. ESI-MS: *m/z* (%) 224.1185 ($[M + H]^+$, 100%). HRMS (ESI) Calcd for $C_{14}H_{15}N_3$, $[M + H]^+$: 224.1188, found: 224.1185.

*2.2.2.2. N-(1H-benzimidazol-2-ylmethyl)-2-bromoanaline (**L2**)*

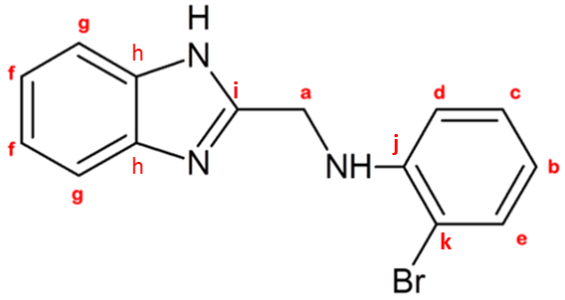

Following the same procedure for **L1** using 2-(chloromethyl) benzimidazole (1.08 g, 6.55 mmol), 2-bromoaniline (1.10 ml. 6.45 mmol) and KI (0.73 ml, 6.45 mmol) in absolute ethanol (50 ml) and KOH (0.37 g, 6.45 mmol) solution. The product was purified by column chromatography using 5:1 ether: hexane solvent system to yield a pale yellow solid. Yield: 1.53 g (79 %). ^1H NMR (400 MHz, DMSO-d_6): δ_H/ppm: 4.77 (s, 2H, H_a); 5.94 (t, 1H, $^3J_{HH}$ = 8.0 Hz, H_b); 6.63 (t, 1H, $^3J_{HH}$ = 8.0 Hz, H_c); 6.67 (d, 1H, $^3J_{HH}$ = 8.0 Hz, H_d); 7.12 (d, 1H, H_e); 7.14 (d, 2H, $^3J_{HH}$ = 8.0 Hz, H_f); 7.49 (d, 2H, $^3J_{HH}$ = 4.0 Hz, H_g). $^{13}C\{^1H\}$ NMR (DMSO-d_6): δ/ppm: 42.23 (C_a), 109.26 (C_k), 112.08 ($2C_g$), 118.31 (C_b), 121.92 ($2C_f$), 129.09 (C_c), 132.74 (C_e), 141.60 ($2C_h$); 145.23 (C_i), 153.34 (C_j) FT-IR (cm^{-1}): $\nu_{(N-H)}$: 3060; $\nu_{(C=N)}$: 1599. ESI-MS: *m/z* (%) 324.0120 ($[M + Na]^+$, 100%).

*2.2.2.3. N-(1H-benzimidazol-2-ylmethyl)-2-methoxyanaline (**L3**)*

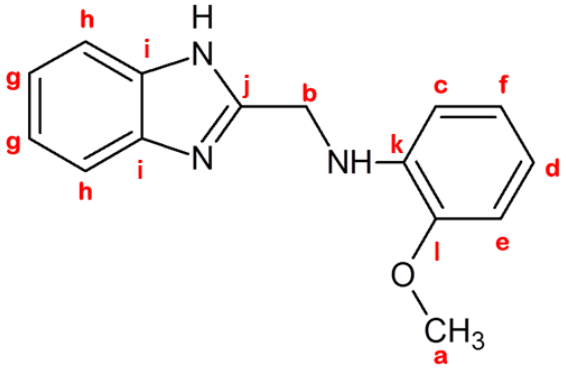

2-(chloromethyl) benzimidazole (3.36 g, 20.00 mmol), 2-methoxyanaline (1.72 ml, 15.00 mmol) and KI (3.34 g, 20.00 mmol) were dissolved in absolute ethanol (50 ml) and refluxed for 6 h at 80 °C. KOH (0.90 g, 16.00 mmol) was dissolved in water and ethanol mixture (1:1) and it was added to the reaction mixture and the reaction was allowed to reflux for further 2 h at the same temperature. The mixture was then cooled to room temperature and transferred into ice/water and filtered off. The dark brown precipitate was then re-dissolved in methanol (50 ml) and filtered off to remove impurities and the solvent removed under vacuum. The dark brown product dried in *vacuo* was obtained at a mass of 4.13 g (97%). ^{1}H NMR (400 MHz, $CDCl_3$): δ_H/ppm: 3.80 (s, 3H, H_a); 4.65 (s, 2H, H_b); 6.53 (d, 1H, $^{3}J_{HH}$ = 8.0 Hz, H_c); 6.76 (dd, 3H, $^{3}J_{HH}$ = 8.0 Hz, H_d, H_e and H_f); 7.25 (dd, 2H, $^{3}J_{HH}$ = 8.0 Hz, H_g); 7.53-7.55 (dd, 2H, $^{3}J_{HH}$ = 8.0 Hz, H_h). $^{13}C\{^{1}H\}$ NMR ($CDCl_3$): δ/ppm: 42.21 (C_b), 55.78 (C_a), 110.00 (C_c), 116.88 ($4C_{deh}$), 121.44 ($3C_{fg}$), 138.08 ($3C_{ki}$), 147.07 (N=C, C_j), 154.06 (C-O, C_l) FT-IR (cm^{-1}): $\nu_{(N-H)}$: 3149; $\nu_{(C=N)}$: 1600. ESI-MS: *m/z* (%) 276.1121 ($[M + Na]^+$, 100 %); 277.1160 ($[M + Na]^+$, 20 %).

*2.2.2.4. N-(1H-benzimidazol-2-ylmethyl)-2-phenolanaline (**L4**)*

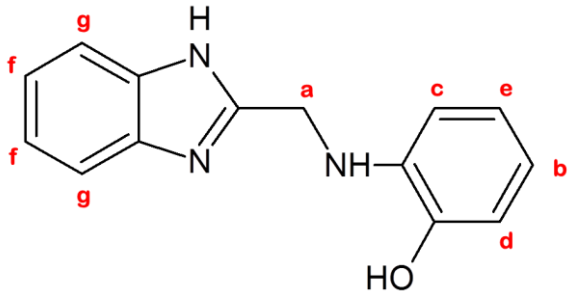

2-chloromethyl benzimidazole (1.69 g, 10.00 mmol) was first dissolved in absolute ethanol (20 ml) followed by the addition of potassium iodide (1.66 g, 10.00 mmol) which resulted in a light yellow to orange solution. 2-aminophenol (1.10 g, 10.00 mmol) was then added to the mixture and a brown to red solution resulted. The mixture was then allowed to reflux for 6 h at 80 °C. KI (0.56 g, 10.00 mmol) was then added which resulted in a dark brown to red solution which was allowed to further reflux for 2 hours. The resultant solution with a precipitate at the bottom was cooled, poured in ice/water. The product was observed sticking at the walls of the beaker. It was then dissolved in methanol, rotary evaporated to remove solvent and dried under vacuum. The product was obtained at a mass of 0.72 g (33%). ^{1}H NMR (400 MHz, DMSO-d_6): δ_H/ppm: 4.45 (d, 2H, H_a); 5.41 (t, 1H, H_b); 6.44 (m, 1H, H_c); 6.60 (t, 1H, H_d); 6.70 (d, 1H, H_e); 7.14 (q, 2H, H_f); 7.51 (s, 2H, H_g). FT-IR (cm^{-1}): $\nu_{(O-H)}$: 3162cm^{-1}; $\nu_{(N-H)}$: 3349 cm^{-1}; $\nu_{(C=N)}$: 1611 cm^{-1}. ESI-MS: *m/z* (%) 240.1133 ([M + H]$^+$, 100 %). HRMS (ESI) for $C_{14}H_{14}N_3O$, [M + H]$^+$: 240.1137, found: 240.1133.

*2.2.2.5. [{N-(1H-benzoimidazol-2-ylmethyl)-2-analine} $NiBr_2$] (**1**)*

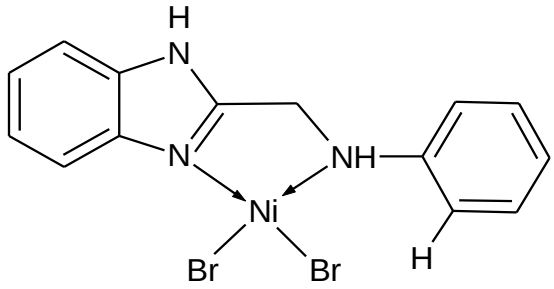

Complex **1** was prepared by adding a solution of $NiBr_2$ (0.10 g, 0.47 mmol) in dichloromethane (5 ml) to a solution of **L1** (0.11 g, 0.47 mmol) in dichloromethane (5 ml). The light brown mixture was then stirred for 24 h at room temperature to give a green precipitate which was filtered off, washed with dichloromethane to afford complex **1** as a green solid. Yield: 0.21 g (89%). FT-IR (cm^{-1}): $\nu_{(N-H)}$: 3328; $\nu_{(C=N)}$: 1622. TOF MS ESI: *m/z* (%), 222.0842 ($[M-NiBr_2]^+$ 100%), 360.1100 ($[M-Br]^+$, 18%), 441.8250 ($[M]^+$, 14%). μ_{obs} = 2.67 BM. Anal. Calcd for $C_{14}H_{14}N_3NiBr_2{\cdot}3CH_2Cl_2$: C 29.27, H 2.89, N 6.04. Found: C 29.53, H 2.70, N 7.59.

Complexes **2**-**6** were prepared following the same procedure adopted for complex **1.**

*2.2.2.6. [{N-(1H-benzoimidazol-2-ylmethyl)-2-bromoanaline} $NiBr_2$] (**2**)*

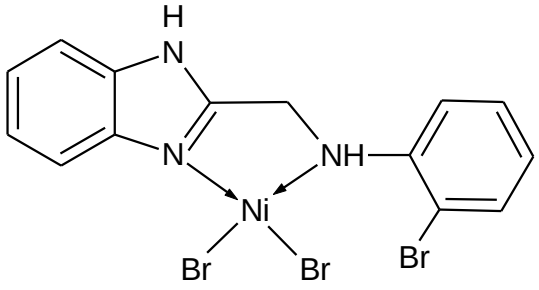

$NiBr_2$ (DME) (0.08 g, 0.26 mmol) was mixed with **L2** (0.08 g, 0.26 mmol) to give a lime solid obtained of complex **2**. Yield: 0.06g (66%). FT-IR (cm^{-1}): $\nu_{(N-H)}$: 3344; $\nu_{(C=N)}$: 1623. TOF MS ESI: *m/z* (%), 520.3353 [M^+, 10%], 302.0250 ([M-$NiBr_2$]$^+$, 100%). μ_{obs} = 3.33 BM. Anal. Calcd for $C_{14}H_{12}N_3NiBr_3 \cdot 10H_2O$: C 24.00, H 4.46, N 6.00. Found: C 24.10, H 2.61, N 6.20.

*2.2.2.7. [{N-(1H-benzoimidazol-2-ylmethyl)-2-methoxyanaline} $NiBr_2$] (**3**)*

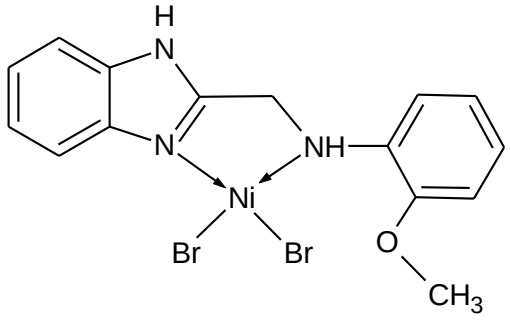

$NiBr_2$ (0.10 g, 0.46 mmol) and **L3** (0.11 g, 0.56 mmol). Light green solid obtained. Yield: 0.15 g (73%). Upon recrystallization from methanol/diethyl-ether solution mixture, **3** rearranged to afford lime crystals suitable for single-crystal X-ray analysis of nickel(II) complex **3a**. FT-IR (cm^{-1}): $\nu_{(N-H)}$: 3348, $\nu_{(C=N)}$: 1622. TOF MS ESI: m/z (%), 391.9781 ([M-Br]$^+$, 50%), 254.1197 ([M-$NiBr_2$]$^+$ 100%). μ_{obs} = 2.60 BM. Anal. Calcd for $C_{15}H_{15}N_3ONiBr_2 \cdot 6H_2O$: C 31.12, H 4.53, N 7.26. Found: C 31.19, H 2.51, N 7.61.

*2.2.2.8. [{N-(1H-benzoimidazol-2-ylmethyl)-2-methoxyanaline} $NiCl_2$] (**4**)*

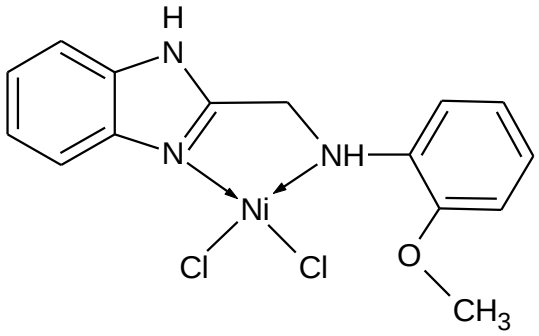

$NiCl_2.6H_2O$ (0.24 g, 1.00 mmol) and **L3** (0.25 g, 1.00 mmol). Yield: 0.11 g (25%). FT-IR (cm^{-1}): $\nu_{(N-H)}$: 3422, $\nu_{(C=N)}$: 1621. TOF MS ESI: *m/z* (%), 434.1031 ($[M + H]^+$, 14%). μ_{obs} = 4.08 BM. Anal. Calcd for $C_{15}H_{15}N_3ONiCl_2$: C 47.00, H 3.90, N 10.97. Found: C 46.74, H 3.50, N 11.15.

*2.2.2.9. [{N-(1H-benzoimidazol-2-ylmethyl)-2-phenolanaline} $NiBr_2$] (**5**)*

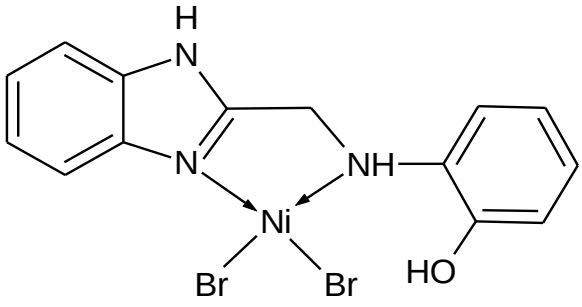

$NiBr_2$ (0.10 g, 0.44 mmol) and **L4** (0.10 g, 0.44 mmol). Yield: 0.15 g (75%). FT-IR (cm^{-1}): $\nu_{(N-H)}$: 3434, $\nu_{(C=N)}$: 1629. TOF MS ESI: *m/z* (%), 376.0251 ($[M - Br]^+$, 9%), 296.0190 ($[M - 2Br]^{2+}$ 100%), 240.1024 ([M - $NiBr_2$], 12%). μ_{obs} = 3.33 BM. Anal. Calcd for $C_{14}H_{13}N_3ONiBr_2 \cdot 1.5CH_2Cl_2$: C 31.81, H 2.76, N 7.18. Found: C 32.26, H 2.71, N 8.10.

*2.2.2.10. [{N-(1H-benzimidazol-2-ylmethyl)-2-phenolanaline} $NiCl_2$] (**6**)*

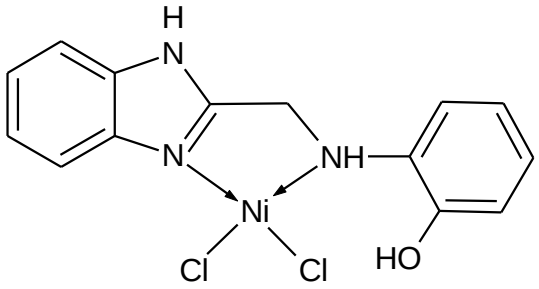

$NiCl_2$ (0.06 g, 0.46 mmol) and **L4** (0.11 g, 0.46 mmol). Light brown product obtained. Yield: 0.11 g (67%). FT-IR (cm^{-1}): $\nu_{(N-H)}$: 3435; $\nu_{(O-H)}$: 3172; $\nu_{(C=N)}$: 1592. TOF MS ESI: *m/z* (%), 296.0204 ($[M - 2Cl]^{2+}$, 100%), 240.1035 ($[M - NiCl_2]$, 13%). μ_{obs} = 3.16 BM. Anal. Calcd for $C_{14}H_{13}N_3ONiCl_2 \cdot 5CH_2Cl_2$: C 28.70, H 3.00, N 7.28. Found: C 29.10, H 4.00, N 7.30.

2.2.3. X-ray crystallography

X-ray crystallographic data collection for compound **3a** was recorded on a Bruker Apex Duo diffractometer equipped with an Oxford Instrument Cryojet operating at 100(2) K and an Incoatec microsource operating at 30 W power. The molecular crystal structure of nickel(II) complex **3** is given in Figure 2.7 but structure refinements data provided since the solution to the crystal structure was not obtained. The data was collected with Mo Kα (λ = 0.71073 Å) radiation at a crystal-to-detector distance of 50 mm. The data collections were performed using omega and phi scans with exposures taken at 30 W X-ray power and 0.50˚ frame width using APEX2.[8] The data was reduced with the program SAINT[8] using outlier rejection, scan speed scaling, as well as standard Lorentz and polarisation correction factors. A SADABS semi-empirical multi-scan absorption correction was also applied to the data. Direct methods, SHELXS-2014[9] and WinGX[10]

were used to solve the structure. All non-hydrogen were located in the difference map and refined anisotropically with SHELXZ-2014.[9] All the hydrogen atoms were included as idealized contributors in the least squares process. Their positions were calculated using a standard riding model with C-$H_{aromatic}$ distances of 0.93 Å and U_{iso} = 1.2 U_{eq} and C-$H_{methylene}$ distances of 0.99 Å and U_{iso} = 1.2 U_{eq} and C-H_{methyl} distances of 0.98 Å and U_{iso} = 1.5 U_{eq}. The amine N-H and hydroxyl O-H hydrogen atoms were located in the difference density map and refined isotropically.

2.2.4. General procedure for ethylene oligomerization reactions

Ethylene oligomerization reactions were performed in a 400 ml stainless steel Parr reactor equipped with a mechanical stirrer, temperature controller and an internal cooling system. The reactor was pre-heated to 100 °C in *vacuo* and then cooled to room temperature. The appropriate amount of the synthesized catalyst precursor (10.0 µmol) was weighed out and transferred into a dry Schlenk tube under nitrogen and toluene (20 ml) was added utilizing a syringe. The required amount of a co-catalyst ($EtAlCl_2$, 1.40 ml, 2.52 mmol) was then injected into the Schlenk tube containing the pre-catalyst to form an active catalyst system. The solution mixture in the Schlenk tube was then transferred through the cannula into the reactor. An additional 60 ml of toluene solvent was also transferred through the cannula into the reactor to give a total of 80 ml. Before the reaction was started, the reactor was flashed three times with ethylene and the appropriate temperature and pressure was set and the reaction (stirring) started. After the reaction time was over, the reactor was cooled to approximately -10 °C using ice and liquid nitrogen and the excess ethylene vented off to facilitate fast cooling through the reduction of pressure. The reaction was then quenched by the addition of 10 % hydrochloric acid (5 ml). A portion of the reaction mixture

was sampled in a GC-vial for GC and GC-MS analyses to determine the product distribution. The mass of the product formed was initially determined using the mass difference of 80 ml toluene solvent (69.90 g) or 80 ml chlorobenzene solvent (88.80 g) and the mass of the final solution after the reaction. In subsequent reactions, the mass of the product formed was determined using the calibration curve of the R-factors for the standards versus number of carbons of the standards (Equations 1 and 2).[11] Hexene (0.849), octene (0.744), decene (0.496), dodecene (0.389) and tetra-decene (0.327) standards were used to obtain calibration curve and n-heptane was used as an internal standard. The R-factor for butene was extrapolated as 0.981 from the calibration curve.

$$RF_A = \frac{P_A}{[A]} \div \frac{P_{IS}}{[IS]} \qquad \textit{Equation} (1)$$

Rearranging to solve for the concentration of the analyte,

$$[A] = \frac{P_A}{P_{IS}} \times \frac{[IS]}{RF_A} \qquad \textit{Equation} (2)$$

RF – Response factor,

P_A – Peak area of the analyte,

P_{IS} – Peak area of the internal standard,

[A] – Concentration of the analyte,

[IS] – Concentration of the internal standard,

2.3. Results and discussion

2.3.1. Syntheses of benzimidazolylmethylamine ligands and their respective nickel(II) complexes

The synthesis of the benzimidazolylmethylamine ligands was carried out by employing the previously described method[12] through the reaction of the 2-chloromethylbenzimidazole and potassium iodide in a 1:1 ratio in absolute ethanol at 80 °C. This was followed by the addition of the appropriate aniline as illustrated in Scheme 2.1. Potassium hydroxide was added to deprotonate the acidic proton which resulted in the formation of a salt. The first step is the nucleophilic substitution whereby the chlorine is replaced with iodine which is a better leaving group and promotes the bond formation between the aniline precursor and 2-iodomethylbenzimidazole after the proton has been removed. All the ligands (**L1**–**L4**) were obtained in moderate to high yields (42% - 87%).

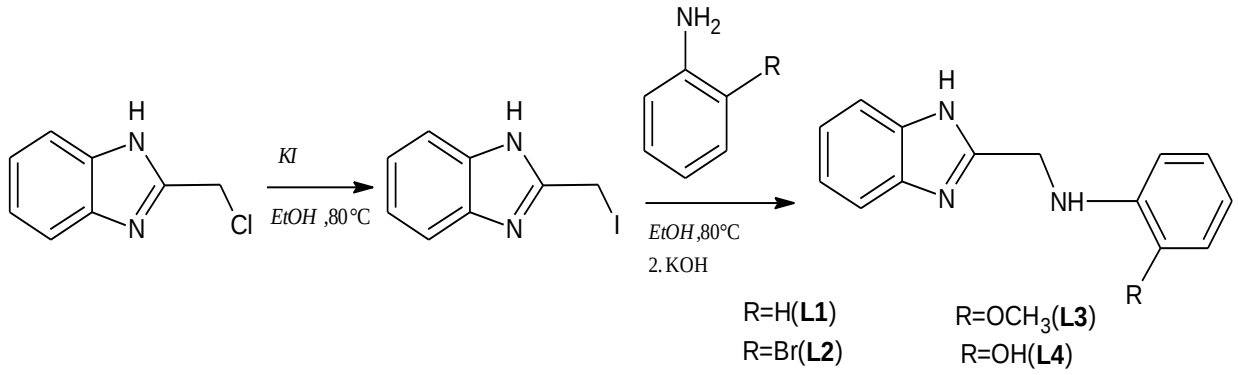

Scheme 2.1: The two-step synthetic protocol of the benzimidazolylmethylamine ligands.

The structural elucidation of ligands **L1**-**L4** was achieved using ^{1}H NMR, ^{13}C{^{1}H} NMR, IR spectroscopies and mass spectrometry. In Figure 2.1 is the ^{1}H NMR spectrum of ligand **L1** which shows a signature peak of the two methylene protons of the linker carbon, N-CH_2, which were

observed as singlet at a chemical shift of 4.71 ppm as previously observed by Attandoh *et al.*[12] The $^{13}C\{^{1}H\}$ NMR spectrum of ligand **L1** was found to be consistent with ^{1}H NMR spectrum. For example, the signal at 42.51 ppm which corresponds to the methylene linker carbon was observed downfield as opposed to aromatic carbons which were found up field between 113 ppm – 154 ppm (Figure 2.2). The peak at 78 ppm is due to the solvent, deuterated chloroform.

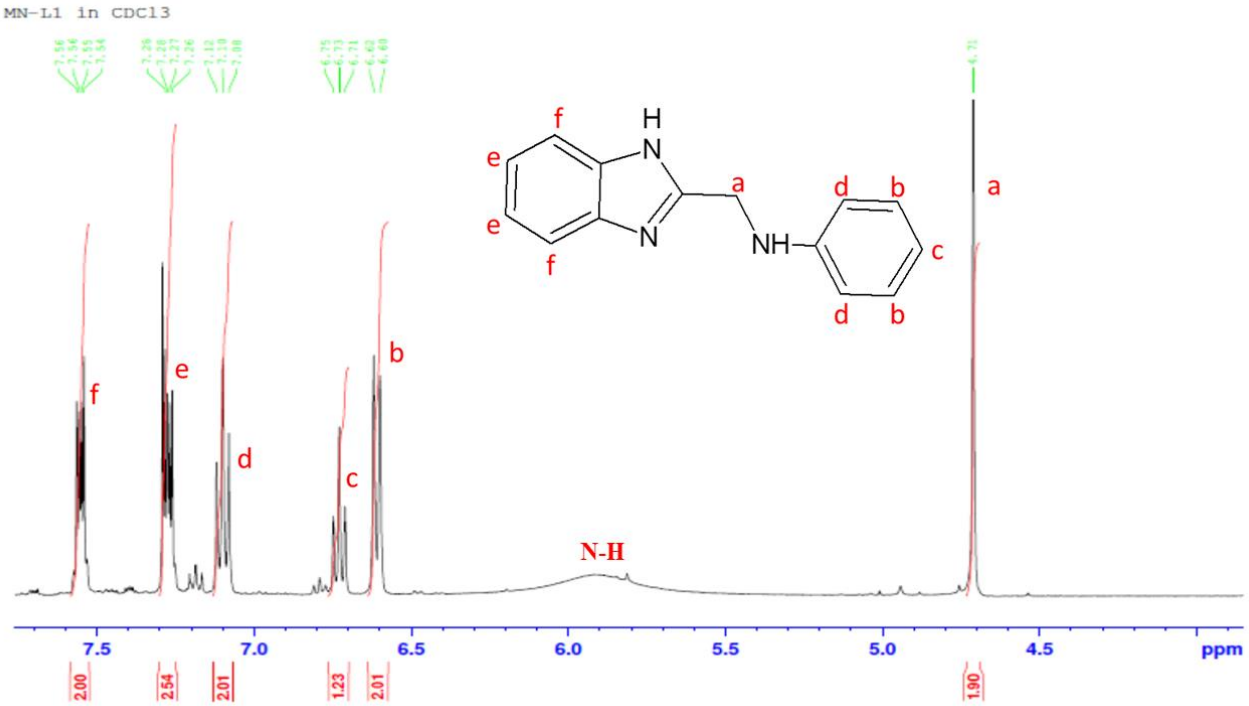

Figure 2.1: ^{1}H NMR spectrum of N-(1H-benzoimidazol-2-ylmethyl)-2-aniline (**L1**) in $CDCl_3$.

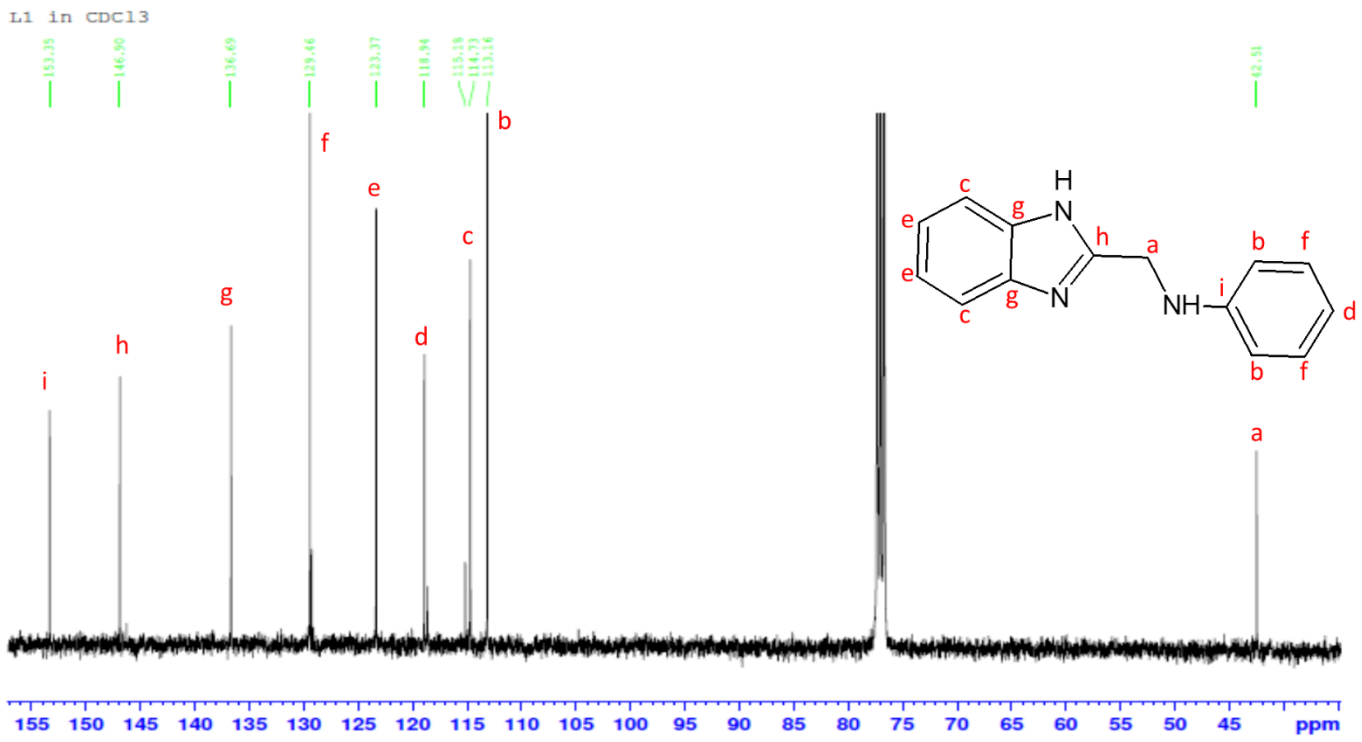

Figure 2.2: $^{13}C\{^{1}H\}$ NMR spectrum of N-(1H-benzoimidazol-2-ylmethyl)-2-aniline (**L1**) in $CDCl_3$.

FT-IR spectroscopy also aided in the determination of the formation of the benzimidazolylmethylamine ligands **L1, L2, L3** and **L4**. The IR spectra of ligands showed absorption bands in the region 3054 - 3358 cm^{-1} (N-H stretching), an attribute to the conversion of the primary amines into secondary amines. The FT-IR spectrum of ligand **L3** (Figure 2.3) shows the broad peak at 3149.45 cm^{-1} which was assigned to the N-H stretching mode. The benzimidazolylmethylamine ligands were further characterized using mass spectrometry as shown in Figure 2.4. The low resolution mass spectrum of **L3** showing $[M + Na]^+$ peak at 276.1021 confirmed the formation of the respective ligand. Similar mass spectra were also achieved for other ligands (**L1**, **L2** and **L4**) revealing a successful synthesis of the benzimidazolylmethylamine ligands.

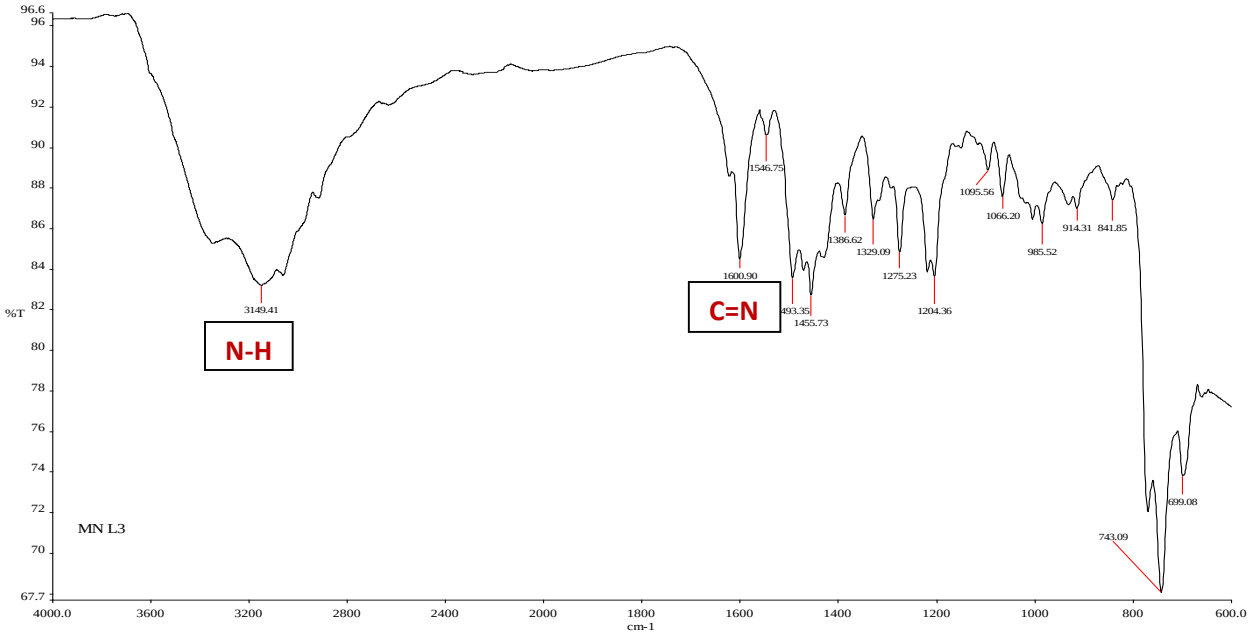

Figure 2.3: FT-IR spectrum of compound **L3** displaying N-H (broad) and C=N (sharp) peaks at 3149.45 cm^{-1} and 1600.93 cm^{-1} respectively.

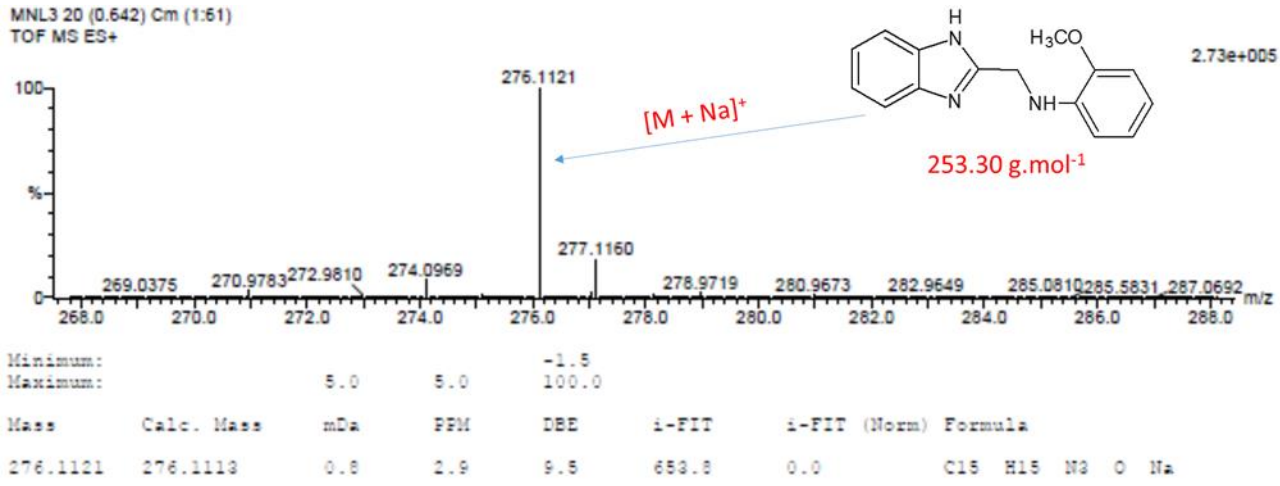

Figure 2.4: The mass spectrum of ligand **L3** showing a molecular ion peak at m/z of 276.1121 amu.

The reactions of the compounds **L1**–**L4** with the equimolar amounts of nickel(II) halides produced the corresponding nickel(II) complexes **1**–**6** in good to high yields (25% - 89%). (Scheme 2.2). Due to the paramagnetic nature of the nickel(II) complexes, the use of NMR spectroscopy was not helpful in their structural determination. The complexes were therefore characterized by mass spectrometry, infrared spectroscopy, magnetic moment measurements and single crystal X-ray crystallography.

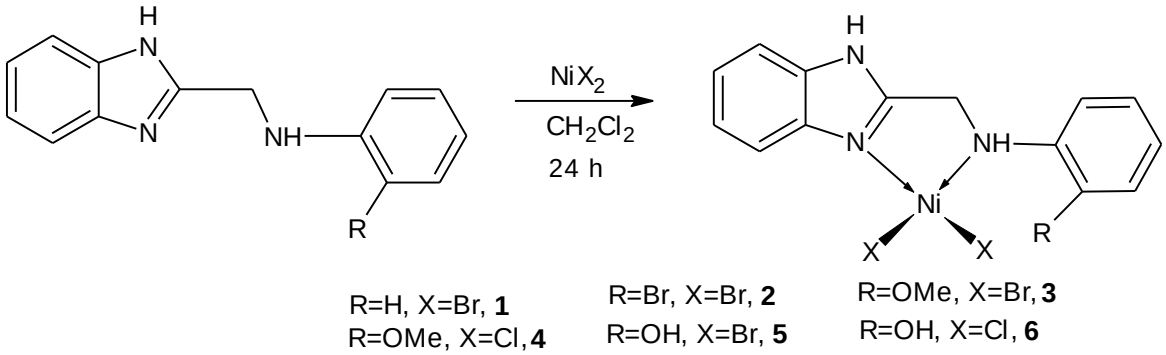

Scheme 2.2: The syntheses of benzimidazolylmethylamine N^N chelated nickel(II) complexes.

Mass spectrometry proved to be useful in confirming the formation and determining the identity of the nickel(II) complexes. In Figure 2.5 is the mass spectrum of complex **1** showing the complex peak at m/z of 441.8240 amu and the loss of the bromide ion to give m/z peak at 359.9186 amu. Another m/z peak at 293.0150 amu corresponds to the loss of the second bromide ion. The peak at m/z of 222.0842 amu corresponds to the ligand molecular ion. Similar fragmentation patterns were also observed for the other nickel(II) complexes **2-6**. The molecular ion peaks corresponding to the molecular weights of the nickel(II) complexes were also observed for complexes **2** ($[M]^+$ = 520.3353 amu) and **4** ($[M]^+$ = 434.1031 amu) in relatively low percentages of 10% and 14% respectively.

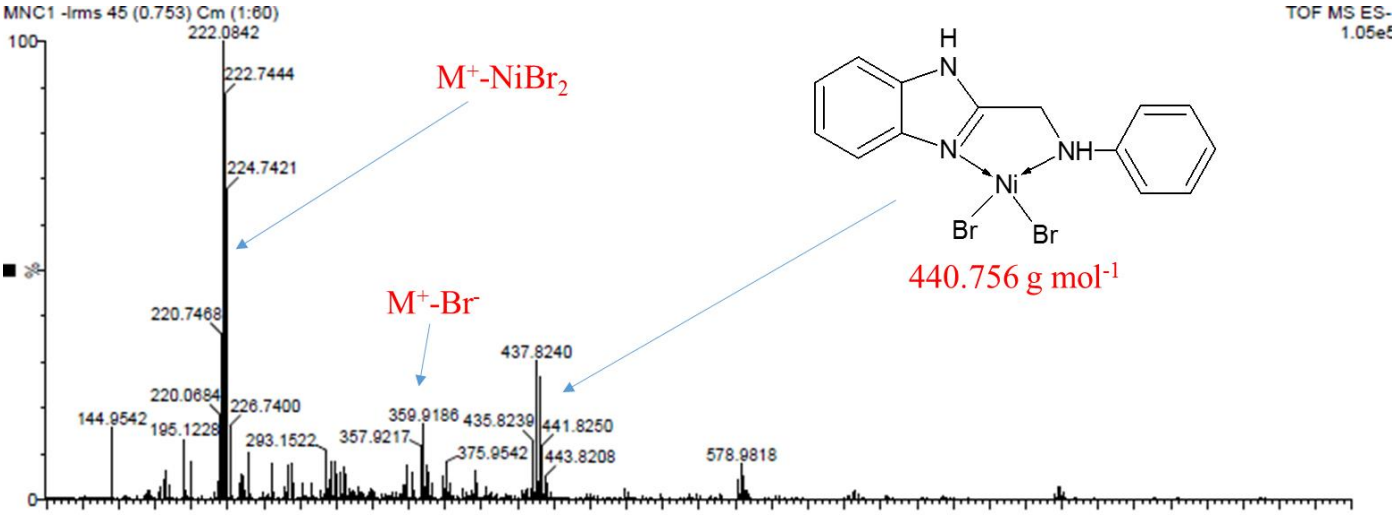

Figure 2.5: The mass spectrum of **1** showing the complex peak at 441.8250 amu and fragmentation of a bromide ion at m/z of 359.9186 amu.

The structural elucidation of the nickel(II) complexes was also accomplished using FT-IR spectroscopy. The peak corresponding to the N-H stretching frequency was observed broad signals in the range 3054 cm^{-1} - 3349 cm^{-1} for the ligands. These peaks were observed to be shifted to a slightly higher frequencies the respective nickel(II) complexes which confirmed the formation of the nickel(II) complexes. The IR spectra of complexes **1-6** showed N-H stretching absorption bands in the region of 3328 cm^{-1} - 3515 cm^{-1} (Table 2.1). An increase in frequency for the N-H band confirmed the coordination of the metal to the ligand. The IR spectra of ligand **L2** and its corresponding complex **2** shown in Figure 2.6 are consistent with this argument.

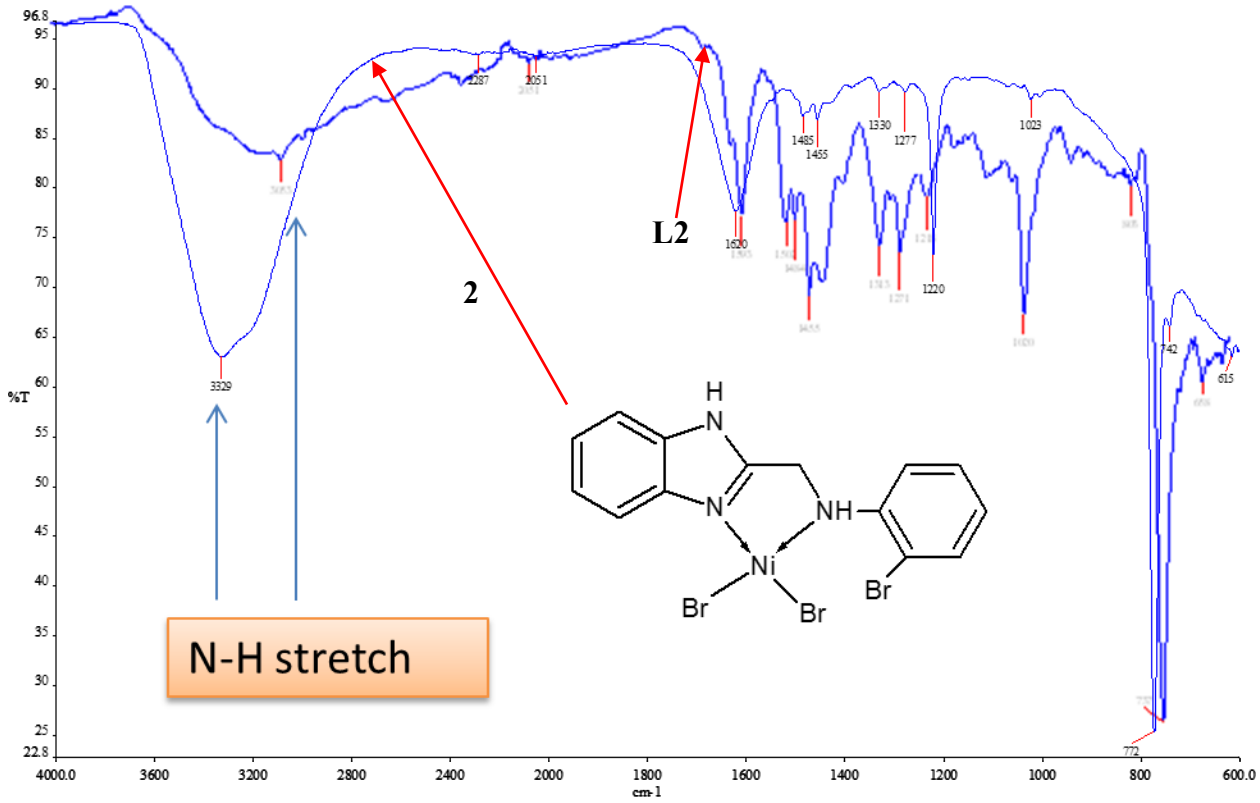

Figure 2.6: The IR spectra of ligand **L2** and its corresponding complex **2** showing N-H peaks at 3060.84 cm^{-1} (broad peak) and 3151.64 cm^{-1} respectively.

The magnetic moments of the complexes **1-6** were found to be within the expected range for high spin nickel(II) complexes which is 2.9 - 4.2 BM[13] even though complexes **1** and **3** showed slightly lower values 2.67 and 2.60 respectively. The magnetic moments for complexes **2** and **4** were found to be 3.33 and 4.08 BM respectively confirming the paramagnetic nature of the nickel(II) complexes and high spin configuration of the nickel(II) metal centre. Table 2.1 gives a summary of the spectroscopic, mass spectral and magnetic measurement data obtained for the nickel(II) complexes **1**–**6**.

Table 2.1. The spectroscopic and physical data obtained for nickel(II) complexes **1-6**.

Complex	FT-IR: ν(N-H) / CM^{-1} (Ligands)	FT-IR: ν(N-H) / CM^{-1}	M/Z (%)	μ_{obs} (BM)
1	3054 **(L1)**	3328	M^+ (14%)	2.67
2	3060 **(L2)**	3344	M^+ (10%)	3.33
3	3149 **(L3)**	3348	M^+-Br^- (50%)	2.60
4	3149 **(L3)**	3422	M^++H^+ (12%)	4.08
5	3049 **(L4)**	3334	M^+-2Br^- (100%)	3.33
6	3049 **(L4)**	3434	M^+-2Cl^- (100%)	3.16

The benzimidazolylmethylamine nickel(II) complexes **1**–**6** were further characterized using elemental analyses to establish the purity and the molecular weight of the complexes. There was a good correlation between the experimentally obtained and calculated elemental analyses data of the proposed structures of **1**–**6** in which the nickel(II) complexes have one ligand unit as shown in Scheme 2.2. However, the nickel(II) complexes obtained were however hygroscopic in nature which affected purity and as a result, correction for solvent was made in order to balance the molecular composition.

In contrast to the elemental analyses data obtained for complex **3**, the crystal structure of complex **3a**, which is a derivative of complex **3,** contains two benzimidazolylmethylamine ligand units of ligand **L3** coordinated to one nickel(II) metal centre (Figure 2.7). This revealed an interesting aspect about the interaction between the benzimidazolylmethylamine ligand **L3** and the nickel(II)

metal centre. Therefore, it could be inferred that a mononuclear complex **3** with one ligand motif upon recrystallization transformed to give a monometallic octahedral complex **3a** with two ligand units of **L3** coordinated to the nickel(II) metal centre. Despite, the unambiguous deduction of the coordination chemistry of complex **3a** (Figure 2.7), the crystal data collected was of low quality for complete refinement. Thus, the bond lengths, bond angles and the geometry could not be fully determined.

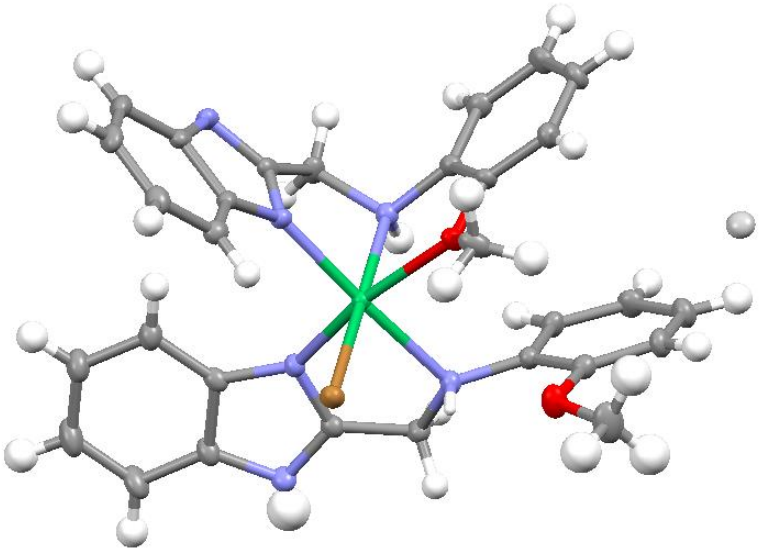

Figure 2.7: Molecular structure of complex **3a** showing the presence of two ligands units in the nickel(II) coordination sphere. Orthorhombic crystal lattice with Z=4, Space Group: $Pca2_1$.

2.3.2. Evaluation of the nickel(II) complexes 1-6 as catalysts for the ethylene oligomerization reactions

The catalytic abilities of complexes **1-6** on ethylene oligomerization reactions were evaluated by first activating the complexes with ethylene aluminium dichloride ($EtAlCl_2$) co-catalyst in toluene and chlorobenzene solvents. The complexes displayed considerably high catalytic activities in all performed reactions to a maximum of 1 254 kg mol^{-1} h^{-1} resulting in the formation of butene and hexene oligomers and alkyl-alkylated toluenes as the main products. In chlorobenzene solvent there was no Friedel-craft alkylated products observed, only oligomers i.e. butenes, hexenes and octenes were produced. The sections that follow gives a detailed analyses of the products identities and provides a discussion regarding the catalysis data obtained.

The nickel(II) complexes **1**–**6** were investigated for their abilities to catalyze ethylene oligomerization reactions using $EtAlCl_2$ as co-catalyst in toluene solvent. All the pre-catalysts **1**–**6** showed significant catalytic activities toward ethylene oligomerization producing butene (C_4), hexene (C_6) and alkylated toluenes (Scheme 2.3). The identities of these products were established by a combination of GC (Figure 2.8) and GC–MS (Figure 2.9). Table 2.2 shows a summary of the data obtained for all the pre-catalysts.

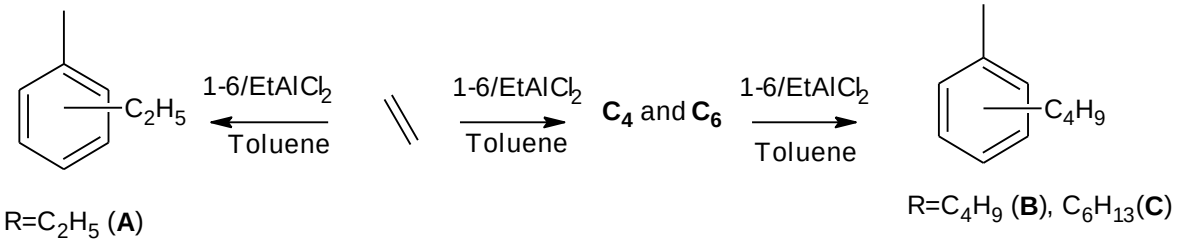

Scheme 2.3: Ethylene oligomerization reactions and unusual Friedel alkylation catalysts.

The results obtained revealed the fact that the pre-formed oligomers underwent *in situ* Friedel-Crafts alkylation of the toluene solvent used. Therefore, the formation of hexyl-alkylated toluene evidently denotes that minimal amounts of hexene oligomers were produced before forming Friedel-crafts alkylated toluene product denoted as **C** in Figure 2.8. Moreover, it is with evident that the complexes selectively oligomerized ethylene to predominantly butene compared to hexene. Since the toluene solvent can be alkylated in the *ortho-*, *para-* and *meta-* position besides the branched products, multiple peaks which are possibly due to isomerism of the *ortho-*, *para-* and *meta-* alkyl toluene products are observed in the GC spectra of the complexes. The presence Friedel-Craft alkylated toluene products has been previously reported by our research group and other researchers.[14-18]

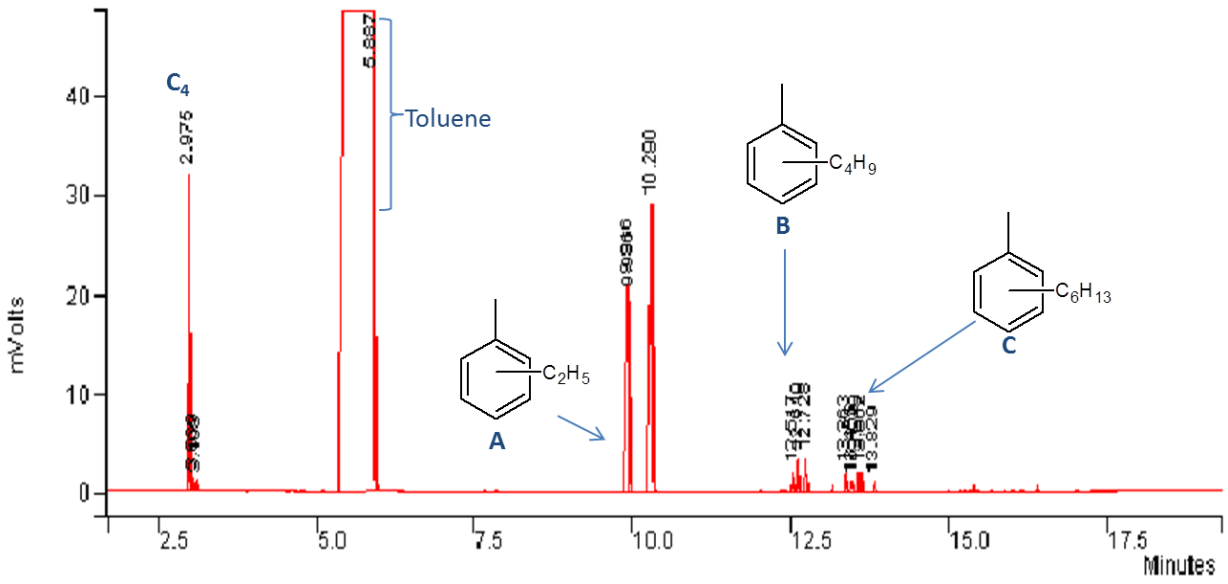

Figure 2.8: A typical gas chromatogram obtained for ethylene oligomerization reaction by complex **3** using $EtAlCl_2$ as co-catalyst in toluene solvent showing the alkylation of the pre-formed oligomers to form alkyl-toluenes.

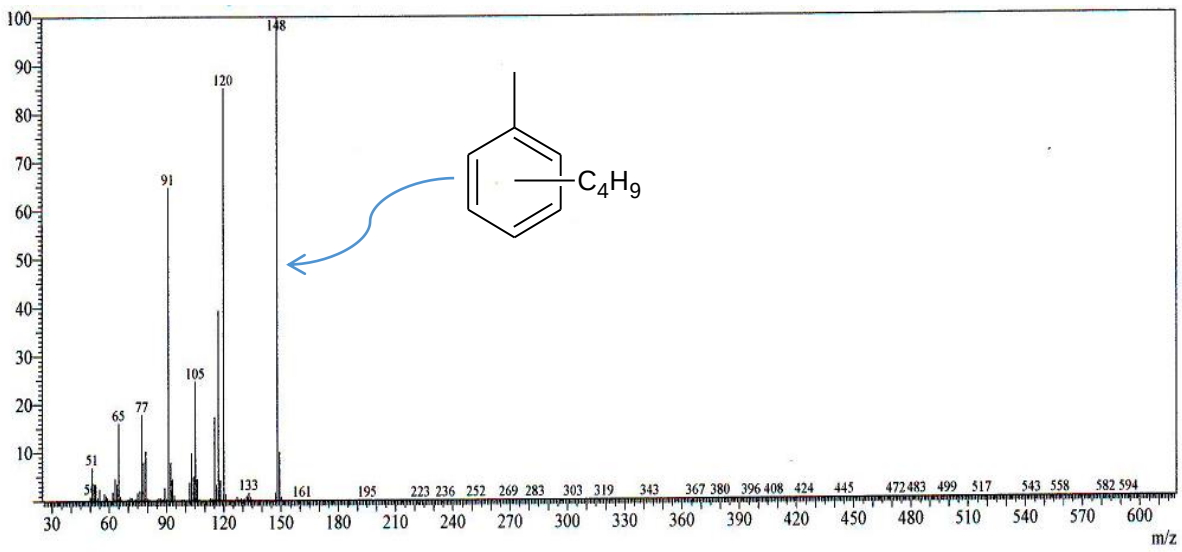

Figure 2.9: The GC-MS of the product obtained when using complex **3**, showing the butyl-alkylated toluene product.

The subsequent Friedel–Crafts alkylation of the toluene solvent by the preformed ethylene oligomers during the oligomerization reactions could be attributed to the pre-catalyst structure and the decrease in the catalytic activities exhibited by catalysts **1-6**. This is in comparison to the previously reported 2-(benzimidazol-2-yl)-1,10-phenanthrolines catalysts which exhibited higher catalytic activities of 2 770 kg mol^{-1}(Ni) h^{-1} without Friedel-Craft alkylation reaction being reported.[19] However, it is noteworthy to point out that while in previous reports all the pre-formed oligomers underwent subsequent Friedel-Crafts alkylation, the present catalysts (**1**–**6**) catalyzed partial alkylation of the toluene solvent in addition to significant amounts of C_4 and C_6 oligomers. Hence, it is apparent that the ligand structure confers some influence on product distribution. It is also apparent that the nature of the co-catalyst, the solvent used and the identity of the catalyst precursor plays a crucial role in the formation of Friedel-Craft alkylated products or oligomers. The formation of C_4 oligomers as the major products when $EtAlCl_2$ in toluene solvent is used to activate the nickel(II) complexes has been widely reported.[20-25]

Table 2.2: The Effect of the catalyst structure on ethylene oligomerization reactions using complexes **1-6** and $EtAlCl_2$ as a co-catalyst in toluene [a]

Entry	Catalyst	T_{min}/T_{min} (°C)[b]	Yield[c] (g)	TON (kg mol^{-1} h^{-1})[d]	Product Distribution (%)[e]			
					C_4	A	B	C
1	**1**	30/34	6.92	692	36	64	-	-
2	**2**	30/32	6.45	645	30	66	4	-
3	**3**	30/36	5.25	525	33	9	24	34
4	**4**	30/40	3.95	395	48	52	-	-
5	**5**	30/38	3.37	337	28	72	-	-
6	**6**	30/41	5.30	530	70	30	-	-

[a] Reaction conditions: [Catalyst]= 10µmol; solvent, toluene, 80 ml; Pressure, 10 Bar; Time, 1h; Al/Ni: 250; Temperature, 30 °C.
[b] Initially the temperature was 30 °C, T_{min} and T_{max}=lowest and highest temperature achieved during the course of the reaction.
[c] Yield as determined by mass difference of 80ml toluene (69.90 g) and the mass of the final solution.
[d] TON, kg oligomer produced per mol. Catalyst per hour.
[e] Determined by Gas Chromatography.

2.3.2.1. The influence of the catalyst structure on ethylene oligomerization reactions

The catalytic reactions investigated revealed a significant effect of complex structure on both the catalytic activities and product distributions observed. The ligand framework had a remarkable effect on the catalytic activities of the nickel(II) complexes. To give an illustration, the substitution of a hydrogen in complex **1** with the hydroxyl (complex **5**) in the phenyl ring was followed by a decrease in catalytic activity from 692 kg mol^{-1} h^{-1} to 337 kg mol^{-1} h^{-1} respectively (Table 2.2, entries 1 and 5). The lower catalytic activity in complex **5** could be assigned to the electron withdrawing destabilization on the phenyl ring due to the hydroxyl group in comparison to the unsubstituted phenyl ring in **1**.[26] This behavior was also reported by Wang *et al.*[27] in their tri-dentate N^N^N catalytic systems where replacing a hydrogen with

the chlorine in the phenyl ring resulted in a decrease in the catalytic activity of the nickel complexes from 6.4 x 10^6 g mol^{-1}(Ni) h^{-1} to 2.7 x 10^6 g mol^{-1}(Ni) h^1.[27] Since oxygen also forms hydrogen bonding, this decrease in catalytic activity might also be due to the coordination behavior of oxygen in forming a hydrogen bond with the nearest halogen which results in the formation of a more stable and less active intermediate. The observed trend of catalytic activity decrease in the order **1> 2> 3> 6> 4>5.** On the other hand, the nickel(II) complexes showed comparable selectivity towards the formation of C_4 and ethylene-alkylated toluene with the exception of **3** which also produced butyl-alkylated and hexyl-alkylated products. Thus, the nature of the ligand motif did have a major influence in product distribution.

The identity of the halides also had noticeable effect on the catalytic behavior of the resultant catalysts. For example, the chloride complex **6** (530 kg mol^{-1} h^{-1}) was found to be more active than its bromide analogue complex **5** (337 kg mol^{-1} h^{-1}), (Table 2.2, entries 6 and 5). This is consistent with observations in literature[15] and has been assigned to electronic and steric factors and also could possibly be due to favorable activation processes by the activator. There was an observed trend in the competition between C_4 and C_2-toluene formation in the product distribution of the complexes. The nickel(II) bromide pre-catalysts preferentially produced C_2-toluene in a higher proportion with the exception of **3**. In contrast, the nickel(II) chloride complexes selectively produced C_4 in higher yields than C_2-toluene alkylated products.

2.3.2.2. Effect of reaction conditions on ethylene oligomerization reactions.

The influence of reaction parameters such as Al/M ratio, time of the reaction, pressure of ethylene and the type of co-catalyst employed on the catalytic abilities of these complexes was accomplished using complex **3** due to its high yield and ease in preparation and the data obtained is given in Table 2.3.

2.3.2.2.1. Effect of Al/Ni ratio on the catalytic behavior of complex 3.

The influence of Al/Ni ratio was investigated by varying the ratio from 200 to 300 using complex **3** (Table 2.3, entries 1, 6 and 7). We observed that variation of Al/Ni ratio greatly influenced the catalytic activity and selectivity of complex **3**. For example, increasing Al/Ni ratio from 200 to 300 was accompanied by a increment in catalytic activity from 387 kg mol^{-1} h^{-1} - 525 kg mol^{-1} h^{-1} and then decreased to 469 kg mol^{-1} h^{-1} with an optimum activity reported at Al/Ni ratio of 250 (Table 2.3, entry 1). This is in accordance with the reports by Shi *et al.*[28] and can be rationalized by stating that as the Al/Ni ratio increases, a maximum catalytic activity is reached beyond which a decline in catalytic activity is observed. Lower catalytic activities at high Al/Ni ratio could be assigned to trialkylaluminium impurities which leads to catalyst deactivation or poisoning.[29] Increasing Al/Ni ratio was also found to affect product distribution of the complexes. For instance, the production of butene was found to decrease from 38% - 21% (Table 2.3, entries 6 and 7) with increased Al/Ni ratio from 200 - 300 whilst the amount of C_6-alkylated toluene increased from 23% - 46%. The proportion of C_2 and C_4 alkylated to toluene remained unchanged.

Table 2.3: The effect of reaction conditions on ethylene oligomerization reactions of nickel(II) complex **3** and $EtAlCl_2$ as a co-catalyst in toluene[a].

Entry	Catalyst	Time (h)	Pressure (Bar)	T_{min}/T_{min} (°C)[b]	Al/Ni	Yield[c] (g)	TON (kg mol^{-1} h^{-1})[d]	Product Distribution (%)[e]				
								C_4	C_6	A	B	C
1	**3**	1	10	30/36	250	5.25	525	33	-	9	24	34
2	**3**	1	20	30/40	250	8.11	811	54	-	16	11	19
3	**3**	1	30	30/45	250	12.54	1 254	70	-	5	7	18
4	**3**	0.5	10	30/35	250	1.59	318	38	-	8	36	18
5	**3**	2	10	30/41	250	9.04	452	29	-	5	18	48
6	**3**	1	10	30/39	200	3.87	387	38	-	4	25	23
7	**3**	1	10	30/42	300	4.69	469	21	-	4	29	46
8[f]	**3**	1	10	30/38	250	2.32	232	95	5	-	-	-
9[f]	**2**	1	10	30/40	250	3.20	320	92	8	-	-	-

[a] Reaction conditions: [Catalyst]= 10 µmol; solvent, toluene, 80 ml; Co-catalyst: $EtAlCl_2$; Temperature, 30 °C.
[b] Initially the temperature was 30 °C, T_{min} and T_{max}=lowest and highest temperature achieved during the course of the reaction.
[c] Determined using the calibration curve of the R-factors versus the number of carbons (Equation 1).
[d] TON, kg oligomer produced per mol catalyst per hour.
[e] Determined by Gas Chromatography.
[f] Using MAO as a co-catalyst.

2.3.2.2.2. Effect of time on the catalytic behavior of the nickel(II) complex 3.

The reaction time was varied from 0.5 h to 2 h in order to investigate the stability of the activated species using complex **3** (Table 2.3, entries 1, 4 and 5). We noted that increasing reaction time from 0.5 h to 1 h was accompanied by an increased in the catalytic activity of **3** from 318 kg mol^{-1} h^{-1} to 525 kg mol^{-1} h^{-1} respectively (Table 2.3, entries 1 and 4), consistent with an induction period between 0.5 to 1 h. The decrease in catalytic activity from 525 kg mol^{-1} h^{-1} to 452 kg mol^{-1} h^{-1} after 2 h (Table 2.3, entry 5) demonstrated catalyst deactivation with

longer reaction times. Nevertheless, the observed increase in product yields with time is an indication of considerable stability of the active species.

The variation of reaction time also had a significant influence on product distribution. It is evident from Table 2.3 that shorter reaction times favor the formation of higher amounts of butyl-toluenes, and in contrast, prolonged reaction times produce more of hexyl-toluenes revealing that the percentage distribution of butene is decreasing with time. To give a supporting example, increasing reaction time from 0.5 h to 2 h led to a decrease of selectivity of butene from 38% - 29% and an increase in hexyl-toluene content from 38% - 48%. In addition, butyl-toluene decreased from 36% - 18% (Table 2.3, entries 4 and 5). The results showed that there is a slight decrease in the production of butenes with time. Yang *et al.*[30] also observed a similar trend. Prolonged time favors chain termination than chain propagation hence more oligomers were produced. In addition, hexyl-toluene proportion also increased with time which implies that reinsertion of butene to produce more C_6 was also favored.

2.3.2.2.3. Effect of ethylene pressure on the catalytic behavior of complex 3

The effect of ethylene pressure was also probed using **3**/$EtAlCl_2$ and the results showed that there is a significant increase in the catalytic activity of **3** with increasing pressure. For example, increasing the ethylene pressure from 10 bar to 20 bar was followed by an increase in the catalytic activity of **3** from 525 kg mol^{-1} h^{-1} to 811 kg mol^{-1} h^{-1} respectively (Table 2.3, entries 1 and 2). This is not a new concept but also have been reported in literature by several workers including Ojwach *et al.*[17] This could be assigned to increased concentration of the ethylene monomer. In addition, ethylene concentration had a significant effect on the

selectivity of the complex. For example, varying ethylene pressure from 10 bar to 30 bar was followed by an increase in the product distribution of butene as shown by increased amounts of C_4 from 33% - 70%. This is consistent with enhanced chain termination due to rapid chain transfer at high ethylene concentration.[17 & 31] The alkylated-toluene oligomers C_6 and C_4 were observed to decrease with increasing pressure.

2.3.2.2.4. Effect of the nature of the co-catalyst on the catalytic behavior of complexes 2 and 3.

The effect of employing different co-catalyst was also investigated using **3**/$EtAlCl_2$ and **3**/MAO systems. Higher and lower catalytic activities of 525 kg mol^{-1} h^{-1} and 232 kg mol^{-1} h^{-1} were observed for **3**/$EtAlCl_2$ and **3**/MAO respectively (Table 2.3, entries 1 and 8). This implies that activation using MAO results in the formation of a less active species compared to $EtAlCl_2$ co-catalyst. In most cases, activation with MAO results in a high catalytically active species for ethylene polymerization.[1] Therefore, the decrease in the catalytic activity observed for complex **3** when activated with MAO could be due to its structure, as it also forms oligomer products and not polymers. In addition, the acidity of the co-catalyst plays a crucial role in the type and formation of the active species.[28] Despite the lower catalytic activities observed, MAO co-catalyst was more selective since it predominantly gave C_4 (95%) and C_6 (5%) oligomers without the formation of Friedel-craft alkylated products. Similar results were observed for complex **2** (Table 2.3, entry 9) which is in accord with the results reported in literature.[28, 30]

2.3.2.3. The effect of the solvent on the catalytic activity and selectivity of complexes 1, 3 and 4.

The effect of solvent on the oligomerization of ethylene was probed using complexes **1**, **3** and **4** in chlorobenzene and toluene solvents using $EtAlCl_2$ co-catalyst (Table 2.4). The solvent played a very important role in the determination of the catalytic activity of the nickel(II) complexes and in the oligomer distribution. The results obtained revealed that the solvent used greatly affects the catalytic activity and selectivity of the catalyst which also have been reported in literature.[17, 32-33]

Table 2.4: The effect of the solvents chlorobenzene and toluene on the catalytic activity and selectivity of the nickel(II) complexes **1**, **3** and **4** [a]

Entry	Catalyst	Yield [d] (g)	Activity (kg mol^{-1} h^{-1})	Product distribution (%) [e]		
				C_4	C_6	FC[f]
1	**1** [b]	6.92	692	36	64	-
2	**1** [c]	4.07	407	87	13	-
3	**3** [b]	5.25	525	33	9	58
4	**3** [c]	5.10	510	66	34	-
5	**4** [b]	3.95	395	48	52	-
6	**4** [c]	5.42	542	25	75	-

[a] Reaction conditions: [M]=10 µmol; Co-catalyst, $EtAlCl_2$; Temperature, 30 °C; Time, 1h; Pressure, 10 bar; Al:M = 250.
[b] Solvent, toluene, 80 ml.
[c] Solvent, chlorobenzene, 80 ml.
[d] Determined using the calibration curve of the r-factors versus the number of carbons.
[e] Determined by GC.
[f] Friedel-Craft alkylated products.

The catalytic activity of **1** drastically decreased from 692 kg mol^{-1} h^{-1} when toluene solvent was used compared to 407 kg mol^{-1} h^{-1} reported in chlorobenzene solvent (Table 2.4 entries 1 and 2). Similar trend was also observed for the other complex **3** with an exception of complex **4** bearing the methoxy phenyl substituent and the chloride halides (Table 2.4, entries 5 and 6). This could be attributed to the slightly poor solubility of the nickel(II) catalysts in chlorobenzene. Most nickel(II) complexes bearing benzimidazole moiety have high solubility in toluene than in chlorobenzene and hexane.[31]

The effect of the solvent on the product distribution is also demonstrated in Tables 2.4. In chlorobenzene solvent, only C_4 and C_6 oligomers were produced and no Friedel-Craft alkylated products were observed. Figure 2.10 shows gas chromatogram of the products obtained using nickel(II) complex **3** revealing the absence of Friedel-Craft alkylated products when ethylene oligomerization reactions were performed in chlorobenzene solvent using $EtAlCl_2$ co-catalyst as opposed to Figure 2.8. High proportions of C_4 were observed for nickel(II) complexes **1** (87%) and **3** (66%) in chlorobenzene (Table 2.4, entries 2 and 4) whilst catalyst **4** produced C_6 in a higher proportion of 75% than C_4 (25%), Table 2.4 entry 6. This could be assigned to the improved solubility of the chloride based complex **4** in chlorobenzene as can be witnessed in its observed high catalytic activity as opposed to bromide based complexes **1** and **3** which showed lower catalytic activities. It can also be inferred that **4** favours chain propagation over chain termination due to the active species formed upon activation. The absence of Friedel-Craft alkylation in chlorobenzene have also been reported by Ojwach *et al.*[18] and Nyamato *et al.*[17]

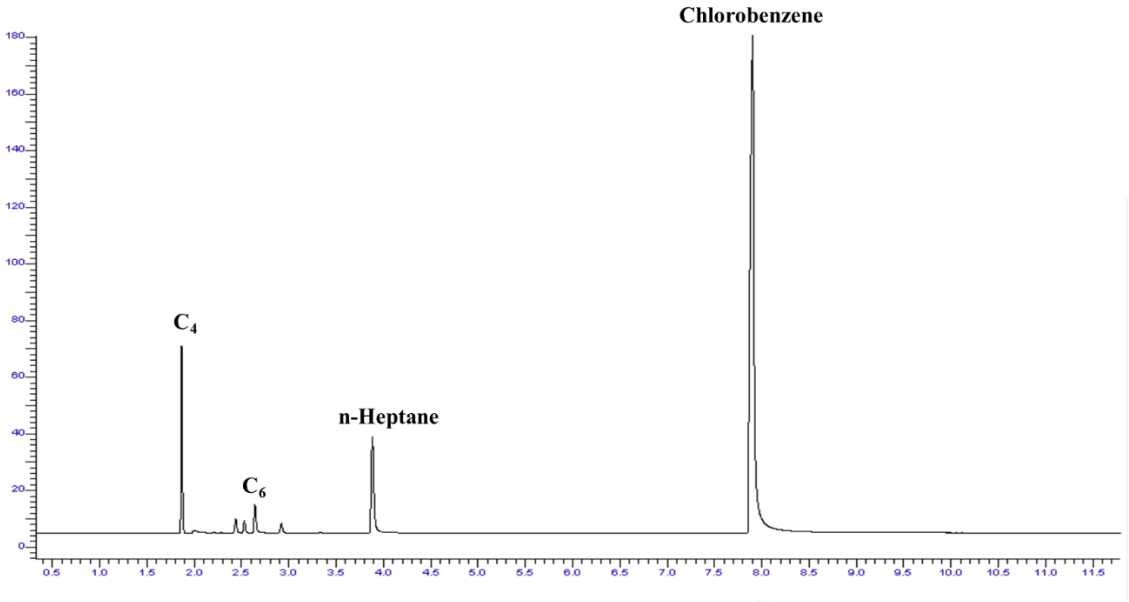

Figure 2.10: Gas chromatogram showing C_4 and C_6 oligomers obtained when complex **3** is activated with $EtAlCl_2$ co-catalyst in chlorobenzene solvent.

2.4. Conclusions

The N^N bidentate ligands based on benzimidazolylmethylamine moiety were successfully prepared and used to synthesize their nickel(II) complexes. The nickel(II) complexes were characterized using mass spectrometry, IR spectroscopy, magnetic moments measurements, elemental analyses and X-ray crystallographic analyses. The nickel complexes were found to be catalytic active toward the oligomerization reaction of ethylene to predominantly butene, hexene and alkylated toluenes as the major products depending on the solvent and co-catalyst used. The catalytic activity and selectivity of the nickel(II) complexes relied extensively on the nature of the ligand backbone and catalytic reaction parameters. The solvent used greatly influenced the catalytic activities and selectivities of the nickel(II) complexes.

2.5. References

1. Piel, C., Kaminsky, W., Kulickle, Ing. W. -M., *Dissertation: Hamburg, Chem.* **2005**.

2. Nodono, M., Novak, B. M., Boyle, P. T., *Polymer.* **2004**, *36*, 140-145.

3. Sun, W.-H., Zhang, D., Zhang, S., Jie, S., Hou, J., *Kinetics and Catalysis.* **2006**, *47*, 278-283.

4. Nyamato George, S., Alam, M. G., Ojwach, S. O., Akerman, M. P., *J. Organomet. Chem.* **2015**, *783*, 64-72.

5. Zhang, D., Nadres, E. T., Brookhart, M., Daugulis, O., *Organometallics.* **2013**, *32*, 5136-5143.

6. Zhang, C., Sun, W.-H., Wang, Z,-X., *Eur. J. Inorg. Chem.* **2006**, *23*, 4895-4900.

7. Trofymchuk, O. S., Gutsulyak, D. V., Quintero, C., Parvez, M., Daniliuc, C. G., Piers, W. E., Rojas, R. S., *Organometallics.* **2013**, *32*, 7323-7333.

8. Bruker, *A.*, *SAINT and SADABS*, Bruker AXS Incl., Madison, Wisconsin, USA. , **2012**.

9. Sheldrick, G. M., *Acta Crystallogr., Sect. A: Found. Crystallogr.* **2007**, *64*, 112-122.

10. Farrugia, L. J., *Appl. Crystallogr.* **2012**, *45*, 849-854.

11. Rome, K., Mclntyre, A., *Chromatography Today.* **2012**, *52*.31-36.

12. Attandoh, N. W., Ojwach, S. O., Munro, O. Q., *Eur. J. Inorg. Chem.* **2014**, 3053-3064.

13. Cotton, F. A., Wilkinson, G., Murillo, C. A., Bochmann, M., Advanced Inorganic Chemistry 6th Ed. John Wiley and Sons: New York, **1999**; p 835.

14. Ainooson, M. K., Ojwach, S. O., Guzei, I. A., Spencer, L. C., Darkwa, J., *J. Organomet. Chem.* **2011**, *696*, 1528-1535.

15. Budhai, A., Omondi, B., Ojwach, S. O., Obuah, C., Osei-Twum, E. Y., Darkwa, J., *Catal. Sci. Technol.* **2013**, *3*, 3130-3135.

16. Dyer, P. W., Fawcett, J., Hanton, M. J., *Organometallics.* **2008**, *27*, 5082-5087.

17. Nyamato, G. S., Ojwach, S. O., Akerman, M. P., *J. Mol. Catal. A: Chem.* **2014**, *394*, 274-282.

18. Ojwach, S. O., Guzei, I. A., Benade, L. L., Mapolie, S. F., Darkwa, J., *Organometallics.* **2009**, *28*, 2127-2133.

19. Shi, Q., Zhang,S., Chang, F., Hao, P., Sun, W. -H., *Comptes Rendus Chimie.* **2007**, *10*, 1200-1208.

20. Boudier, A., Breuil, P. R., Magna, L., Olivier-Bourbigou, H., Braunstein, P., *J. Organomet. Chem.* **2012**, *718*, 31-37.

21. Boudier, A., Breuil, P. R., Magna, L., Olivier-Bourbigou, H., Braunstein, P., *Chem. Commun.* **2014**, *50*, 1398-1407.

22. Hao, P., Zhang, S., Sun, W.-H., Shi, Q., Adewuyi, S., Lu, X., Li, P., *Organometallics.* **2007**, *26*, 2439-2446.

23. Schweinfurth, D., Su, C.,Wei, S., Braustein, P., Sarkar, B., *Dalton Trans.* **2012**, *41*, 12984-12990.

24. Yu, J., Hu, X., Zeng, Y., Zhang, L., Ni, C., Hao, X., Sun, W-H., *New. J. Chem.* **2011**, *35*, 178-183.

25. Schweinfurth, D., Su, C., Wei, S., Braunstein, P., Sarkar, B., *Dalton. Trans.* **2012**, *41*, 12984-12990.

26. Nyamato G. S., O., S. O., Akerman, M. P., *Organometallics.* **2015**, *34*, 5647-5657.

27. Wang, K., Shen, M., Sun, W-H., *Dalton Trans.* **2009**, *568*, 4085-4095.

28. Shi, Q., Zhang,S., Chang, F., Hao, P., Sun, W. -H., *C. R. Chimie.* **2007**, *10*, 1200-1208.

29. Chen, L., Hou, J., Sun, W., *Appl. Catal. A: Gen.* **2003**, *246*, 11-16.

30. Yang, P., Yang, Y., Zhang, C., Yang, X. –J., Hu, H. –M., Gao, Y., Wu, B., *Inorg. Chim. Acta.* **2009**, *362,* 89-96.

31. Liu, H., Zhang, L., Chen, L., Redshaw, C., Li, Y., Sun, W. -H., *Dalton Trans.* **2011**, *40*, 2614-2621.

32. Killian, C. M., Johnson, L. K., Brookhart, M., *Organometallics.* **1997**, *16*, 2005-2007.

33. Obuah, C., Omondi, B., Nozaki, K., Darkwa, J., *J. Mol. Catal. A: Chem.* **2014**, *382*, 31-40.

Chapter Three

Chelated N^O donor nickel(II) complexes of 2-[(ethylimino)ethyl]phenol ligands: Coordination chemistry and catalytic behavior on ethylene oligomerization reactions.

3.1. Introduction

Ethylene oligomerization reactions have become a process of high interest due to the high demand of oligomers.[1] Approximately 10^8 tons of oligomers are consumed each year in South Africa alone. In varying densities, oligomers are commonly used in the production of lubricants, surfactants, detergents and in pharmaceuticals.[2] The shell higher olefin process (SHOP) which employs N^O donor ligands and a nickel metal centre as catalyst is one of the most important industrial process and have paved its way towards the future of ethylene oligomerization reactions.[3, 4-5]

The discovery of highly active nickel(II) catalysts by M. Brookhart and R. H. Grubbs in 1970 have stimulated great interest in the development of highly active and stable catalysts based on nickel(II) late transition metal catalysts for ethylene oligomerization reactions.[6-7] Recent reports have shown that nickel complexes are promising catalysts due to their high catalytic activity and selectivity towards oligomerization of ethylene.[8, 9, 10-11] The major challenges to date in using nickel(II) complexes as catalysts of ethylene oligomerization is in improving and balancing their catalytic activity, stability and selectivity for the formation of α-olefins and controlling the properties of the resulting polymer.[3]

Previous studies have revealed that the ligand framework plays a crucial role in controlling both the electronic and steric properties of the resulting complex.[12-17] Ligands of the type N^N, N^O, N^P, O^P, P^P, N^N^N donor atoms have been intensely studied and the outputs showed that the ligand structure plays a vital role in the resulting activity of the complex.[19] Thus internalization of the bulky groups, variation in the donor atom as well as the addition of the electron donating and withdrawing groups can assist in optimizing the catalytic performances of the complexes. The O^N^N and N^N^N systems have been reported to produce mostly polymers and oligomers that undergo *in-situ* Friedel-Crafts alkylation reaction respectively depending on the co-catalyst and solvent utilized.[18]

Based on the knowledge that the ligand architecture plays a crucial role in the catalytic performance of the resulting pre-catalyst, we therefore aim to use mixed donor atoms in order to achieve a balanced systems i.e. in terms of stability, activity and selectivity; for the ethylene oligomerization reactions. Ligands incorporating mixed donor atoms have been used by various researchers and have shown promising future. For example, the well-known SHOP process utilizes the chelating P^O ligands for neutral nickel(II) catalysts to produce linear α-olefins.

In this chapter the design of O^N mixed donor system is based on 2-[(ethylimino)ethyl]phenol moiety and is expected to give active and stable nickel(II) catalysts since hybrid ligands show distinct dynamic features such as hemilability which provides molecular activation procedure under mild condition and adds extensively in the stability of the resulting complex.[20] This chapter explores the synthesis and characterization of the O^N based nickel(II) complexes. The catalytic behavior of the nickel(II) complexes towards ethylene oligomerization is also discussed in details. In addition to fine-tuning the ligand electronic and steric properties, the

reaction conditions and the co-catalyst employed can also be altered to enhance catalytic selectivity and the activity of the nickel(II) catalysts.[11]

3.2. Experimental section

3.2.1. Materials and methods

All synthetic manipulations were performed using standard Schlenk-line techniques under a nitrogen atmosphere. The solvents obtainable from Merck were dried by distillation using appropriate drying agent prior to use. The reagents; 2'-hydroxy acetophenone (98%), 2-methoxy amine (99%), ethanolamine (99%), *N*,*N*-(diethyl)ethylenediamine (99%), sodium borohydride (98%), nickel(II) bromide (98%), nickel(II) bromide-1,2-dimethoxyethane complex [$NiBr_2$(DME)] (97 %) and nickel(II) chloride (98%) were obtained from Sigma Aldrich and used as received. ^{1}H NMR and ^{13}C{^{1}H} NMR (100 MHz) spectra were obtained from a 400 MHz proton NMR on a Bruker Ultra shield in $CDCl_3$ and DMSO-d_6 solvent at room temperature using tetramethylsilane (TMS) as a reference compound. The infrared spectra were recorded from the Perkin Elmer, Spectrum 100 in the range of 4000 - 650 cm^{-1}. LC Premier micro-mass Spectrometer model LCMS-2020, was used for the mass spectral analyses. Elemental analyses were performed on a Thermal Scientific Flash 2000. The magnetic moments of the complexes were determined using Evans balance (Sherwood MK-1). Varian CP-3800 gas chromatograph equipped with a CP-Sil 5 CB (30 m x 0.2 mm x 0.25 µm) carpillary column was used for GC analyses while GC-MS analyses were performed on a Shimadzu GCMS-QP2010SE.

3.2.2. Preparation of ligands and their respective nickel (II) complexes

3.2.2.1. *Phenol, 2-[1-[(2-methxyethyl) imino] ethyl]* (**L5**)

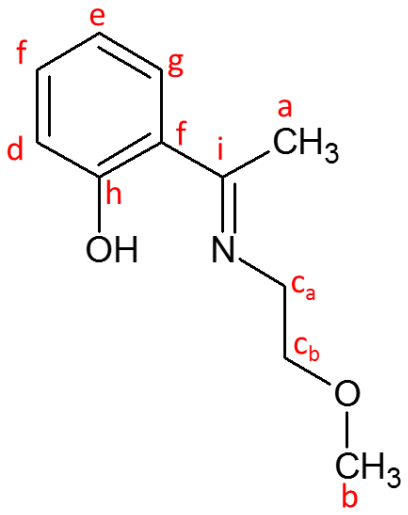

A solution of 2'-hydroxy acetophenone (1.50 g, 11.00 mmol) in ethanol (30 ml) was added 2-methoxyethyl amine (0.83 g, 11.00 mmol). Then a catalytic amount of Para toluene sulfonic acid (5.00 mg) was added resulting in a light green solution which was refluxed for 24 h at 60 °C. After the reaction period, the solvent was removed under vacuum to give **L5** as brown liquid oil. Yield: 2.12 g (87%). ^{1}H NMR (400 MHz, $CDCl_3$): δ_H/ppm: 2.35 (s, 3H, H_a); 3.45 (s, 3H, H_b); 3.74 (t, 4H, $^{3}J_{HH}$ = 4.0 Hz, H_c); 6.80 (d, 1H, $^{3}J_{HH}$ = 8.0 Hz, H_d); 6.94 (dd, 1H, $^{3}J_{HH}$ = 8.0 Hz, H_e); 7.34 (dd, 1H, $^{3}J_{HH}$ = 8.0 Hz, H_f), 7.54 (d, 1H, $^{3}J_{HH}$ = 8.0 Hz, H_g). $^{13}C\{^{1}H\}$ NMR ($CDCl_3$): δ/ppm: 14.61 (C_a), 49.18 (C_b), 50.18 (C_{ca}), 72.09 (C_{cb}), 116.98 (C_d), 128.05 (C_e), 132.52 ($C_{f\&g}$), 164.05 (C_h), 172.53 (C_i). FT-IR (cm^{-1}): $\nu_{(O-H)}$: 3059; $\nu_{(C=N)}$:1615. TOF MS ESI: m/z (%), 216.0995 ($[M + Na]^+$, 100%). HRMS (ESI) for $C_{11}H_{15}NO_2$, $[M^+]$: 194.1181, found: 194.1187.

3.2.2.2. *Phenol, 2-[1-[(2-hydroxyethyl) imino] ethyl]* (**L6**)

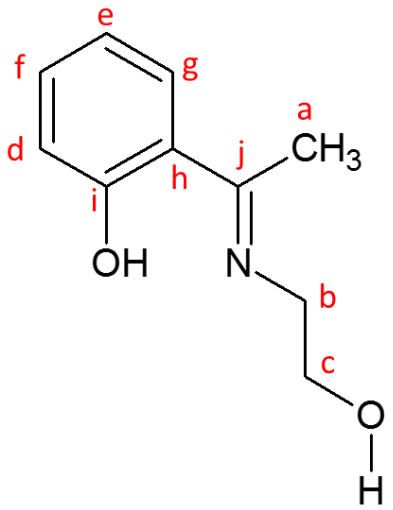

Following the same procedure for **L5**, equimolar amounts of 2'-hydroxy acetophenone (1.50 g, 11.00 mmol) and ethanolamine (0.67 g, 11.00 mmol) were mixed and refluxed in ethanol (30 ml) at 60 °C for 24 h using a catalytic amount of *p*-TsOH (5.00 mg). The product was obtained as a light brown oil. Yield: 2.58 g (80%). ^{1}H NMR (400 MHz, $CDCl_3$): δ_H/ppm: 2.37 (s, 3H, H_a); 3.75 (t, 2H, $^{3}J_{HH}$ = 8.0 Hz, H_b); 3.99 (t, 2H, $^{3}J_{HH}$ = 8.0 Hz, H_c); 6.75 (d, 1H, $^{3}J_{HH}$ = 8.0 Hz, H_d); 6.92 (d, 1H, $^{3}J_{HH}$ = 8.0 Hz H_e); 7.28 (dd, 1H, $^{3}J_{HH}$ = 8.0 Hz, H_f), 7.48 (d, 1H, $^{3}J_{HH}$ = 8.0 Hz, H_g). $^{13}C\{^{1}H\}$ NMR ($CDCl_3$): δ/ppm: 42.62 (C_a), 58.25 (C_b), 63.70 (C_c), 116.59 (C_d), 128.25 (C_e), 130.72 (C_f), 133.08 (C_g), 136.47 (C_h), 162.37 (C_i), 173.40 (C_j). FT-IR (cm^{-1}): $\nu_{(O-H)}$: 3164; $\nu_{(C=N)}$:1604. TOF MS (ESI): *m/z* (%), 180.1028 ($[M + H]^+$, 100%). HRMS (ESI) Calcd for $C_{10}H_{13}NO_2$, $[M + H]^+$: 180.1025, found: 180.1028.

3.2.2.3. *Phenol, 2-[(E)-[(2-hydroxyethyl) imino] methyl]* (**L7**)

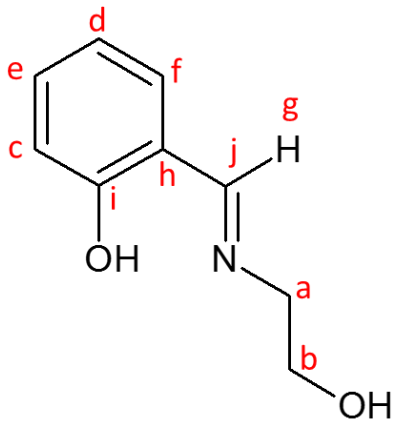

L7 synthesis was carried out by reacting salicyladehyde (1.50 g, 0.01 mol) and ethanolamine (0.73 g, 0.01 mol) in ethanol (30 ml). A catalytic amount (5 mg) of *p*-TsOH was also added and the resultant solution was refluxed for 24 h at 60 °C. A brown oily product was obtained after removing the solvent through rotary evaporator. Yield: 1.87 g (84 %). ^{1}H NMR (400 MHz, $CDCl_3$): δ_H/ppm: 3.79 (t, 2H, $^{3}J_{HH}$ = 4.0 Hz, H_a); 3.96 (t, 2H, $^{3}J_{HH}$ = 4.0 Hz, H_b); 6.89 (t, 1H, $^{3}J_{HH}$ = 8.0 Hz, H_c); 6.98 (d, 1H, $^{3}J_{HH}$ = 8.0 Hz, H_d); 7.28 (d, 1H, $^{3}J_{HH}$ = 8.0 Hz, H_e); 7.36 (d, 1H, $^{3}J_{HH}$ = 8.0 Hz, H_f), 8.42 (s, 1H, H_g). $^{13}C\{^{1}H\}$ NMR ($CDCl_3$): δ/ppm: 61.73 (C_b), 62.12 (C_a), 117.08 (C_c), 118.68 (C_d), 131.46 (C_f), 132.47 (C_e), 161.20 (C_i), 166.94 ($C_{h\&j}$). FT-IR (cm^{-1}): $\nu_{(O-H)}$: 3353; $\nu_{(C=N)}$:1631. TOF MS (ESI): m/z (%), 166.0866 ($[M + H]^+$, 100%). HRMS (ESI) Calcd for $C_9H_{11}NO_2$. 166.0868, found: 166.0866.

3.2.2.4. *Phenol, 2-[(E)-{[2-(diethylamino) ethyl] imino} methyl]* (**L8**)

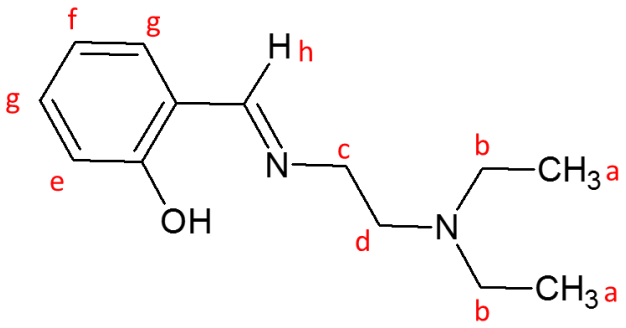

Ligand **L8** was synthesized by following the same method adopted for ligand **L5-L7.** Salicyladehyde (1.50 g, 0.01 mol) and *N*,*N*-diethylethane-1,2 diamine (1.43 g, 0.01 mol) in ethanol (30 ml). Liquid brown oil, Yield: 2.60 g (87%). ^{1}H NMR (400 MHz, $CDCl_3$): δ_H/ppm: 1.11 (t, 6H, $^{3}J_{HH}$ = 8.0 Hz, H_a); 2.68 (q, 4H, $^{3}J_{HH}$ = 8.0 Hz, H_b); 2.83 (t, 2H, $^{3}J_{HH}$ = 8.0 Hz, H_c); 3.72 (d, 2H, $^{3}J_{HH}$ = 4.0 Hz, H_d); 6.88 (d, 1H, $^{3}J_{HH}$ = 8.0 Hz, H_e); 6.98 (d, 1H, $^{3}J_{HH}$ = 8.0 Hz, H_f), 7.33 (qd, 2H, $^{3}J_{HH}$ = 8.0 Hz, H_g), 8.38 (s, 1H, H_h). FT-IR (cm^{-1}): $\nu_{(H-O)}$: 3061; $\nu_{(C=N)}$:1631. TOF MS (ESI): m/z (%), 219.1499 ([M – H]$^+$, 100%), 220.1502 ([M$^+$], 40%). HRMS (ESI) Calcd for $C_{13}H_{20}ON_2$. 219.1497, found: 219.1499.

3.2.2.5. *Phenol, 2-[1-[(2-methxyethyl) amino] ethyl]* (**L9**)

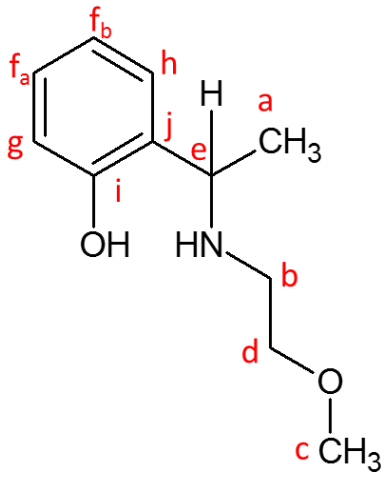

L5 (0.50 g, 2.59 mmol) was dissolved in methanol (30 ml) and five equivalent of $NaBH_4$ (0.49 g, 12.09 mmol) were then added in small portions to give a clear solution which was stirred under reflux for 4 h at 50 °C. The solvent was reduced under vacuum and the residue dissolved in chloroform (30 ml) and washed with distilled water (3 x 20 ml) to remove excess $NaBH_4$. The organic layer was then separated and dried over $MgSO_4$, filtered and solvent was removed under reduced pressure to afford **L9** as a light yellow oil. Yield: 0.28 g (51%). ^{1}H NMR (400 MHz, $CDCl_3$): δ_H/ppm: 1.46 (d, 3H, $^{3}J_{HH}$ = 8.0 Hz, H_a); 2.75 (d, 2H, $^{3}J_{HH}$ = 8.0 Hz, H_b); 3.39 (s, 3H, $^{3}J_{HH}$ = 8.0 Hz, H_c); 3.52 (d, 2H, $^{3}J_{HH}$ = 8.0 Hz, H_d); 3.95 (q, 1H, $^{3}J_{HH}$ = 8.0 Hz, H_e);

6.78 (m, 2H, $^{3}J_{HH}$ = 8.0 Hz, H_f), 6.98 (d, 1H, $^{3}J_{HH}$ = 8.0 Hz, H_g); 7.15 (d, 1H, $^{3}J_{HH}$ = 8.0 Hz, H_h). ^{13}C {^{1}H} NMR ($CDCl_3$): δ/ppm: 22.37 (C_a), 30.91 (C_b), 49.13 (C_e), 58.91 (C_c), 61.33 (C_d), 116.78 (C_g), 119.17 (C_{fb}), 126.44 (C_j), 128.45 (C_{fa}), 128.12 (C_h), 157.14 (C_i). FT-IR (cm^{-1}): $\nu_{(N-H)}$: 3310; $\nu_{(H-O)}$:2870. TOF MS (ESI): m/z (%), 194.1189 ([M – H]$^+$, 100%), 195.1350 ([M$^+$], 40%). HRMS (ESI) Calcd for $C_{11}H_{17}NO_2$, 194.1181, found: 194.1189.

3.2.2.6. *Phenol, 2-[1-[(2-hydroxyethyl) amino] ethyl]* (**L10**)

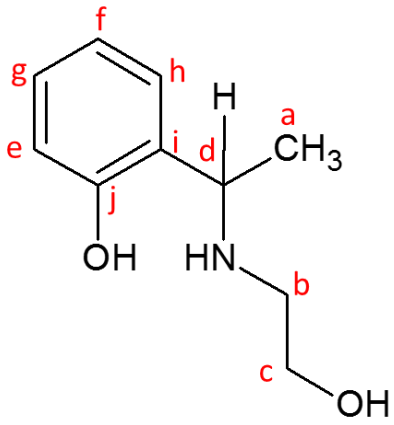

L10 was synthesized in a similar manner to **L9**, using $NaBH_4$ (0.54 g, 13.90 mmol) and **L6** (0.50 g, 2.79 mmol). Yield of a yellow oil: 0.16 g (32%). ^{1}H NMR (400 MHz, $CDCl_3$): δ_H/ppm: 1.51 (d, 3H, $^{3}J_{HH}$ = 4.0 Hz, H_a); 2.74 (t, 2H, $^{3}J_{HH}$ = 4.0 Hz, H_b); 3.79 (t, 2H, $^{3}J_{HH}$ = 4.0 Hz, H_c); 4.00 (q, 1H, $^{3}J_{HH}$ = 4.0 Hz, H_d); 6.80 (d, 1H, $^{3}J_{HH}$ = 8.0 Hz, H_e); 6.98 (dd, 1H, $^{3}J_{HH}$ = 8.0 Hz, H_f), 7.15 (d, 1H, $^{3}J_{HH}$ = 8.0 Hz, H_g); 7.20 (d, 1H, $^{3}J_{HH}$ = 8.0 Hz, H_h). ^{13}C {^{1}H} NMR ($CDCl_3$): δ/ppm: 22.37 (C_a), 49.13 (C_d), 58.91 (C_b), 61.33 (C_c), 116.78 (C_e), 119.17 (C_f), 126.44 (C_i), 128.12 (C_g), 128.45 (C_h), 157.14 (C_j). FT-IR (cm^{-1}): $\nu_{(O-H)}$: 3363; $\nu_{(C=N)}$:1594. TOF MS (ESI): m/z (%), 180.1023 ([M – H]$^+$, 100%), 181.1078 ([M]$^+$, 14%). HRMS (ESI) Calcd for $C_{10}H_{15}NO_2$, 180.1025, found: 180.1023.

3.2.2.7. *Phenol, 2-{[(2-hydroxyethyl) amino] methyl}* (**L11**)

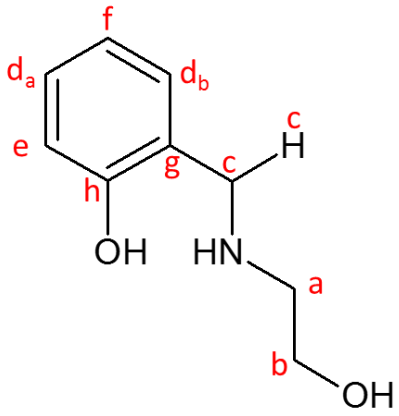

L11 was synthesized in a similar manner as **L9** and **L10**, using $NaBH_4$ (0.62 g, 16.25 mmol) and **L7** (0.54 g, 3.25 mmol). Yield of a light yellow oil: 0.058 g (11%). ^{1}H NMR (400 MHz, $CDCl_3$): δ_H/ppm: 2.89 (t, 2H, $^3J_{HH}$ = 4.0 Hz, H_a); 3.83 (t, 2H, $^3J_{HH}$ = 4.0 Hz, H_b); 4.06 (s, 2H, H_c); 6.85 (p, 2H, $^3J_{HH}$ = 8.0 Hz, H_d); 7.02 (d, 1H, $^3J_{HH}$ = 8.0 Hz, H_e); 7.21 (dd, 1H, $^3J_{HH}$ = 8.0 Hz, H_f). TOF MS (ESI): m/z (%), 166.0864 ($[M - H]^+$, 100%). HRMS (ESI) Calcd for $C_{11}H_{17}NO_2$, 166.0868, found: 166.0864.

3.2.2.8. *Phenol, 2-({[2-(diethylamino)ethyl]amino}methyl)* (**L12**)

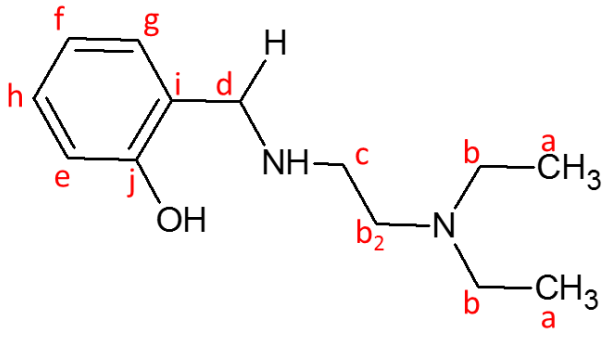

Using the same procedure for **L9**, compound **L12** was synthesized by dissolving **L8** (1.01 g, 4.54 mmol) in methanol (30 ml) and $NaBH_4$ (0.89 g, 22.60 mmol). A clear yellow oil of **L12** was obtained. Yield: 0.66 g (65%). ^{1}H NMR (400 MHz, $CDCl_3$): δ_H/ppm: 1.09 (t, 6H, $^3J_{HH}$ = 8.0 Hz, H_a); 2.60 (m, 6H, $^3J_{HH}$ = 8.0 Hz, H_b); 2.73 (t, 2H, $^3J_{HH}$ = 8.0 Hz, H_c); 4.04 (d, 2H, $^3J_{HH}$

= 8.0 Hz, H_d); 6.78 (d, 1H, $^3J_{HH}$ = 8.0 Hz, H_e); 6.85 (d, 1H, $^3J_{HH}$ = 8.0 Hz, H_f), 7.07 (d, 1H, $^3J_{HH}$ = 8.0 Hz, H_g); 7.20 (d, 1H, $^3J_{HH}$ = 8.0 Hz, H_h). ^{13}C {^1H} NMR ($CDCl_3$): δ/ppm: 11.75(C_a), 45.95 (C_d), 47.07 (C_c), 51.91 (C_b), 52.49 (C_{b2}), 116.36 (C_e), 118.83 (C_f), 122.76 (C_i), 128.24 (C_h), 128.57 (C_g), 158.46 (C_j). FT-IR (cm^{-1}): $\nu_{(O-H)}$: 3634. TOF MS (ESI): m/z (%), 221.1650 ($[M- H]^+$, 100%), 222.1701 ($[M^+]$, 14%). HRMS (ESI) Calcd for $C_{13}H_{22}ON_2$, 221.1654, found: 221.1650.

3.2.2.9. *Phenol, 2-[1-[(2-hydroxyethyl) imino] ethyl] $NiBr_2$* (**7**)

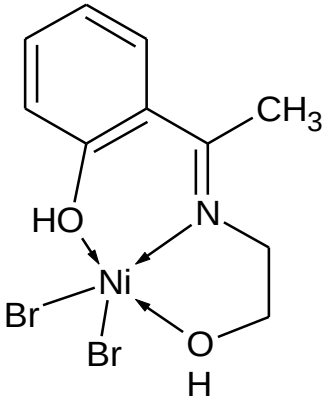

Complex **C7** was synthesized by adding a solution of $NiBr_2$ (DME) (0.10 g, 0.33 mmol) in dichloromethane (5 ml) to a solution of **L6** (0.12 g, 0.66 mmol) in dichloromethane (5 ml). Then the solution was allowed to stir for 24 h at room temperature to give a yellow precipitate which was filtered and washed with dichloromethane (10 ml). Yield: 0.04 g (28%). TOF MS ESI: m/z (%), 397.0925 ($[M]^+$, 18%). FT-IR (cm^{-1}): $\nu_{(O-H)}$: 3292; $\nu_{(C=N)}$:1626. μ_{obs} = 3.10 BM. Anal. Calcd for $C_{11}H_{17}NO_2NiBr_2{\cdot}3H_2O$: C 26.59, H 4.24, N 3.10. Found: C 26.58, H 4.37, N 3.26.

Complexes **8**-**13** were synthesized following procedure described for complex **7**, using appropriate ligand and nickel(II) salt.

3.2.2.10. *Phenol, 2-[1-[(2-hydroxyethyl) imino] ethyl] $NiCl_2$* (**8**)

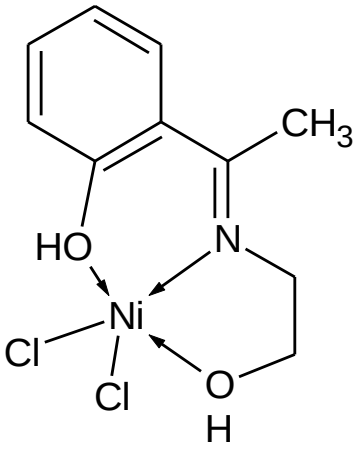

$NiCl_2$ (0.10 g, 0.80 mmol) and **L6** (0.15 g, 0.80 mmol). Green solid. Yield: 0.07 g (30%). TOF MS ESI: m/z (%), 236.0220 ($[M^+ - 2Cl]^{2+}$, 100%). FT-IR (cm^{-1}): $\nu_{(O-H)}$: 3307; $\nu_{(C=N)}$:1630. μ_{obs} = 3.14 BM. Anal. Calc. for $C_{10}H_{13}NO_2NiCl_2{\cdot}CH_2Cl_2{\cdot}2H_2O$: C 30.74, H 4.46, N 3.26. Found: C 31.53, H 4.93, N 3.81.

3.2.2.11. *Phenol, 2-[1-[(hydroxyethyl) imino] methyl $NiCl_2$* (**9**)

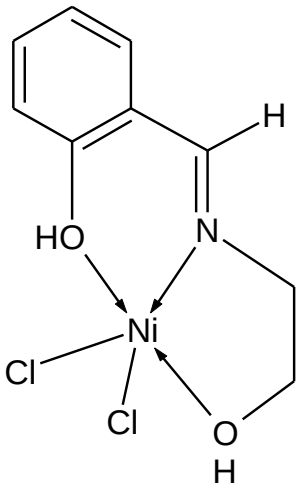

L7 (0.22 g, 1.32 mmol) and $NiCl_2$ (0.17 g, 1.32 mmol). Rearrangement of complex **9** during recrystallization from methanol/diethyl-ether solution mixture, afforded a derivative of **9**, that is, nickel(II) complex **9a** as blue crystals which were suitable for single-crystal X-ray analysis.

Yield: 0.22g (59%). TOF MS (ESI): m/z (%), 222.0021 ([M - 2Cl]$^{2+}$, 100%); 443.0172 ([(L7)$_2$Ni]$^+$, 40 %). FT-IR (cm^{-1}): $\nu_{(O-H)}$: 3426; $\nu_{(C=N)}$:1644. μ_{obs} = 3.55 BM. Anal. Calc. for $C_9H_{11}NO_2NiCl_2 \cdot H_2O$: C 34.56, H 4.19, N 4.48. Found: C 34.92, H 4.39, N 6.02.

3.2.2.12. *Phenol, 2-[1-[(2-methxyethyl) amino] ethyl] NiBr$_2$* (**10**)

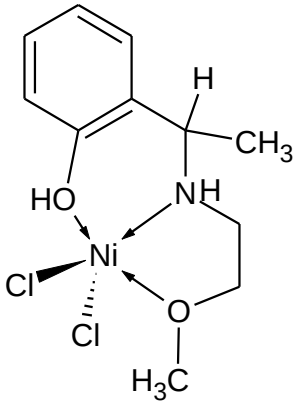

L9 (0.60 mmol, 0.12 g) and $NiCl_2$ (0.08 g, 0.60 mmol). Yield: 0.05 g (23%). TOF MS-ESI: m/z (%), 326.9065[M$^+$, 67%], 250.90 ([M - 2Cl]$^{2+}$, 40 %). FT-IR (cm^{-1}): $\nu_{(N-H)}$: 3314. μ_{obs} = 3.76 BM.

3.2.2.13. *Phenol, 2-[1-[(2-hydroxyethyl) amino] ethyl] NiBr$_2$* (**11**)

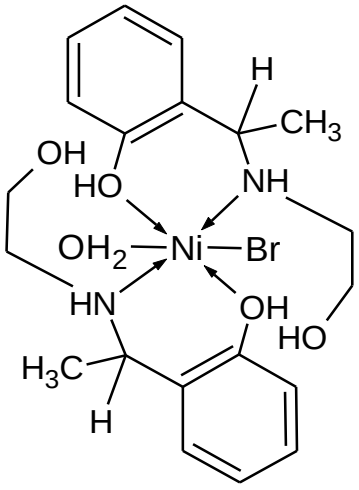

Ligand **L10** (0.10 g, 0.56 mmol and $NiBr_2$ (DME) (0.15 g, 0.55 mmol). Blue solid. Yield: 0.20 g (90%). TOF MS ESI: m/z (%), 239.9875 ([M- 2Br]$^{2+}$, 50%). FT-IR (cm^{-1}): $\nu_{(N-H)}$: 3237; $\nu_{(O-}$

$_{H)}$:3058. μ_{obs} = 3.75 BM. Anal. Calc. for $C_{20}H_{30}N_2O_4NiBr{\cdot}H_2O$: C 46.28, H 6.21, N 5.40 Found: C 46.24, H 5.95, N 5.28.

3.2.2.14. *Phenol, 2-[1-(2-Hydroxyethyl) amino] methyl] $NiCl_2$* (**12**)

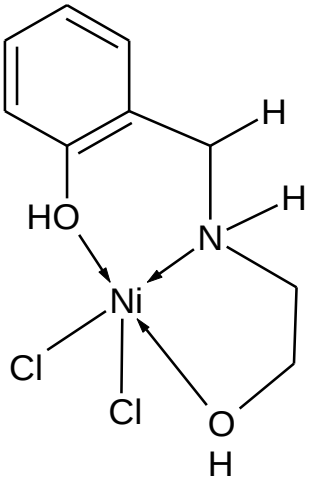

$NiCl_2{\cdot}6H_2O$ (0.12 g, 0.48 mmol) and **L11** (0.08 g, 0.48 mmol). Green solid. Yield: 0.03 g (21%). TOF MS (ESI): m/z (%), 224.0218 ($[M - 2Cl]^{2+}$, 100%). FT-IR (cm^{-1}): $\nu_{(O-H)}$: 3179. μ_{obs} = 3.58 BM. Anal. Calc. for $C_9H_{13}NO_2NiCl_2$: C 36.42, H 4.41, N 4.72. Found: C 36.39, H 4.38, N 4.65.

3.2.2.15. *Phenol, 2-(1-{[2-(diethylamino) ethyl] amino} methyl) $NiCl_2$* (**13**)

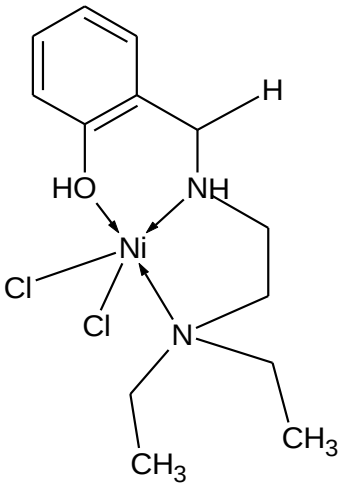

$NiCl_2$ (0.13 g, 0.96 mmol) and **L12** (0.21 g, 0.96 mmol). Green solid. Yield: 0.03 g (21%). TOF MS (ESI): m/z (%), 281.1196 ($[M - 2Cl]^{2+}$, 62%). FT-IR (cm^{-1}): $\nu_{(O-H)}$: 3250. μ_{obs} = 3.54 BM.

3.2.3. X-ray crystallography data collection

X-ray crystallographic data collection for compound **9a** was recorded on a Bruker Apex Duo diffractometer equipped with an Oxford Instrument Cryojet operating at 100(2) K and an Incoatec microsource operating at 30 W power. Crystal and structure refinements data of **9** is provided in Table 3.3. The data was collected with Mo Kα (λ = 0.71073 Å) radiation at a crystal-to-detector distance of 50 mm. The data collections were performed using omega and phi scans with exposures taken at 30 W X-ray power and 0.50˚ frame width using APEX2.[21] The data was reduced with the program SAINT[21] using outlier rejection, scan speed scaling, as well as standard Lorentz and polarisation correction factors. A SADABS semi-empirical multi-scan absorption correction was also applied to the data. Direct methods, SHELXS-2014[22] and WinGX[23] were used to solve the structure. All non-hydrogen were located in the difference map and refined anisotropically with SHELXZ-2014.[22] All the hydrogen atoms were included as idealized contributors in the least squares process. Their positions were calculated using a standard riding model with $C\text{-}H_{aromatic}$ distances of 0.93 Å and U_{iso} = 1.2 U_{eq} and $C\text{-}H_{methylene}$ distances of 0.99 Å and U_{iso} = 1.2 U_{eq} and $C\text{-}H_{methyl}$ distances of 0.98 Å and U_{iso} = 1.5 U_{eq}. The amine N-H and hydroxyl O-H hydrogen atoms were located in the difference density map and refined isotropically.

3.2.4. General procedure for ethylene oligomerization reactions

Ethylene oligomerization reactions were performed in a 400 ml stainless steel Parr reactor equipped with a mechanical stirrer, temperature controller and an internal cooling system. The

reactor was pre-heated to 100 °C in *vacuo* and then cooled to room temperature. The appropriate amount of the synthesized catalyst precursor (10.0 µmol) was weighed out and transferred into a dry Schlenk tube under nitrogen and toluene (20 ml) was added utilizing a syringe. The required amount of a co-catalyst ($EtAlCl_2$, 1.40 ml, 2.52 mmol) was then injected into the Schlenk tube containing the pre-catalyst to form an active catalyst system. The solution mixture in the Schlenk tube was then transferred through the cannula into the reactor. An additional 60 ml of toluene solvent was also transferred through the cannula into the reactor to give a total of 80 ml. Before the reaction was started, the reactor was flashed three times with ethylene and the appropriate temperature and pressure was set and the reaction (stirring) started. After the reaction time was over, the reactor was cooled to approximately -10 °C using ice and liquid nitrogen and the excess ethylene vented off to facilitate fast cooling through the reduction of pressure. The reaction was then quenched by the addition of 10 % hydrochloric acid (5 ml). A portion of the reaction mixture was sampled in a GC-vial for GC and GC-MS analyses to determine the product distribution. The mass of the product formed was determined using the calibration curve of the R-factors for the standards versus number of carbons (Equations 1 and 2).[24] Hexene (0.849), octene (0.744), decene (0.496), dodecene (0.389) and tetra-decene (0.327) standards were used to obtain calibration curve and n-heptane was used as an internal standard. The R-factor for butene was extrapolated as 0.981 from the calibration curve.

$$RF_A = \frac{P_A}{[A]} \div \frac{P_{IS}}{[IS]} \qquad \textit{Equation (1)}$$

Rearranging to solve for the concentration of the analyte,

$$[A] = \frac{P_A}{P_{IS}} \times \frac{[IS]}{RF_A} \qquad \textit{Equation (2)}$$

RF – Response factor,

P_A and P_{IS} – Peak area of the analyte and internal standard respectively,

[A] and [IS] – Concentration of the analyte and internal standard respectively,

3.3. Results and discussion

3.3.1. Syntheses of ligands and their respective nickel (II) complexes

The phenol,2-[1-[(2-methoxyethyl)imino]ethyl], phenol,2-[1-[(2-hydroxyethyl)imino]ethyl], phenol,2-[1-[(2-hydroxyethyl)imino]methyl] and phenol,2-[(E)-{[2-(diethylamino)ethyl] imino}methyl] ligands **L5**-**L8** were synthesized by reacting equimolar amounts of 2'-hydroxy acetophenone and salicylaldehyde with appropriate amine precursor in ethanol solvent with para toluene sulphonic acid as a catalyst (Scheme 3.1). The imino and amino ligands were obtained in high yields 80% – 99%. The characterization of the imine ligands was accomplished using ^{1}H and ^{13}C NMR spectroscopy, mass spectrometry and IR spectroscopy.

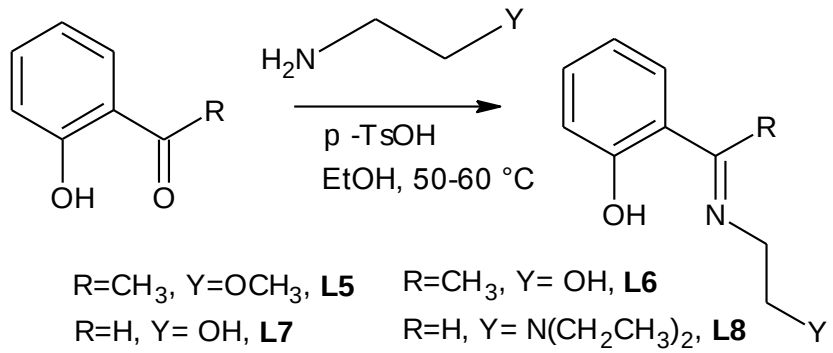

Scheme 3.1: Syntheses of 2-[(ethylimino)ethyl]phenol, N^O donor ligands.

The ^{1}H NMR spectrum of **L5** (Figure 3.1) shows the expected number of protons in their respective chemical shifts. For instance, a singlet peak around 2.35 ppm which was due to the imine methyl while the singlet peak at 3.50 ppm corresponds to the methoxy protons. The four ethylene hydrogen appeared as a single triplet peak at 3.80 ppm. The $^{13}C\{^{1}H\}$ NMR spectrum of ligand **L5** (Figure 3.2) was found to be in good agreement with the ^{1}H NMR of the molecule.

For example, the carbon double bonded to the nitrogen appeared at 164.05 ppm and the methyl at 14.61 ppm (a). The number of fragment peaks observed was also consistent with the number of carbons in the molecule.

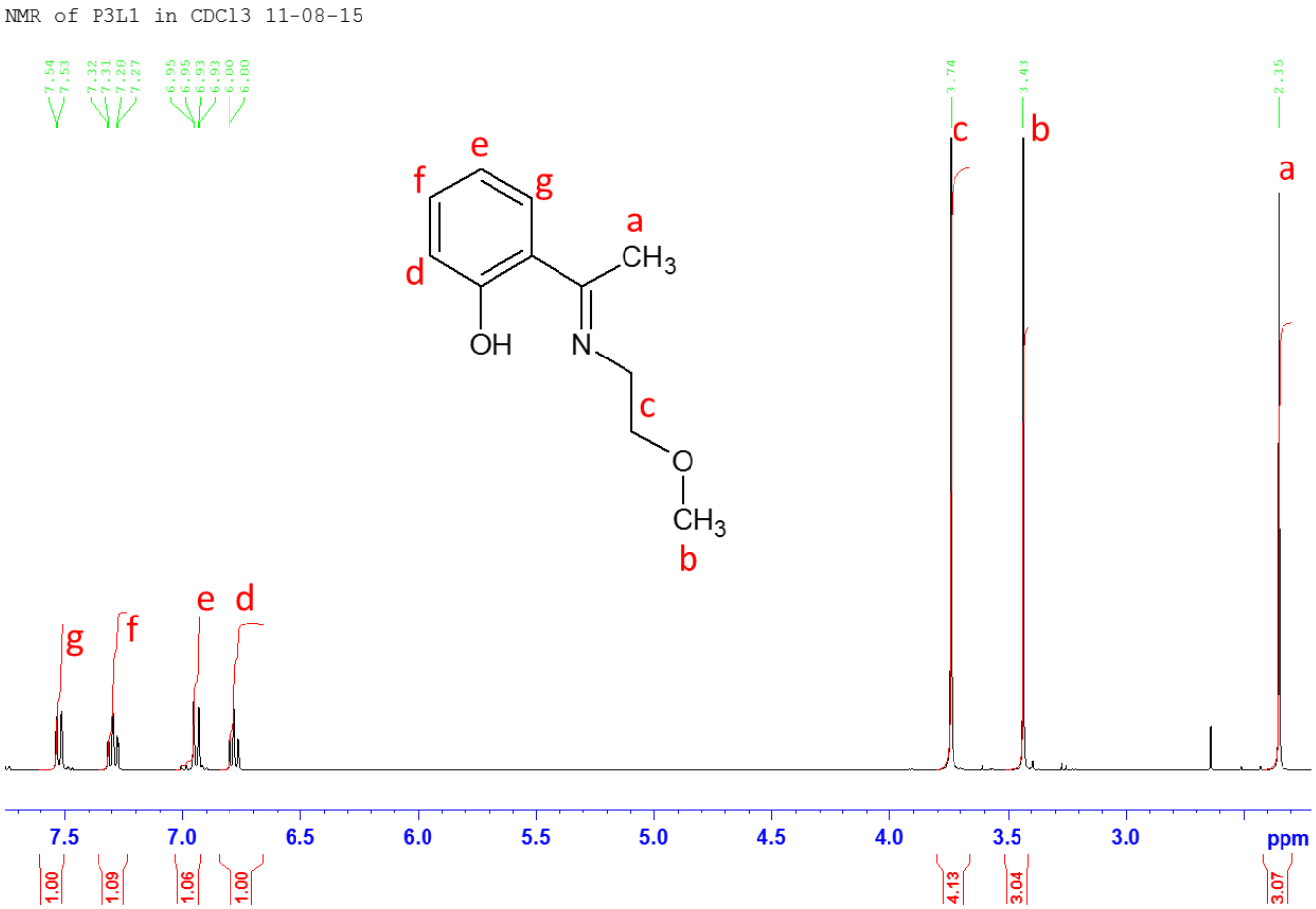

Figure 3.1: ^{1}H NMR spectrum of ligand **L5** in $CDCl_3$.

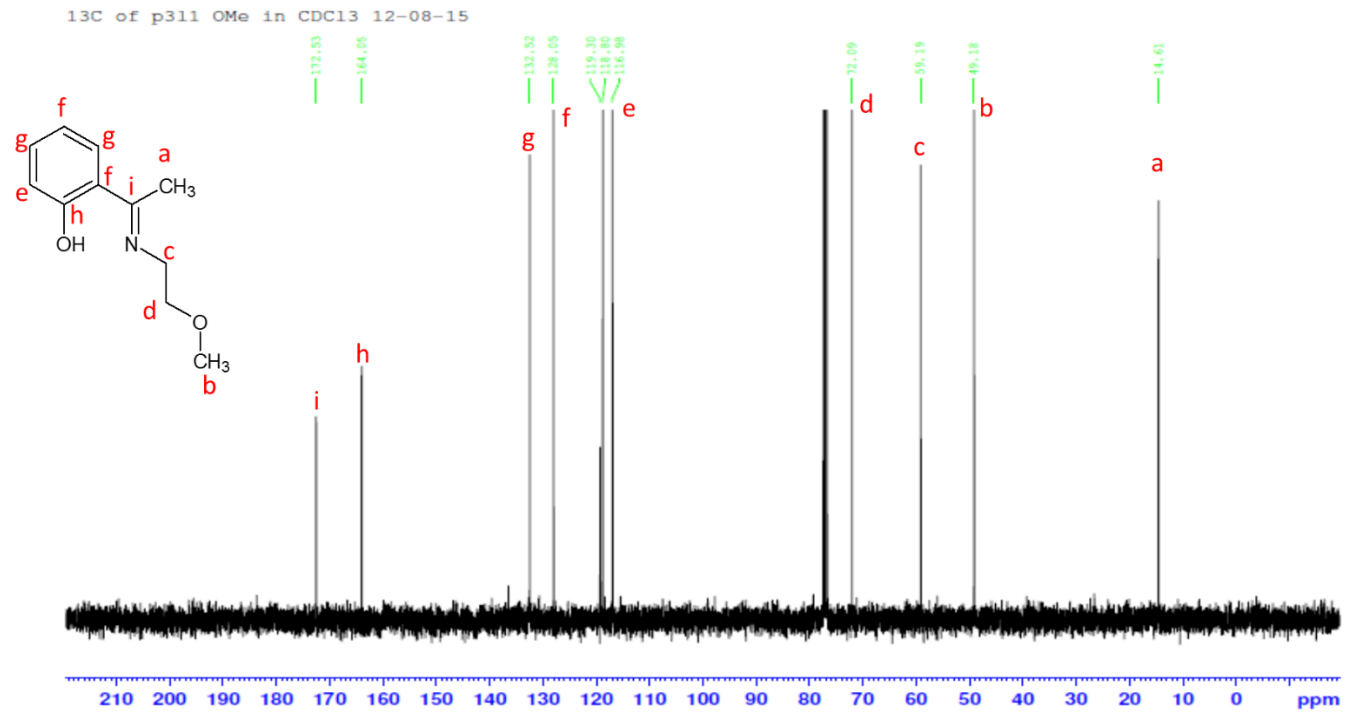

Figure 3.2: $^{13}C\{^{1}H\}$ NMR of spectrum of ligand **L5** in $CDCl_3$.

The mass spectrum of ligand **L5** shown in Figure 3.3 also confirmed the formation of the imine ligand. The base peak at m/z = 216.0995 amu corresponds to $[M + Na]^+$ fragment.

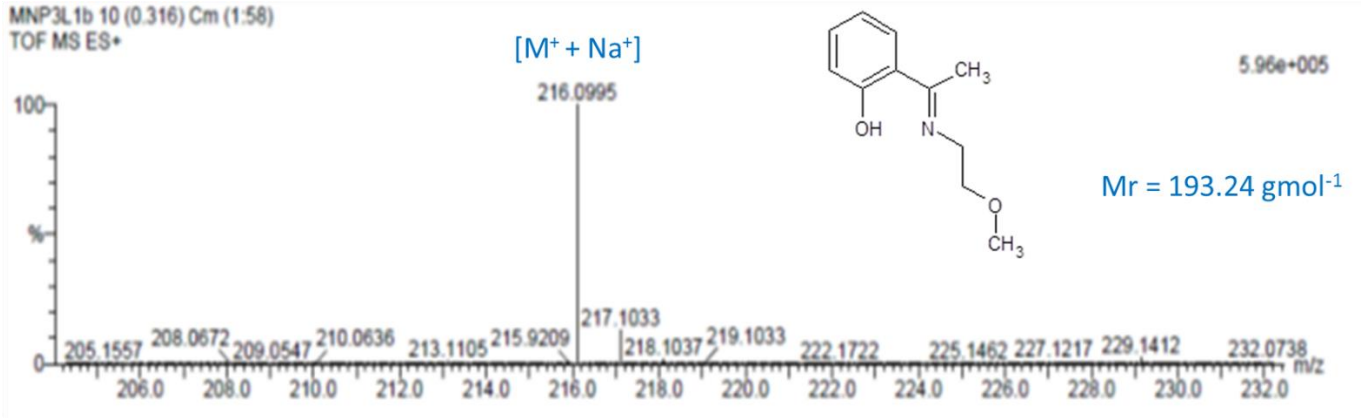

Figure 3.3: The mass spectrum of **L5** showing $[M + Na]^+$ fragment at m/z = 216.0995 amu.

The amine ligands **L9-L12** were synthesized *via* the reduction of the imine ligands **L5-L8** respectively using sodium borohydride ($NaBH_4$) in methanol solvent according to Scheme 3.2.

All the ligands were obtained in low to moderate yields (11% - 65%). The structural characterization of **L9**-**L12** was achieved using ^{1}H and $^{13}C\{^{1}H\}$ NMR spectroscopy, mass spectrometry and IR spectroscopy.

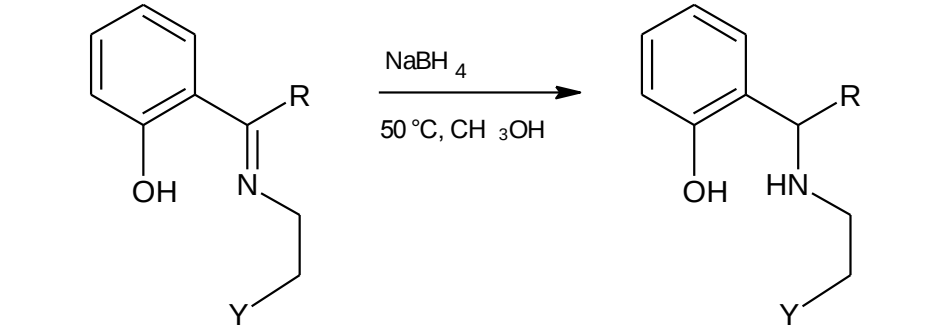

R=CH_3, Y=OCH_3, **L5**
R=CH_3, Y= OH, **L6**
R=H, Y= OH, **L7**
R=H, Y= $N(CH_2CH_3)_2$, **L8**

R=CH_3, Y=OCH_3, **L9**
R=CH_3, Y= OH, **L10**
R=H, Y= OH, **L11**
R=H, Y= $N(CH_2CH_3)_2$, **L12**

Scheme 3.2: Reduction of imine ligands (**L5**–**L8)** to form 2-[(ethylamino)ethyl]phenol donor ligands (**L9**–**L12)** respectively.

The ^{1}H NMR spectrum of amine ligand **L9** in Figure 3.4 shows the methylene proton peak at 1.50 ppm as a doublet. This is in contrast to a singlet peak at 2.40 ppm reported for the corresponding imine ligand **L5**. In addition, the appearance of a signal as a quartet at around 2.75 ppm confirmed the reduction of **L5**-**L9**. Similarly, the $^{13}C\{^{1}H\}$ NMR spectrum of **L9** showed the methylene carbon peak shifted down field from 14.41 ppm (**L5**) to 22.44 ppm (**L9**) as given in Figure 3.5.

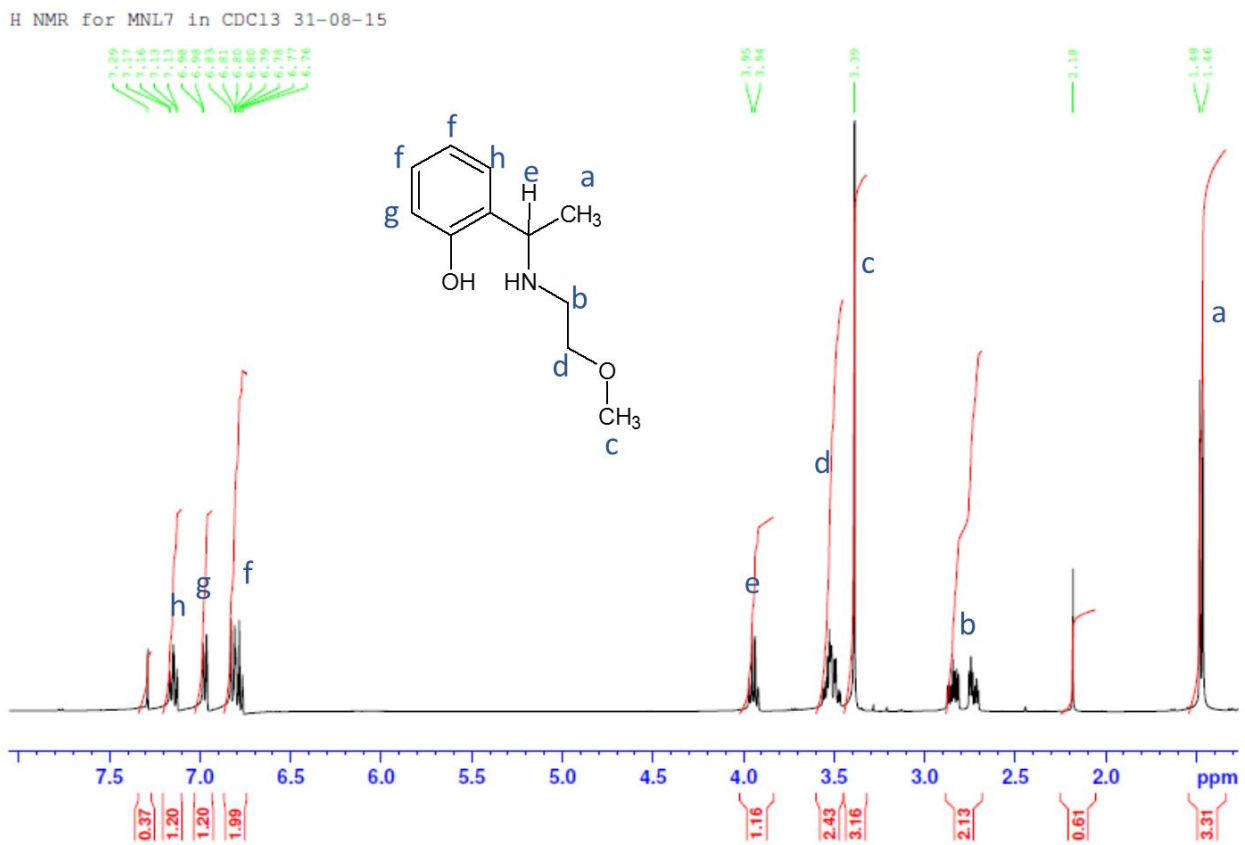

Figure 3.4: ^{1}H NMR spectrum of ligand **L9** showing the reduction of **L5** as shown by the appearance of a doublet methylene peak (a) at 1.50 ppm (in $CDCl_3$).

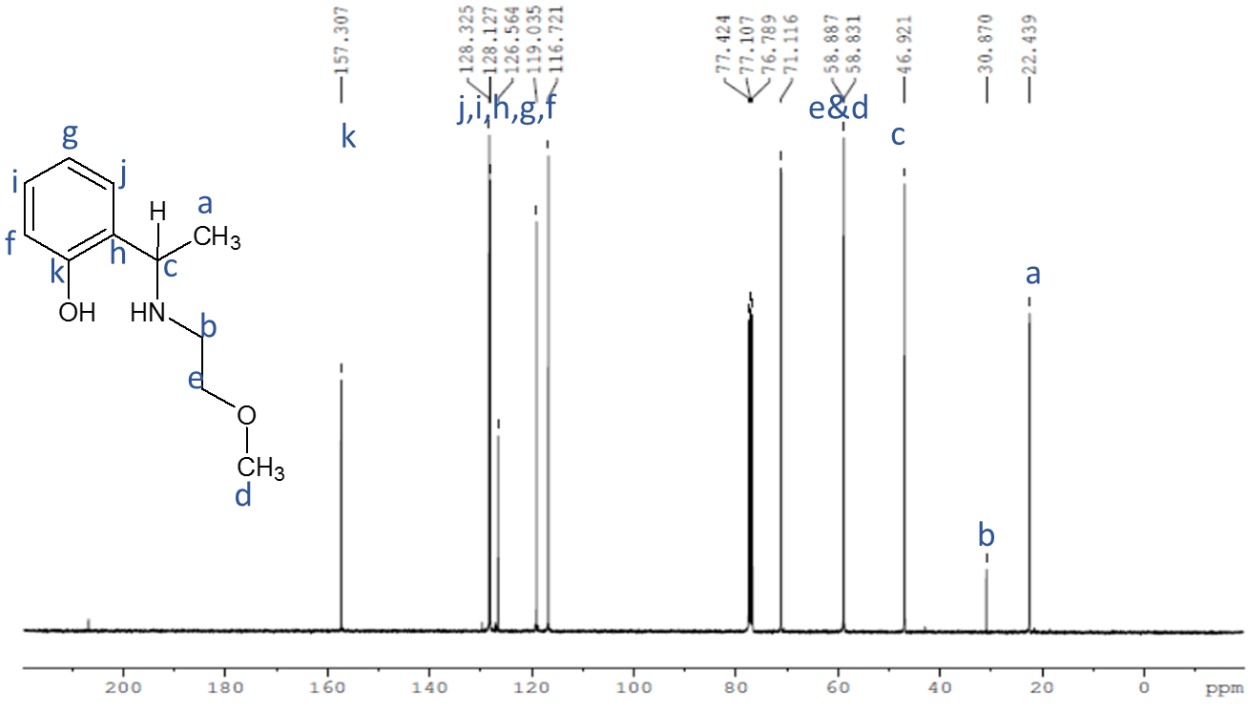

Figure 3.5: $^{13}C\{^{1}H\}$ NMR spectrum of compound **L9** in $CDCl_3$.

The mass spectrum was also used to confirm the formation of the amine ligands, for example Figure 3.6 shows the mass spectrum of **L9**. A molecular ion peak with m/z of 194.1184 amu corresponds to $[M - H]^+$ and the peak with m/z value of 195.1350 amu was due to the ligand ion peak. Similar mass spectra were observed for ligands **L8**–**L12**.

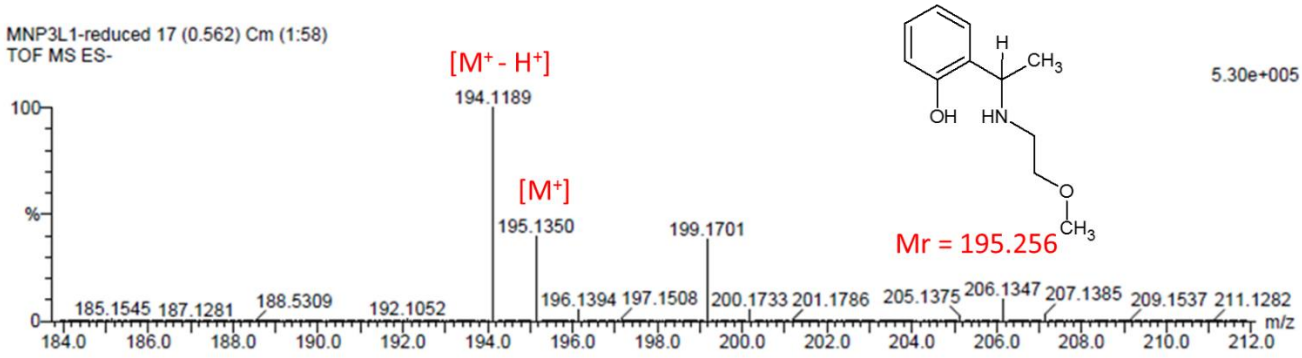

Figure 3.6: Mass Spectrum of **L9** showing a peak at 195.1189 amu corresponding to a molecular ion peak.

Infrared spectroscopy was also helpful in structural elucidation of ligands **L6**-**L12**. It is evident from Figure 3.7 that imine and amine ligands were successfully synthesized. The C=N stretching frequency for ligand **L8** was observed at 1631 cm^{-1}, but upon reduction to form ligand **L12**, this peak disappeared while other peaks remained as it is depicted in Figure 3.7.

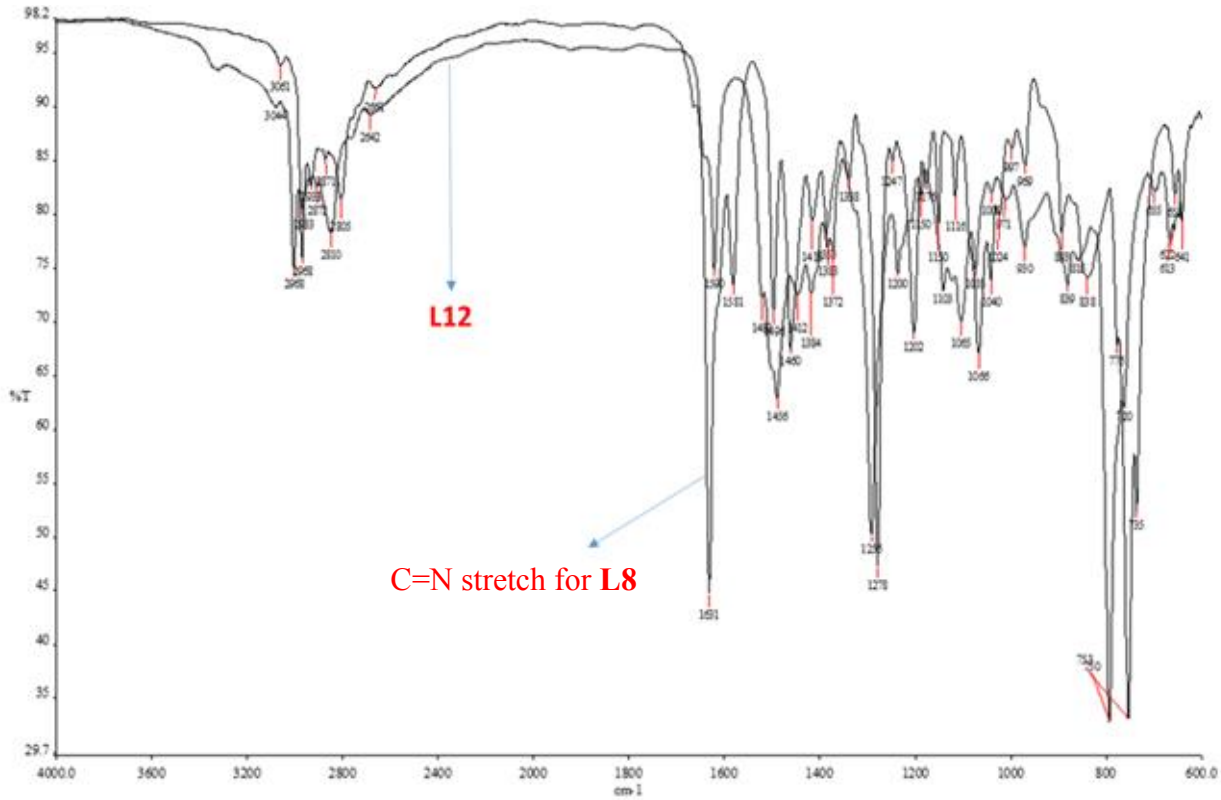

Figure 3.7: The IR spectra of the imine ligand **L8** characterized by a sharp C=N signal around 1631 cm^{-1} and the amine ligand **L12** characterized by the absence of the $C=N_{1631/cm}$ peak.

Complexes **7-13** were synthesized by reacting same number of moles of the 2-[(ethylimino)ethyl]phenol (**L5-L8**) and 2-[(ethylamino)ethyl]phenol (**L9**-L**12**) ligands with the nickel(II) bromide or nickel(II) chloride salts in dichloromethane solvent as illustrated in Scheme 3.3. The complexes synthesized from the imine ligands **L5** and **L8** were relatively unstable and hydrolyzed upon filtration. Nevertheless, the imine complexes **7**, **8** and **9** synthesized from ligands **L6** and **L7** were obtained in reasonable amounts. Thus all the nickel(II) complexes were kept in the desiccator. The amine complexes **10**–**13** were relatively stable and were obtained in good yields. In summary, the nickel(II) complexes derived from the imine and amine N^O ligands were obtained in very low to good yields ranging from 21% - 90%.

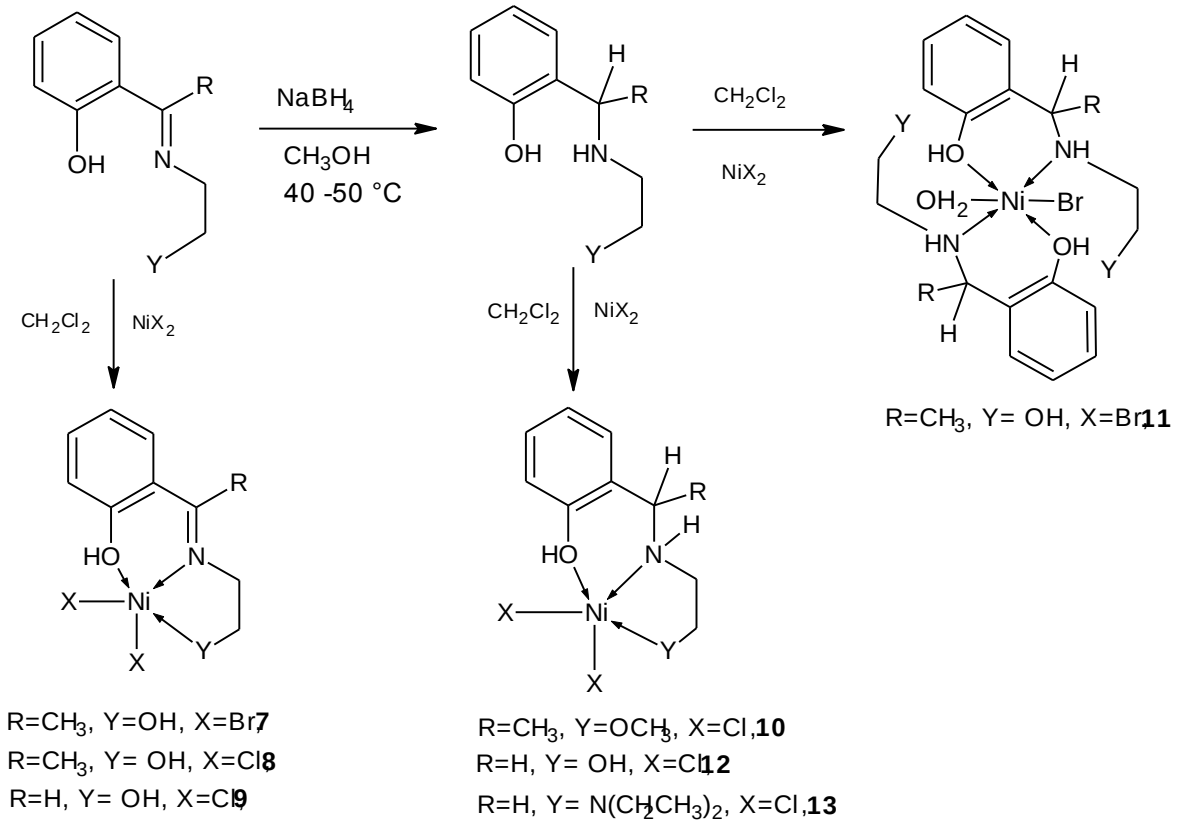

Scheme 3.3: Syntheses of imine and amine N^O chelated nickel(II) complexes **7**–**13**.

The paramagnetic nature of the nickel(II) complexes resulted in the use of NMR spectroscopy for characterization being unhelpful and thus the complexes were characterized using mass spectrometry, infrared spectroscopy, magnetic moments measurements, elemental analyses and single crystal x-ray crystallography. Figure 3.8 shows the mass spectrum obtained for complex **9**. The base peak with m/z value of 222.0113 amu was due to the fragmentation of two chloride ions leaving the ligand and the metal. The peak with m/z value of 443.0172 amu corresponds to the $[(L7)_2Ni]^+$ molecular ion.

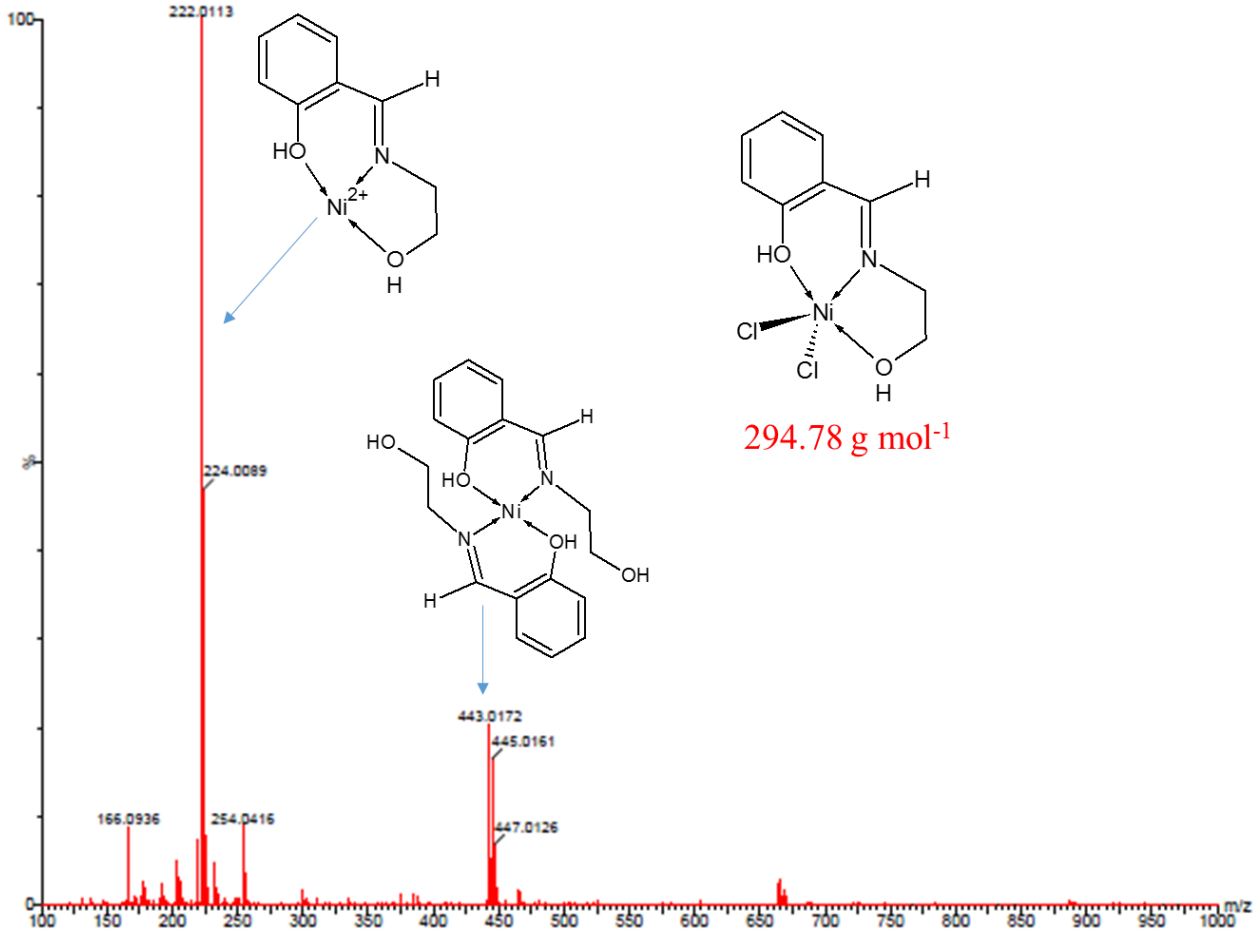

Figure 3.8: The mass spectrum of complex **9** showing a peak at 222.0113 m/z when two chloride ions are lost $[M - 2Cl]^{2+}$ and a peak at 443.0172 corresponding to $[(L7)_2Ni]^{+}$ molecular ion.

The mass spectrum in Figure 3.9 confirmed the formation of complex **10**. For example the signature peak with m/z value of 326.9055 amu corresponded to the molecular ion peak $[M-2H]^{2+}$ of the complex. The base peak at 245.9233 amu was due to the fragmentation of two chloride ions. These fragmentations were also observed for the other nickel(II) complexes, **7**, **8**, **11-13**.

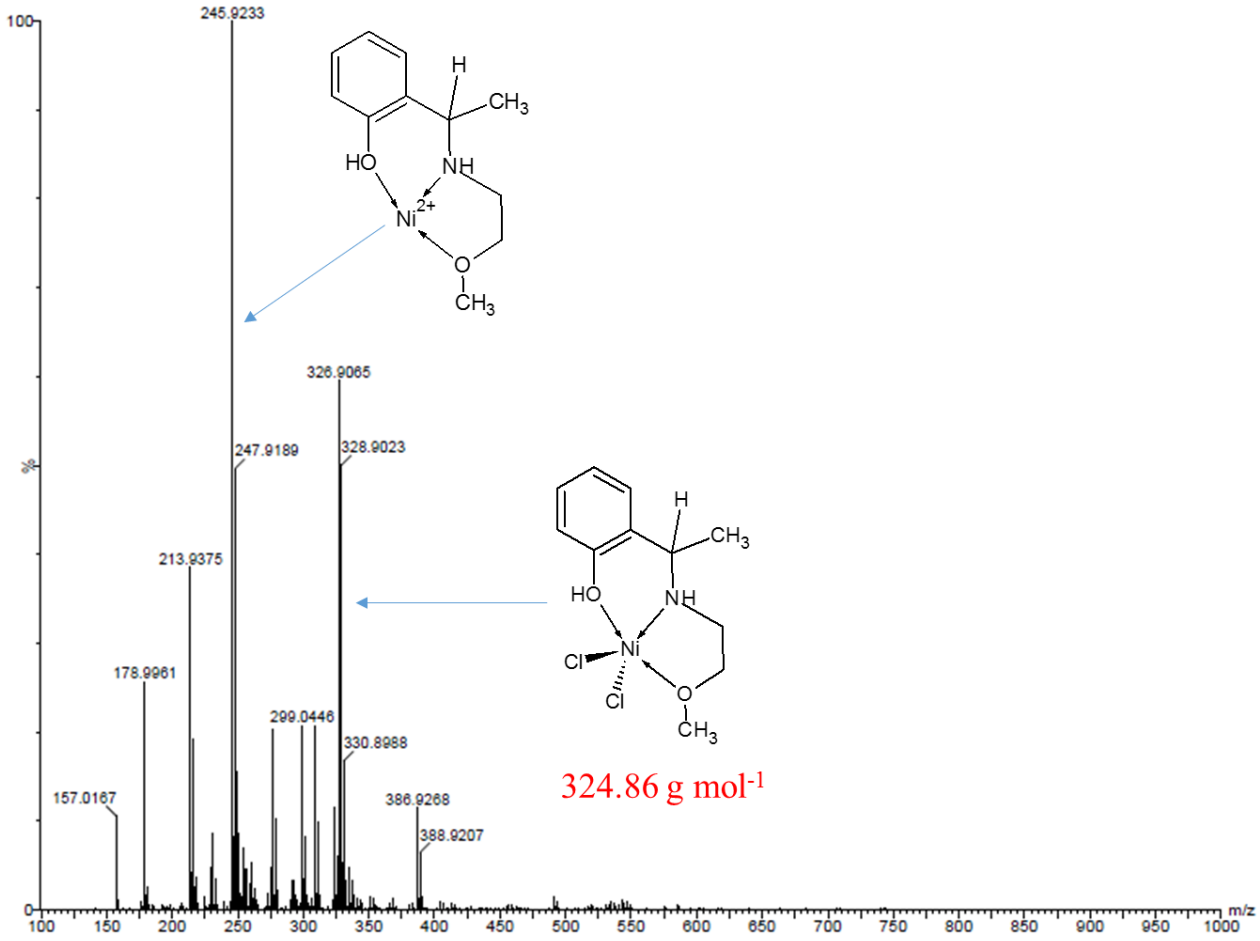

Figure 3.9: The mass spectrum of **10** showing a molecular ion peak at 326.91 ($[M + 2H]^+$ ion peak, 60%).

Infrared spectroscopy also aided in the characterization of the nickel(II) complexes shown in Figure 3.10. The notable difference between the two spectra was the broadening of the strong O-H peak upon the formation the nickel(II) complexes. In the ligands spectra, the O-H peaks were weak and sharp within the range of 2870 cm^{-1} – 3634 cm^{-1}. In contrast, the O-H stretching frequencies for the complexes were found within the range of 3058 cm^{-1} – 3426 cm^{-1} and this was indicative of successful complex formation. The N-H peaks were also observed for amine complexes **10** (3314 cm^{-1}) and **11** (3237 cm^{-1}). Table 3.1 gives a summary of the spectroscopic and physical data obtained for ligands **L9**–**L12** and their respective nickel(II) complexes **7**–**13**.

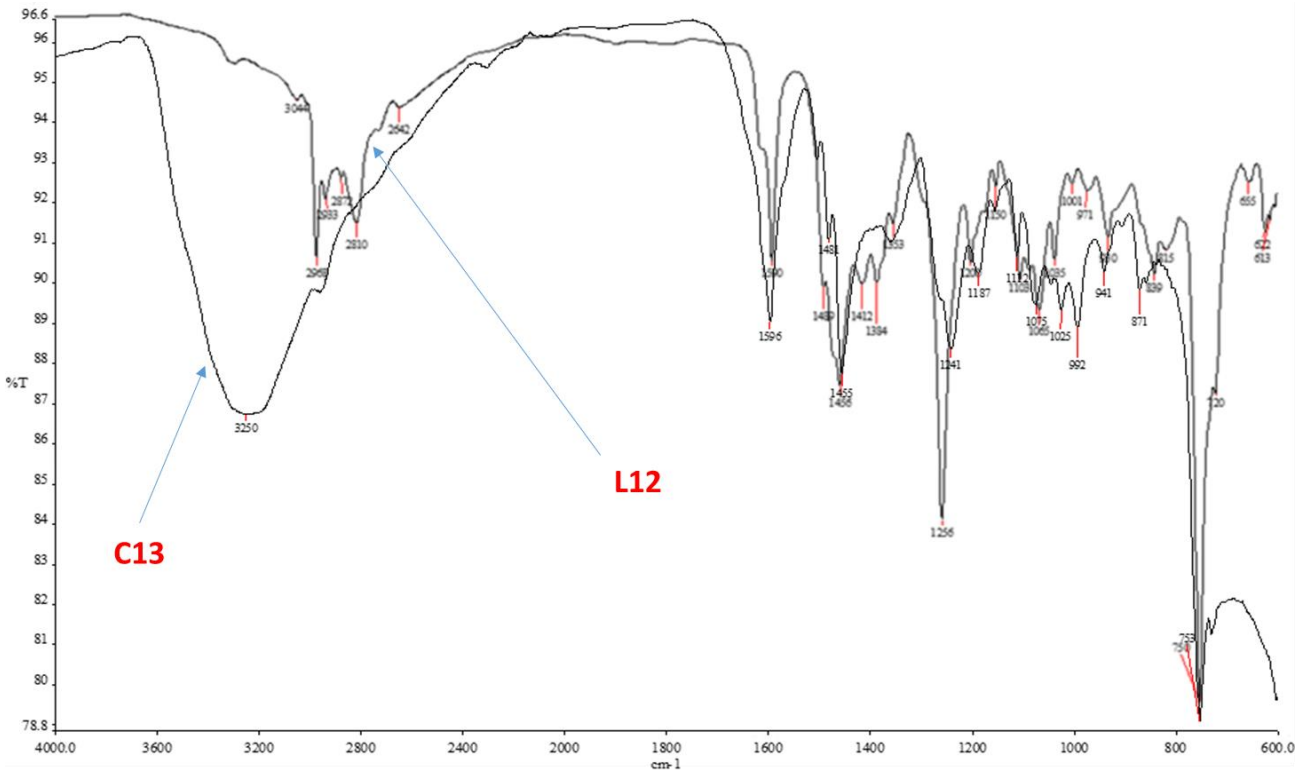

Figure 3.10: The infrared spectra of ligand **L12** and its nickel (II) complex **13** showing strong and broad O-H signal in the complex.

The nickel(II) complexes **7**–**13** were further characterized using magnetic moment measurements and were found to be paramagnetic in nature implying a high spin configuration of the nickel(II) complexes. The magnetic moments of nickel(II) complexes **7**–**13** were found between the ranges of 3.10 – 3.76 BM. The values obtained for complexes **7**–**13** were found to be slightly higher than the literature reported spin only value of 2.83 BM for nickel(II) complexes.[12] The magnetic moment measurement obtained for nickel(II) complexes **7**-**13** nevertheless fell within the anticipated range for high spin nickel(II) complexes of 2.9 – 4.2 BM.[12]

Table 3.1: The IR, mass spectral and magnetic moments data of the ligands **L5**–**L12** and their nickel(II) complexes **7**–**13**.

Imine and amine N^O donor ligands				Nickel(II) complexes				
	FT-IR (cm^{-1})		m/z (%)	complex	FT-IR (cm^{-1})		m/z (%)	μ_{obs} (BM)
	$\nu_{(O-H)}$	$\nu_{(C=N)}$			$\nu_{(O-H)}$	$\nu_{(C=N)}$		
L5	3059	1615	M^+ (100%)	**7**	3292	1626	M^+ (18%)	3.10
L6	3164	1604	M^++H^+ (100%)	**8**	3307	1630	M^+-$2Cl^-$ (100%)	3.14
L7	3353	1631	M^++H^+ (100%)	**9**	3426	1644	M^+-$2Cl^-$ (100%)	3.55
L8	3061	1631	M^+ (100%)	**10**	-	3314 ($\nu_{(N-H)}$)	M^+ (67%)	3.76
L9	2870	3310 ($\nu_{(N-H)}$)	M^+ (100%)	**11**	3058	3237 ($\nu_{(N-H)}$)	M^+-Br^- (50%)	3.75
L10	3363	1594	M^++H^+ (100%)	**12**	3179	-	M^+-$2Cl^-$ (100%)	3.58
L12	3634	-	M^+ (100%)	**13**	3250	-	M^+-$2Cl^-$ (62%)	3.54

The elemental analyses data of the nickel(II) complexes **7**, **8** and **9** were found to be consistent with one ligand motif per metal centre as proposed in Scheme 3.3. Interestingly, the elemental analysis data of complex **11** corresponded to two ligand units per nickel(II) metal atom, one bromide atom and one water molecule which was least expected. This showed the effect of the metal used and ligand structure on the resultant interaction between the ligand and metal centre. Nevertheless, the elemental analyses data obtained for the complexes showed that the nickel(II) complexes were obtained with better purity regardless of their air sensitivity. To account for the hygroscopic nature of the nickel(II) complexes, few molecules of water solvent were added to balance the atomic mass fractions. Furthermore, infinitesimal deviations from the calculated C, H and N contents could be an attribute to the presence of smaller amount impurities in the nickel(II) complexes which shows somewhat the necessity of further purification.

3.3.2. Molecular structure determination of the nickel(II) complex 9a by single crystal X-ray crystallography.

Single crystals suitable for X-ray analysis of complex **9a** were grown by slow diffusion of complex **9** in diethyl-ether into methanol solution at room temperature and used for its solid state structure determination. Tables 3.2 and 3.3 give summary of the crystallographic data, structure refinement parameters and the selected bond length and angles respectively. The nickel(II) complex **9a** crystallized in the monoclinic system with space group $P2_1/n$.

Table 3.2: The selected bond lengths [Å] and angles [°] for nickel(II) complex **9a**

Bond lengths [Å]		**Bond angles [°]**	
Ni(1)-N(1)	2.0012(10)	N(1)-Ni(1)-O(1)	91.45(4)
Ni(1)-O(1)	2.0619(8)	O(1)-Ni(1)-O(1)	80.40(4)
Ni(1)-O(2)	2.1400(9)	N(1)-Ni(1)-O(2)	80.65(4)
Ni(1)-O(3)	2.1303(9)	O(1)-Ni(1)-O(2)	107.15(3)
Ni(1)-Cl(1)	2.4083(4)	O(3)-Ni(1)-Cl(1)	173.20(3)
		O(2)-Ni(1)-Cl(1)	90.85(3)

Table 3.3: Crystal data and structure refinement for **9a**.

Parameter	**9a**
Empirical formula	$C_{20}\ H_{28}\ Cl_2\ N_2\ Ni_2\ O_6$
Formula weight	580.72 g/mol
Temperature	100(2) K
Wavelength	0.71073 Å
Crystal system	Monoclinic
Space group	P 2_1/n
a	8.3440(7) Å
b	8.9628(7) Å
c	16.4951(13) Å
α	90°
β	101.127(2)°
γ	90°
Volume	1210.41(17) $Å^3$
Z	2
Density (calculated)	1.593 Mg/m^3
Absorption coefficient	1.814 mm^{-1}
F(000)	600
Crystal size	0.520 x 0.240 x 0.150 mm^3
Theta range for data collection	2.517 to 28.299°.
Reflections collected	10761
Completeness to theta = 25.242°	100.0 %
Max. and min. transmission	0.789 and 0.446
Data / restraints / parameters	2994 / 2 / 154
Goodness-of-fit on F^2	1.044
Final R indices [I>2sigma(I)]	R1 = 0.0197, wR2 = 0.0472
R indices (all data)	R1 = 0.0206, wR2 = 0.0476
Largest diff. peak and hole	0.450 and -0.281 $e.Å^{-3}$

The molecular structure diagram of complex **9a** shown in Figure 3.11 revealed that the two nickel metal centres adopt distorted octahedral geometry in which the coordination sphere

around the metal centres consists of two bidentate ligands **L7** and one chloride atom. In addition, the oxygen of the pendant group is also coordinated to the nickel metal centre to give a six coordinate octahedral geometry. This is an interesting observation since the elemental analysis of **9** corresponded to one ligand motif around the metal centre which is different from what is observed from the X-ray structure of complex **9a**. Therefore, it could be speculated that a mononuclear complex **9** with one ligand motif upon recrystallization transformed to give a binuclear octahedral complex **9a** with two ligand units of **L7** coordinated to each nickel(II) metal centre. Nevertheless, the presence of two ligand units around the nickel(II) metal in complex **9a** is also somewhat supported by the mass spectrum of **9** (Figure 3.8), which showed a peak with m/z value of 443.0172 amu corresponding to the $[(L7)_2Ni]^+$ molecular ion.

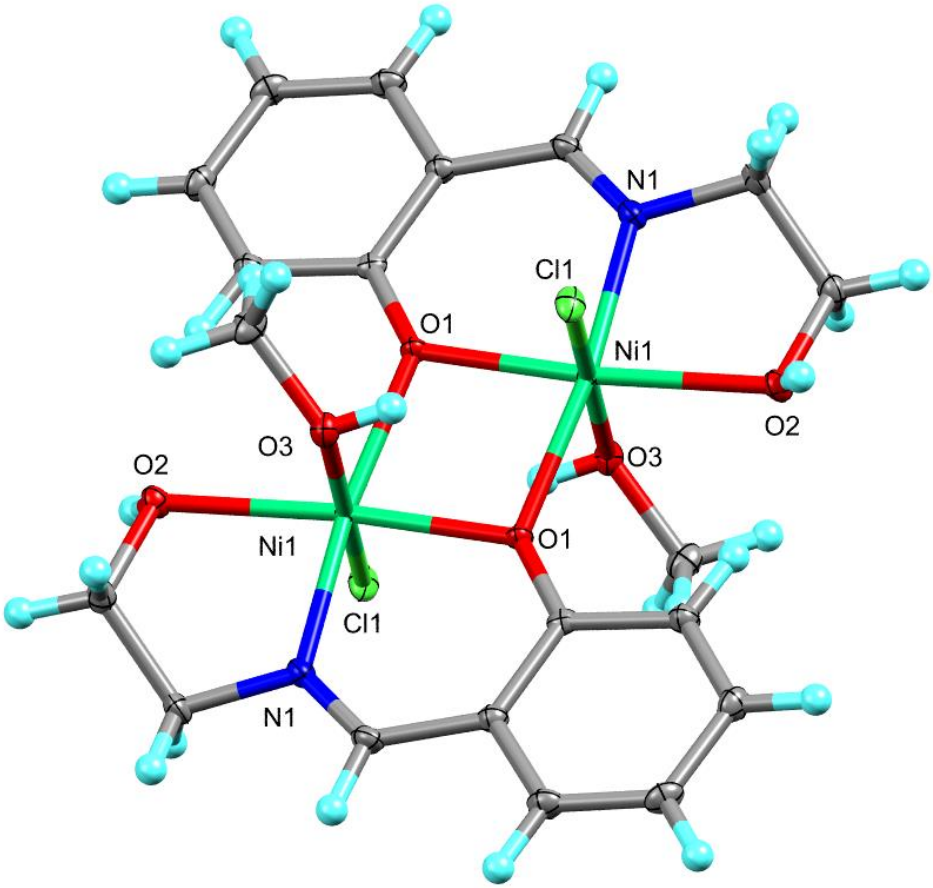

Figure 3.11. Molecular structure diagram of **9a**, the carbons and hydrogens are not labelled for clarity.

The crystal structure of **9a** compares favorably to the one reported by Dey *et al*.[25] for bis(μ$_2$-2-((2-Hydroxyethyl)iminomethyl)phenolato-N,O,O,O')-bis(acetate-O)-diaqua-di-nickel(II) complex obtained from the Cambridge Structural Database (CSD). The Ni-O average bond length of complex **9a** of 2.0619(8) Å was found to be longer than the one obtained in literature of 2.052 Å. In contrast, Ni-N bond length of 2.0012(10) Å was found to be shorter than the one reported in literature of 2.003 Å. The selected bond angles of **9a** revealed a severe distorted octahedral crystal structure. For example, the bond angles of O(1)-Ni(1)-O(1), N(1)-Ni(1)-O(2) and O(3)-Ni(1)-Cl(1) were 80.40(4)˚, 80.65(4)˚ and 173.20(3)˚ respectively (Table 3.2).[26]

3.3.3. The catalytic behavior of complexes 7–13 in the oligomerization of ethylene when activated with EtAlCl$_2$ co-catalyst

The catalytic abilities of the nickel(II) complexes **7-13** in ethylene oligomerization reactions were investigated using EtAlCl$_2$ as an activator in chlorobenzene solvent. Table 3.4 gives a summary of the catalytic results obtained for the pre-catalysts. The ethylene oligomerization reactions predominantly produced C$_4$ and C$_6$ oligomers as main products without Friedel-Craft alkylated products as was reported in Chapter Two for the benzimidazolylmethylamine nickel(II) complexes **1**–**6**.

3.3.3.1. The effect of the catalyst structure on the catalytic activities and product distribution.

The imine and amine nickel(II) complexes **7-13** formed active catalysts after the activation with EtAlCl$_2$. The catalytic results obtained show that the ligand architecture and the identity of the halides had a major effect on the catalytic activities of the nickel(II) complexes (**7-13**). For example, comparing complexes **7** (Table 3.4, entry 1) and **8** (Table 3.4, entry 2), it is clear that the chloride complex was more active than the analogous bromide complex **8**. This is in

good agreement with the report of Zhang *et al.*[27] using nickel(II) complexes ligated by 2, 6-pyridicarboxamide, and could be due to the bromide atom being less electronegative than chloride atom which subsequently results in the less electropositive nickel(II) metal centre.

Table 3.4: Ethylene oligomerization data obtained for nickel(II) complexes **7**-**13** using $EtAlCl_2$ as a co-catalyst in chlorobenzene.[a]

Entry	Catalyst	T_{min}/T_{max} (°C)[b]	Yield [c] (kg)	Activity (kg mol^{-1} h^{-1})	Product distribution (%) [d]	
					C_4	C_6
1	**7**	25/30	0.0250	2 500	27	73
2	**8**	25/27	0.0264	2 640	29	71
3	**9**	25/29	0.0191	1 910	31	69
4	**10**	25/35	0.0333	3 330	25	75
5	**11**	25/26	0.0202	2 020	20	80
6	**12**	25/33	0.0153	1 530	22	78
7	**13**	25/31	0.0255	2 550	30	70

[a]Reaction conditions: [M] = 10 µmol; solvent, chlorobenzene, 80 ml (88.8 g); Temperature, 25 °C; Time, 1h; Pressure, 10 bar; Al:M = 250.
[b]Initial temperature was 25 °C, T_{min} and T_{max} = lowest and highest temperatures obtained during the reaction period.
[c]Determined using the calibration curve of the R-factors versus the number of carbons.
[d]Determined by GC.

There was also an observed decrease in the catalytic activity from 2 640 kg mol^{-1} h^{-1} to 1 910 kg mol^{-1} h^{-1} when the methyl group was substituted with a hydrogen atom in complexes **8** and **9** (Table 3.4, entries 2 and 3). This can be attributed to improved solubility of the complex bearing the methyl group as the alkyl substituent.[18] The imine complexes resulted in the

formation of highly active nickel(II) based catalysts than the corresponding amine complexes. As an illustration, the imine complexes **7** and **9** exhibited high catalytic activities of 2 500 kg mol^{-1} h^{-1} and 1 910 kg mol^{-1} h^{-1} respectively compared to lower catalytic activities of 2 020 kg mol^{-1} h^{-1} and 1 530 kg mol^{-1} h^{-1} for **11** and **12** respectively. This could be due to the electron deficient imine nitrogen withdrawing electrons to itself resulting in a more electropositive nickel(II) metal which subsequently increase the rate of substrate attachment and thereby increasing the catalytic activities of the imine complexes. The opposite is true for the interaction of the amine nitrogen and the nickel(II) metal centre.

The catalytic activities of the nickel(II) complexes were also greatly influenced by the pendant donor group in the ligand structure. In general, the electron donating pendant group gave higher catalytic activity than the electron withdrawing pendant group. For example, complex **13** bearing the $N(CH_2CH_3)_2$ pendant group exhibited high catalytic activity of 2 500 kg mol^{-1} h^{-1} whilst complex **12** bearing an OH pendant group showed a lower catalytic activity of 1 530 kg mol^{-1} h^{-1} (Table 3.4 entries 6 and 7). It is believed that lower catalytic activity by was due to the stronger bond between the hard O-atom and hard Ni-metal (HSAB Theory) which may have created a competition of the vacant coordination site with the incoming ethylene monomer.[28] The selectivity towards the formation of C_4 (20% – 31%) and C_6 (69% - 80%) as the major products was not greatly affected by the variation of the alkyl substituent, pendant group and the identity of the halide.

3.3.3.2. The effect of the reaction parameters on the catalytic behavior of the nickel(II) complexes.

The effect of varying the reaction parameters was investigated using **9**/$EtAlCl_2$ system and the results are summarized in Table 3.5. Both the catalytic activity and the product distribution were significantly affected by the variation of pressure, Al/Ni ratio, time and solvent medium.

Table 3.5. Ethylene oligomerization reactions of the **9**/$EtAlCl_2$ system[a]

Entry	Time(h)	Pressure (Bar)	Al/Ni	Yield[b] (kg)	TON (kg mol^{-1} h^{-1})[c]	Product Distribution (%)[d]	
						C_4	C_6
1	1	10	150	0.0288	2 887	32	68
2	1	10	200	0.0386	3 865	45	55
3	1	10	250	0.0191	1 910	31	69
4	1	10	300	0.0174	1 738	73	27
5	0.5	10	200	0.0154	3 080	62	38
6	2	10	200	0.0568	2 840	33	77
7	1	20	200	0.0622	6 217	66	34
8	1	30	200	0.118	11 850	78	22
9[e]	1	10	200	0.0209	2 094	100	-

[a] Reaction conditions: [**9**] = 10 µmol; solvent, chlorobenzene, 80 ml; Temperature, 25 °C.
[b] Determined using the calibration curve of the R-factors versus the number of carbons.
[c] TON, kg oligomer produced per mol catalyst per hour.
[d] Determined by Gas Chromatography.
[e] In toluene solvent;

3.3.3.2.1. The effect of Al/Ni ratio on ethylene oligomerization reaction using complex 9.

Using **9**/$EtAlCl_2$ system, the Al/Ni ratio was first varied from 150 to 300 (Table 3.5, entries 1 - 4 respectively). An optimum catalytic activity of 3 865 kg mol^{-1} h^{-1} was obtained at Al/Ni ratio of 200. A decrease in the catalytic activity was observed at higher Al/Ni ratios of 250 and 300, which was attributed from an increase in alkylaluminium impurities which might results in the deactivation of the catalyst.[27] As the Al/Ni ratio was increased from 150 to 300, the selectivity of C_4 oligomer was observed to increase from 32% - 73% possibly due to increased chain transfer to the co-catalysts or increased chain termination due to enhanced catalytic activity.[29]

3.3.3.2.2. The effect of time on the catalytic behavior of complex 9.

The reaction times were varied from 0.5 h to 2 h to study the stability of the active species using complex **9** (Table 3.5, entries 2, 5 and 6 respectively). There is an observed increased in the catalytic activity of **9** from 3 038 kg mol^{-1} h^{-1} to 3 865 kg mol^{-1} h^{-1} within 1 h which is consistent with the induction period during the initial stages between 0.5 h and 1 h.[30] This is also marked by the higher amount of C_4 oligomer of 62%, which was observed to decrease to 45% after 1 h. In contrast, further increase to 2 h resulted in a drastic drop in the catalytic activity of **9** to 2 840 kg mol^{-1} h^{-1} due to catalyst degradation after 2 h.[31] The amount of C_6 oligomer was observed to increase after 2 h, and this is due to the fact that longer reaction periods favor chain reinsertion which subsequently results in the formation of higher oligomericproducts.[4]

3.3.3.2.3. The effect of ethylene pressure using complex 9.

The pressure of ethylene was varied from 10 bar to 30 bar to examine the effect of ethylene concentration on the catalytic activity and selectivity of the nickel(II) catalysts. Nevertheless, the catalytic activity of **9** was observed to double from 3 865 kg mol^{-1} h^{-1} to 6 217 kg mol^{-1} h^{-1} (Table 3.5, entries 2 and 7 respectively). Further increase in ethylene pressure resulted in an increase in the catalytic activity of **9**/$EtAlCl_2$ system to 11 850 kg mol^{-1} h^{-1}, Table 3.5, entry 8. This trend is due to an increased in ethylene concentration which also has a profound effect on the product distribution. For example, the selectivity of C_4 oligomer increased from 45% to 78% as the ethylene pressure was increased from 10 bar to 30 bar whilst the opposite was observed for the selectivity of C_6 oligomer. The observed trend in selectivity of C_4 over C_6 is consistent with an increase in the catalytic activity of **9** which subsequently results in rapid chain termination and consequently more C_4 is formed.[32]

3.3.3.2.4. The effect of solvent on the catalytic activity and selectivity of complex 9

The effect of solvent on ethylene oligomerization reactions was investigated using **9**/$EtAlCl_2$ system in chlorobenzene and toluene. The solvent used significantly affected both the catalytic activity and selectivity, for example, the catalytic activities of 2 094 kg mol^{-1} h^{-1} and 3 865 kg mol^{-1} h^{-1} were obtained in toluene and chlorobenzene respectively. Higher catalytic activities observed in chlorobenzene could be attributed to better solubility of the complex in chlorobenzene. Despite lower catalytic activity observed in toluene, the use of toluene solvent resulted in a high selectivity for C_4 oligomer (100%). In contrast, chlorobenzene solvent gave 45% and 55% selectivity for C_4 and C_6 oligomers respectively. These results implied that there is competition between activity and selectivity and therefore it was deducted that high catalytically active conditions results in low catalytic selectivities.

3.4. Conclusion

The imine and amine O^N donor ligands together with their respective nickel(II) complexes were successfully synthesized and characterized using ^{1}H NMR, $^{13}C\{^{1}H\}$ NMR, IR spectroscopy, mass spectrometry, magnetic moment measurements, CHN elemental analyses and single crystal X-ray analysis. The N^O 2-[(ethylimino)ethyl]phenol ligand **L7** gave a binuclear nickel(II) complex **9a** possessing a distorted octahedral geometry. The nickel(II) complexes formed active catalysts for ethylene oligomerization reactions upon activation with $EtAlCl_2$ co-catalyst and afforded butenes and hexenes as the major product. The catalytic activities of the nickel(II) complexes were greatly influenced by the nature of the alkyl substituent, pendant donor group and halide atom.

3.5. Reference

1. Piel, C., Kaminsky, W., Kulickle, Ing. W. -M., *Dissertation: Hamburg, Chem.* **2005**.

2. Speicer, F., Braunstein, P., Saussine, L., *Acc. Chem. Res.* **2005**, *38*, 783-793.

3. Lee, G. M., Appukuttan, V. K., suh, H., Ha, C.-S., Kim, I., *Catal. Lett.* **2011**, *141*, 1608-1615.

4. Nyamato, G. S., Ojwach, S. O., Akerman, M. P., *J. Mol. Catal. A: Chem.* **2014**, *394*, 274-282.

5. Vogt, D., *Oligomerisation of Ethylene to Higher Linear R-Olefins, in Applied Homogeneous Catalysis with Organometallic Compounds*. Cornils, B., Hermann, W. A., Eds.: **1996**; Vol. *1*, pp 245-258.

6. Johnson, L. K., Killian, C. M., Brookhart, M., *J. Am. Chem. Soc.* **1997**, *117*, 6414-6415.

7. Wang, C., Friedrich, S. K., Younkin, T. R., Li, R. T., Grubbs, R. H., Bansleben, D. A., Day, M. W., *Organometallics.* **1998**, *17*, 3149-3151.

8. Lapping, G. R., Sauer, J. D., Alphaolefins Applications Handbook. **1989**.*28*.454-455.

9. Zhang, M., Zhang, S., Hao, P., Jie, S., Sun, W. -H., Li, P., Lu, X., *Eur. J. Inorg. Chem.* **2007**, 3816-3826.

10. Natta, G., Pino, P., Mazzanti, G., Giannini, U., *J. Am. Chem.Soc.* **1957**, *79*, 2975-2976.

11. Nelana, S. M., Darkwa, J., Guzei, A. L., Mapolie, S. F., *J. Organomet. Chem.* **2004**, *689*, 1835-1842.

12. Cotton, F. A., Wilkinson, G., Murillo, C. A., Bochmann, M., Advanced Inorganic Chemistry 6th Ed. John Wiley and Sons: New York, **1999**; p 835.

13. Resconi, L., Cavallo, L., Fait, A., Piemontesi, F., *Chem. Rev.* **2000**, *100*, 1253-1345.

14. Schweinfurth, D., Su, C.,Wei, S., Braustein, P., Sarkar, B., *Dalton Trans.* **2012**, *41*, 12984-12990.

15. Shi, Q., Zhang,S., Chang, F., Hao, P., Sun, W. -H., *Comptes Rendus Chimie.* **2007**, *10*, 1200-1208.

16. Shi, Q., Zhang,S., Chang, F., Hao, P., Sun, W. -H., *C. R. Chimie.* **2007**, *10*, 1200-1208.

17. Sinn, H., Kaminsky, W., *Adv. Organomet. Chem.* **1980**, 99-149.

18. Nyamato George, S., Alam, M. G., Ojwach, S. O., Akerman, M. P., *J. Organomet. Chem.* **2015**, *783*, 64-72.

19. Sun, W.-H., Li, Z., Hu, H., Wu, B., Yang, H., Zhu, N., Leng, X., Wang, H., *New. J. Chem.* **2002**, *26*, 1474-1478.

20. Braunstein, P., Naud, F., *Engew. Chem. Int. Ed.* **2001**, *40*, 680-699.

21. Bruker, *A., SAINT and SADABS*, Bruker AXS Incl., Madison, Wisconsin, USA. **2012**.

22. Sheldrick, G. M., *Acta Crystallogr., Sect. A: Found. Crystallogr.* **2007**, *64*, 112-122.

23. Farrugia, L. J., *Appl. Crystallogr.* **2012**, *45*, 849-854.

24. Rome, K., Mclntyre, A., *Chromatography Today.* **2012**, *52*,52-55.

25. Dey, M., Rao, C. P., Saarenketo, P. K., Rissanen, K., *Inorg. Chem. Commun.* **2002**, *5*, 924-929.

26. Allan, F. H., *Acta Cryst.* **2002**, *B58*, 380-388.

27. Zhang, J., Liu, S., Li, A., Ye, H., Li, Z., *New. J. Chem.* **2016**, *40*, 7027-7029.

28. Nyamato, G. S., Ojwach, S. O., Akerman, M. P., *Dalton Trans.* **2016**, *45*, 3407-3416.

29. Chen, E. Y.-X., Marks, T. J., *Chem. Rev.* **2000**, *100*, 1391-1434.

30. Brookhart, M., Jenkins, J. C., *Organometallics* **2003**, *22*, 250-286.

31. Doherty, M. D., Trudeau, S., White, P. S., Morken, J. P., Brookhart, M. , *Organometallics.* **2007**, *26*, 1261-1269.

32. Killian, C. M., Johnson, L. K., Brookhart, M., *Organometallics.* **1997**, *16*, 2005-2007.

Chapter Four

General concluding remarks and future prospects

4.1. General conclusions

The essence of the research project was to invent catalytically active and stable catalysts for ethylene oligomerization reactions. As a result, nickel(II) complexes based on N^N benzimidazolylmethylamine and N^O 2-[(ethylimino)ethyl]phenol ligands were synthesized, structurally characterized and investigated for ethylene oligomerization reactions. The bidentate benzimidazolylmethylamine ligand **L3** formed a mononuclear nickel(II) complex **3a** in which the oxygen of the methoxy alkyl substituent of the first ligand is bonded to the nickel(II) metal centre. On the other hand, the 2-[(ethylimino)ethyl]phenol ligand **L7** resulted in a formation of a binuclear tridentate (O^N^O donor) nickel(II) complex **9a**. In both complex derivatives, the nickel(II) coordination sphere constituted of two ligand systems coordinated to the metal centre and a chloride or a bromide and also a solvent molecule resulting in a severe distorted octahedral crystal structure.

The nickel(II) complexes upon activation with $EtAlCl_2$ or MAO co-catalysts resulted in active catalysts for ethylene oligomerization reactions and produced butenes, hexenes and Friedel-Craft alkylated toluenes as major products. The selectivity of the catalysts was governed by the catalyst system, nature of the co-catalyst and solvent used. Our findings revealed that the nickel(II) complexes derived from N^O donor ligands of 2-[(ethylimino)ethyl]phenol were highly active than the benzimidazolylmethylamine nickel(II) complexes. Nevertheless, there was a high dependence of the catalytic activity, selectivity and stability on the reaction

parameters such as the nature of the co-catalyst, Al/Ni ratio, ethylene pressure, time and temperature.

The solvent utilized greatly enhanced or diminished the catalytic activities of the nickel(II) complexes and also influenced the product distribution. High catalytic activities were obtained in toluene than in chlorobenzene for the N^N benzimidazolylmethylamine nickel(II) complexes but with low selectivity. In contrast, with the N^O 2-[(ethylimino)ethyl]phenol nickel(II) complexes high catalytic activities were achieved in chlorobenzene with high selectivities. The influence of the solvent is also highlighted in Chapter Two, where the use of toluene solvent and $EtAlCl_2$ co-catalyst resulted in the formation of the Friedel-Craft alkylated products.

The nature of the co-catalyst employed had a great influence on the catalytic activities and selectivities of the catalysts. In Chapter Two, activation of the benzimidazolylmethylamine nickel(II) complexes with MAO co-catalyst resulted in low activities as opposed to the usage of $EtAlCl_2$ co-catalyst but with high selectivity. Activation with $EtAlCl_2$ co-catalyst resulted in the formation of C_4 and C_6 oligomers and Friedel-Craft alkylated products. On the other hand, activation with MAO predominantly produced C_4 and C_6 oligomers as major products.

In Chapter Three, activation of N^O 2-[(ethylimino)ethyl]phenol based nickel(II) complexes with $EtAlCl_2$ in toluene predominantly gave butene as major product. This shows that the formation of the Friedel-Craft alkylated toluene products is a complex concept and cannot be explained using the solvent medium and the nature of the co-catalyst alone, but rather, the catalyst structure also need to be carefully examined.

The single-sited nickel(II) pre-catalysts have been successfully used in the oligomerization reactions of ethylene and this research project has contributed to the ongoing research in the field of homogeneous late transition based metal catalysts. Therefore, it can be concluded that our research project has put forward a great improvements towards the design and synthesis of the new catalysts that would add value to the transformation of α-olefins to higher α-olefins used in the production lubricants, surfactants and plasticizers.

4.2. Future prospects

In addition, to the ongoing research, this project has added value and contributed in the synthesis of new nickel(II) catalysts for ethylene oligomerization reactions in terms of catalytic activity, selectivity and stability. In creating a balance in the stability and activity of the resultant catalysts, the nickel(II) complexes have been incorporated with both electron donating and electron withdrawing substituents and also hemilabile pendant groups. The selectivity of the nickel(II) complexes still remains a challenging aspect.In future we intend to improve the oligomeric product separation by applying heterogeneous systems in our homogeneous nickel(II) catalysts systems. The immobilized system would be based on silica support and are provided in Scheme 4.1.

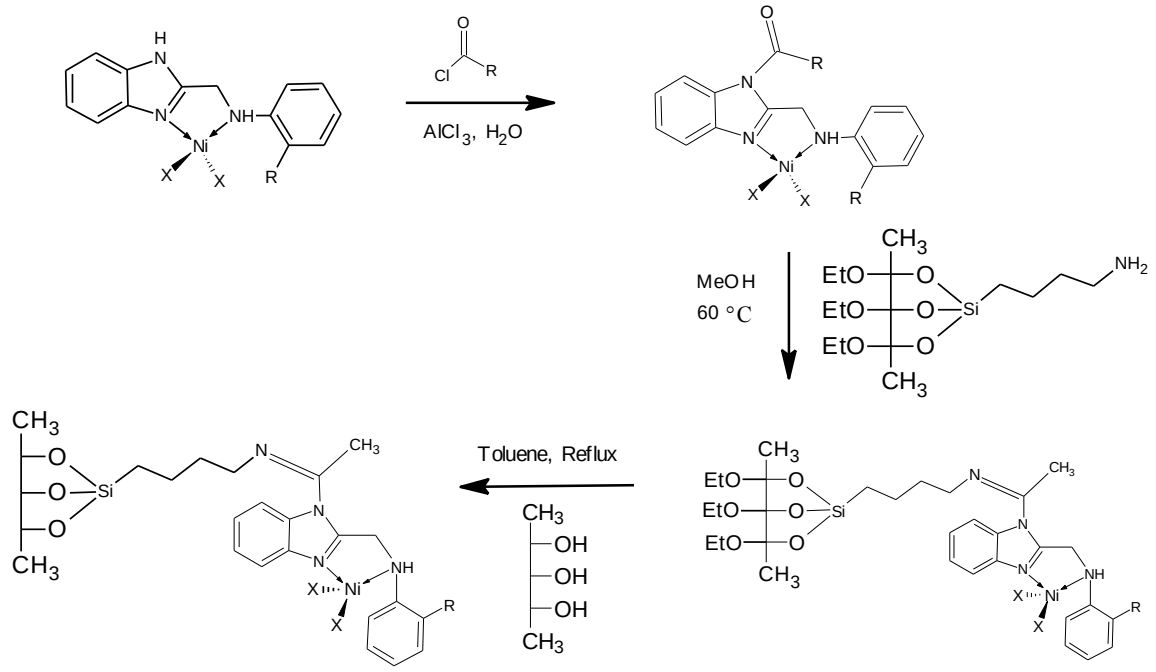

Scheme 4.1. The proposed synthesis for the heterogenized nickel(II) complexes of N^N benzimidazolylmethylamine ligands.